



Master Thesis

**Experiments on adhesion improvement with
sand and its workflow optimization**

Péter Khaut

Graz University of Technology

Faculty of Mechanical Engineering and Economic Sciences

Production Science and Management, MSc.

Institute for Lightweight Design

Ass. Prof. Dipl.-Ing. Dr.techn. Christian Moser

Graz, July 2015



in cooperation with

Knorr-Bremse GmbH Austria



KNORR-BREMSE

STATUTORY DECLARATION

I declare that I have authored this thesis independently, that I have not used other than the declared sources / resources, and that I have explicitly marked all material which has been quoted either literally or by content from the used sources.

date

signature

ABSTRACT

Since the beginning of the railway industry the bottleneck of the braking performance is the adhesion coefficient between the wheel and the rail. Under slippery surface conditions, dropping sand onto the rail is the most common adhesion increasing method. The focus of this thesis is on test rig experiments and its workflow optimization for analysing the benefits and drawbacks of sanding. During these multi-axle experiments various sand amounts and slip values were investigated and compared.

Starting with an overview of the wheel-rail contact the basic theory of adhesion is described. It is followed by a historical and technical review of sanding systems. Next, the test rig facility at Knorr-Bremse Austria is showed with all the details and setting parameters which were used during the experiments. Before presenting the results of the experiments, the whole workflow and input/output variables are exposed. Finally, the optimizations of the workflow are shown and compared to a previous series of experiments.

The thesis has multiple outcomes: the optimized workflow and the results of the experiments. On the one hand, the optimized workflow has enabled a more accurate and reproducible way to carry out the experiments. On the other hand, the results of the experiments show that more sand clearly increases the adhesion coefficient with a higher amount. This advantage however, is showing a falling trend for higher slip values. At the same time the disadvantages of sanding are increasing with more sand output.

ABSTRAKT

Seit dem Anfang der Eisenbahnindustrie ist der Engpass der Bremsleistung der Adhäsionskoeffizient zwischen dem Rad und der Schiene. Unter rutschigen Oberflächenbedingungen, ist Sandung die häufigste Methode um die Adhäsion zu erhöhen. Der Schwerpunkt dieser Masterarbeit liegt auf Prüfstandsversuchen und deren Workflow Optimierung für die Analyse der Vor- und Nachteile von Sandung. Während der Versuche mit Mehrachsüberrollungen wurden verschiedene Sandmengen und Schlupfwerte untersucht und verglichen.

Beginnend mit einem Überblick über den Rad-Schiene Kontakt, ist die grundlegende Theorie der Adhäsion beschrieben. Anschließend erfolgt eine technische und historische Übersicht von Sandungssystemen. Als nächstes wird der Prüfstand bei Knorr-Bremse Österreich mit allen Details und Einstellparameter, die in den Experimenten verwendet wurden, gezeigt. Vor dem Präsentieren der Versuchsergebnisse werden der gesamte Workflow und die Ein-/Ausgangsvariablen dargestellt. Schließlich werden die Optimierungen des Workflows gezeigt und mit einer vorherigen Versuchsreihe verglichen.

Diese Masterarbeit hat mehrere Ergebnisse: der optimierte Workflow und die Ergebnisse der Versuche. Einerseits hat es der optimierte Workflow ermöglicht, die Versuche in einer genaueren und reproduzierbaren Weise durchzuführen. Andererseits zeigen die Ergebnisse der Versuche, dass mehr Sand den Adhäsionskoeffizienten deutlich mit einem höheren Betrag vergrößert. Dieser Vorteil jedoch, zeigt eine fallende Tendenz für höhere Schlupfwerte. Gleichzeitig nehmen die Nachteile der Sandung mit mehr Sandausbringung zu.

ACKNOWLEDGEMENT

Hereby I would like to use the opportunity to express my deepest gratitude to my advisor, Prof. Christian Moser for his support and guidance throughout my thesis. Furthermore, I am very grateful to all the employees of the Institute for Lightweight Design at Graz University of Technology.

I would also like to extend my thankfulness to the employees at Knorr-Bremse Austria, primarily to Florian Hösch. His advice during my work was invaluable.

NOMENCLATURE

Symbol	Meaning	Unit
g	gravitational acceleration	[m/s ²]
F	force	[N]
F_f	friction force	[N]
F_N	normal force	[N]
F_T	tangential force	[N]
m	mass	[kg]
r	radius	[mm]
s	wheel slip according to Kalker's definition	[-]
s_t	wheel slip on the test rig	[-]
t	time	[s]
T	torque	[Nm]
v	speed	[m/s]
v_{rail}	speed of the rail	[m/s]
v_{wheel}	speed of the wheel	[m/s]
x	rail position	[mm]
μ	coefficient of adhesion	[-]
μ_f	coefficient of friction	[-]
φ	speed ratio	[-]
ω	angular velocity	[rad/s]

UIC COORDINATE SYSTEM

x	longitudinal direction, pointing forwards (direction of movement)
y	crosswise to the rail
z	vertical direction, pointing downwards

TABLE OF CONTENTS

STATUTORY DECLARATION	III
ABSTRACT	IV
ABSTRAKT	V
ACKNOWLEDGEMENT	VI
NOMENCLATURE	VII
TABLE OF CONTENTS	VIII
1 INTRODUCTION	1
1.1 BACKGROUND INFORMATION	1
1.2 OBJECTIVES	2
1.3 STRUCTURE AND METHODOLOGY	3
2 WHEEL-RAIL CONTACT	4
2.1 OVERVIEW OF THE WHEEL-RAIL CONTACT	4
2.2 CONTAMINATIONS AND FRICTION MODIFIERS	8
2.3 SLIP	10
2.4 COEFFICIENT OF ADHESION AND FRICTION	12
3 SANDING	16
3.1 THE OBJECTIVE OF SANDING	16
3.2 HISTORY OF THE TECHNOLOGY	16
3.3 SANDING SYSTEMS	17
3.4 OPERATION AND EFFECTS OF SANDING	17
3.5 SANDING PARAMETERS	19
3.5.1 Amount of sand and regulations	19
3.5.2 Properties of sand	20
3.6 DRAWBACKS OF SANDING	22
3.6.1 Isolation	22
3.6.2 Increased wear	22
3.6.3 Need for maintenance	22
3.6.4 Environmental impact	22
4 TESTING FACILITY AT KNORR-BREMSE AUSTRIA	24
4.1 CONSTRUCTION	24
4.2 MEASURING DEVICES, SENSORS, SOFTWARE	25

4.3	INPUT-, OUTPUT PARAMETERS.....	26
4.3.1	Amount of sand.....	26
4.3.2	Slip	27
4.3.3	Test rig output variables.....	28
5	EXPERIMENTS	29
5.1	GOAL OF THE EXPERIMENTS	29
5.2	GENERAL WORKFLOW	29
5.2.1	Multi-axle measurements.....	29
5.2.2	Repetition runs	29
5.2.3	Conditioning with Socolub.....	30
5.2.4	Reference run	30
5.2.5	Sequence of actions.....	32
5.3	PARAMETERS FOR THE EXPERIMENTS.....	33
5.3.1	Sand.....	33
5.3.2	Slip	34
5.3.3	Further parameters and overview	35
5.4	EVALUATION OF THE RESULTS	35
5.4.1	Introduction.....	35
5.4.2	Single overrollings.....	35
5.4.3	Repetition runs	37
5.4.4	Multi-axle results	38
5.4.5	Adhesion curve.....	38
5.4.6	Reference and adhesion improvement.....	39
5.4.7	Isolation.....	39
5.5	PRELIMINARY EXPERIMENTS.....	40
5.5.1	Introduction.....	40
5.5.2	20 % slip.....	40
5.5.3	Modification of the surface condition	42
5.6	RESULTS OF THE EXPERIMENTS	47
5.6.1	Rail at the end of the experiments.....	47
5.6.2	Comparison of the sand amount	48
5.6.3	Comparison of the slip values.....	51
5.6.4	Adhesion curve.....	53
5.6.5	Isolation.....	55
5.7	CONCLUSION	57
5.8	OUTLOOK.....	58

6	WORKFLOW OPTIMIZATION.....	59
6.1	INTRODUCTION	59
6.2	IMPROVEMENTS.....	59
6.2.1	Conditioning	59
6.2.2	Sequence of actions and reference runs.....	62
6.2.3	Evaluation.....	63
6.3	PERFORMANCE OF THE NEW WORKFLOW	64
6.4	COMPARISON OF THE RESULTS.....	67
7	SUMMARY.....	70
	LIST OF REFERENCES.....	71
	LIST OF ABBREVIATIONS.....	73
	LIST OF FIGURES.....	74
	LIST OF TABLES	76
	APPENDIX.....	77

1 INTRODUCTION

1.1 BACKGROUND INFORMATION

The biggest benefit of railway transport compared to other transportation means is clearly the higher energy efficiency. During the evolution of railway vehicles the higher speed of passenger trains and the increased axle load of freight trains had continuously compelled the engineers to strive for better solutions in terms of safety and reliability. The evolved driving capabilities of rolling stocks implied more rigorous prerequisites for the surface condition in the wheel-rail contact.

Technical designers in the railway industry always relied on the friction between the wheel and the rail which permits to transmit the necessary tractive and brake force. For the economical operation of railway vehicles low friction is needed to ensure low rolling resistance, hence low energy consumption. The continuously developing technology enables higher acceleration and operating speed which implies several further measures, e.g. more efficient brake systems in order to be able to stop the rolling stock within the prescribed distance. Since railway is an open system, contaminations (natural or artificial origin) can be present between the contact surfaces which results in a hardly predictable decrease of adhesion. Adhesion is the transmitted tangential force in the longitudinal direction between the wheel and the rail.¹ Both safety and reliable operation can be affected by poor adhesion between the wheel and the rail. Furthermore, adhesion loss can cause skidding marks on the rail surface and wheel flats on the tread, as shown in Figure 1.1, which leads to heavy maintenance costs.

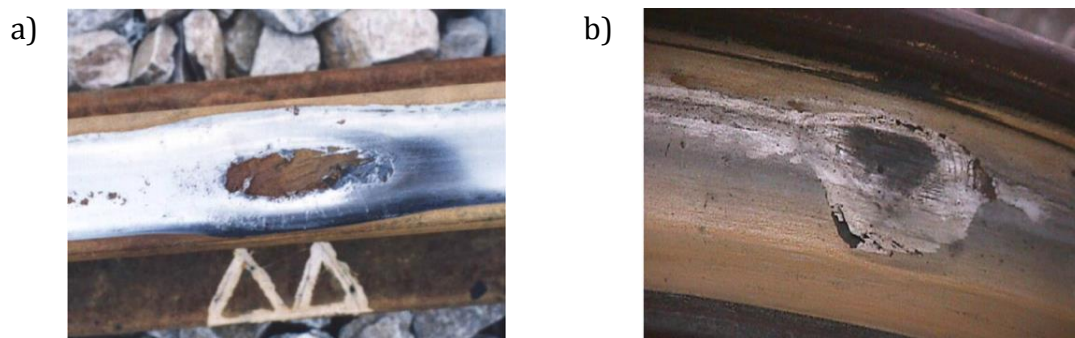


Figure 1.1: The typical damages of wheel/rail under low adhesion, (a) skidding marks on the rail surface; (b) wheel flats on the tread²

¹ Zhu, Adhesion in the wheel-rail contact, 2013, p. 1

² Wang, Zhang, Wang, Liu, & Zhu, 2010, p. 2694

In order to prevent the above described phenomena, sanding is the most common solution to increase adhesion for traction and braking needs. Sand is applied on the surface of the rail which can counteract the harmful effect of contaminations.

1.2 OBJECTIVES

This thesis deals with the analysis of the benefit of sanding. Therefore experiments were made using a test rig at Knorr-Bremse Austria. Furthermore, a big emphasis is on the workflow optimization of these experiments. Namely, the two main objectives of the thesis are:

1. To carry out a series of experiments
2. To perform a workflow optimization of the experiment process

The main objectives in detail and further points of interest which are elaborated in the thesis are:

- The overview of the literature in order to be able to summarize the most recent scientific approach about the wheel-rail interface and the state of the art technological achievements about sanding systems.
- The examination and improvement of the existing workflow which is used for the experiments on the wheel-rail test rig. Basically the goal is to compose a setting instruction which enables a more accurate way of carrying out the experiments.
- The completion of tests for the new workflow with direct comparison between the old and new method.
- Performing a series of experiments with predefined input variables, thus a parameter study where the effectiveness and drawbacks of sanding are investigated. The results will be used by Knorr-Bremse Austria for the development of sanding equipment.

1.3 STRUCTURE AND METHODOLOGY

The content of the thesis can be divided in two major parts. In the first section the theoretical overview of the wheel-rail contact (in Chapter 2) and the basic principles of sanding (in Chapter 3) can be found. Chapter 4 is a transition chapter, describing the test rig facility at Knorr-Bremse Austria. The second major section about the performed practical work starts with Chapter 5, where the carried out experiments are presented. Next, the workflow optimization is outlined in Chapter 6. Finally, the summary closes the thesis.

Information is obtained from scientific papers, dissertations and reputable Internet sources. Furthermore, the experience of the advisors and employees at Knorr-Bremse Austria and at TU Graz are implemented in the thesis as well. The experiments and the workflow optimization which have taken place in the factory of Knorr-Bremse Austria are entirely the own work of the author.

2 WHEEL-RAIL CONTACT

2.1 OVERVIEW OF THE WHEEL-RAIL CONTACT

The wheel-rail system is being used for long-distance trips for many centuries. During the evolution of technology, a lot of forms of transportation have been developed which are based on the principles of the wheel-rail system. Figure 2.1 shows the classification of rolling stocks according to the standard DIN 25003. Furthermore, the wheel-rail system is also widely used among others in machines, cranes, materials-handling technologies and mining applications. This thesis deals with the wheel-rail contact of rolling stocks.

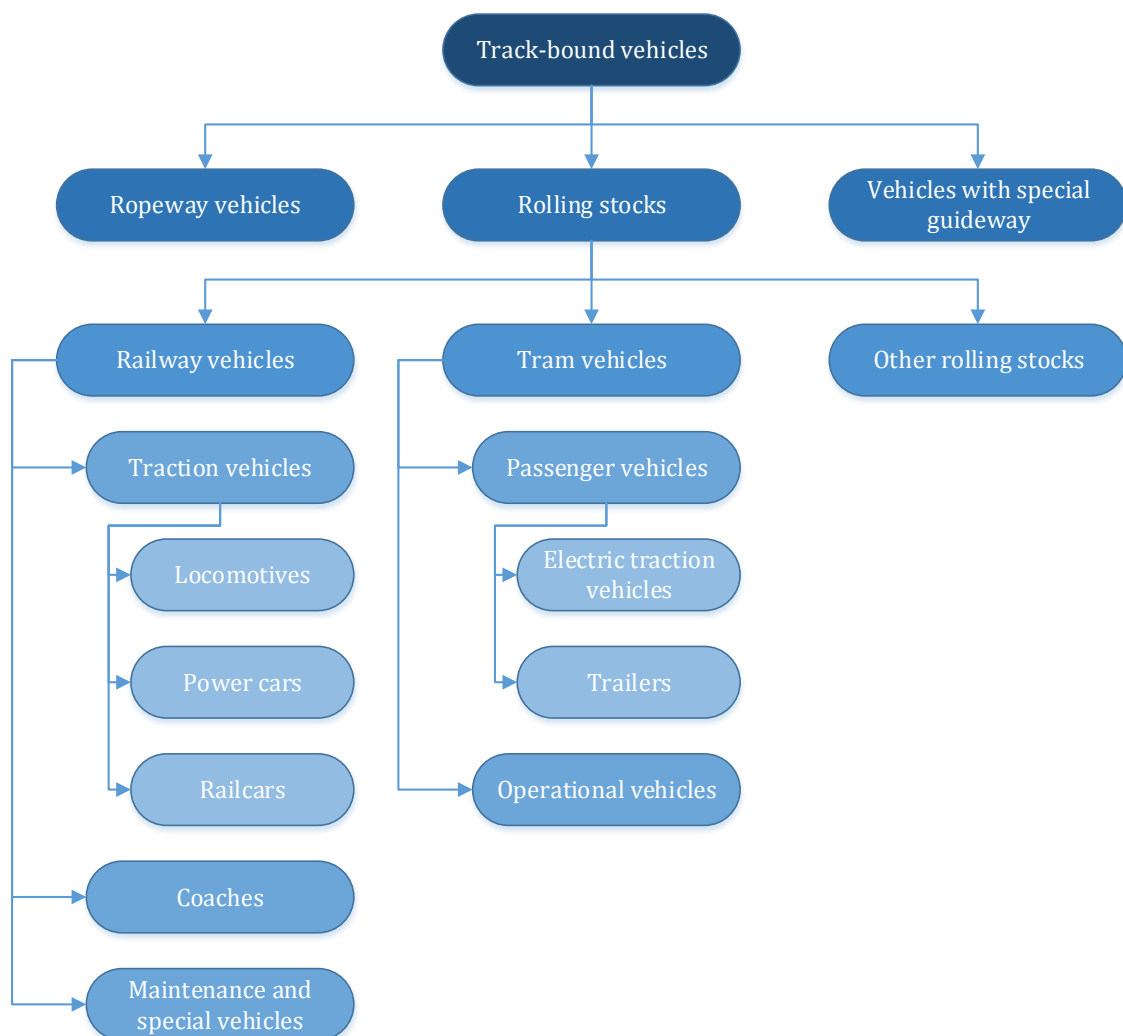


Figure 2.1: Classification of rolling stocks³

³ German National Standard, 2001

Both the wheel and the rail are made of steel and the contact area between the two parts is approximately 1 cm². The reason for the comparatively small contact area is the high hardness of the materials which does not result in excessive elastic deformation despite the high amount of applied normal load.⁴ This property can be considered as a prerequisite for low rolling resistance but there exist additional important factors which will be reviewed in this chapter.

For a deeper understanding of the load states between the wheel and the rail, the geometrical relationship and the technical realization of the two parts has to be investigated. Figure 2.2 shows a common layout of a railway bogie.

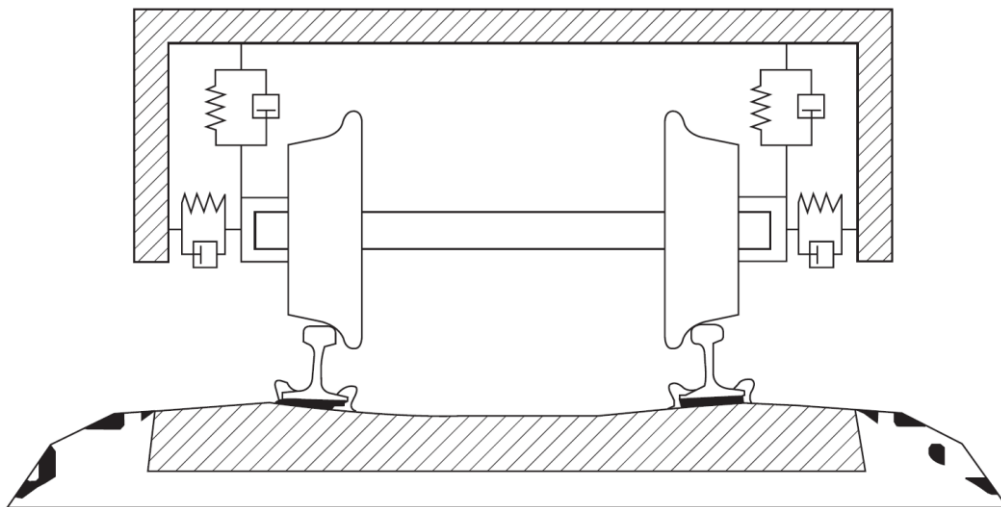


Figure 2.2: Sketch of bogie with primary suspension and wheelset in contact with rails on railpads, sleepers and ballast⁵

Based on the above figure the reasonable conclusion is, that for an accurate determination of the forces in the wheel-rail contact a system-level approach is clearly inevitable. For the research topic of this thesis, however, only the wheel-rail interface is of interest and will be considered.

The wheel tread has a conical shape which is needed to provide a self-centring of the bogie in case of small deflections. The conicity enables the steering capacity and the running stability of the wheel set.⁶ Nevertheless, this geometrical constraint can provide a safe motion of the rolling stock only until a limited extent. For sharp cornering and travelling at high speed, the wheel flange partly overtakes the role of the track guidance.

⁴ Zhu, Adhesion in the wheel-rail contact, 2013, p. 3

⁵ Andersson, Berg, & Stichel, 2007

⁶ Lundén & Paulsson, 2009, p. 7

Therefore, in reality there are multiple areas where the wheel and the rail are in contact. Figure 2.3 shows a closer look on the wheel-rail contact referring to the following details:

- a) Conical wheel profile
- b) Rail inclination
- c) Wheel tread-railhead contact
- d) Wheel flange-rail gauge contact

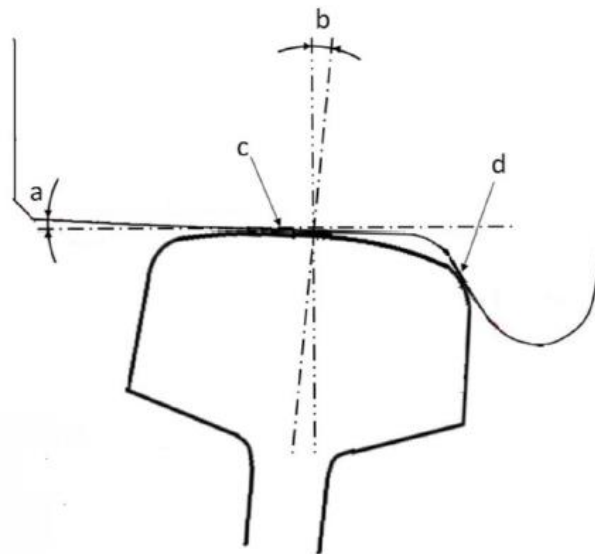


Figure 2.3: Schematic of wheel-rail contact positions⁷

Mainly the two contact areas (“c” and “d”) on Figure 2.3 are responsible for the transfer of all load cases which are present in the dynamical system of the rolling stock. The most important acting forces are:

- Normal force → caused by the gravitation and the mass of the rolling stock
- Longitudinal forces → moves and brakes the rolling stock
- Lateral forces → acts mainly in case of cornering

The above mentioned forces can arise in many ways, causing highly dynamic load cases. Furthermore, the resulting contact pressure and sliding velocity can be very different between the two contact zones. This phenomenon of the contact conditions in the wheel-rail contact is depicted in Figure 2.4.

⁷ Zhu, Adhesion in the wheel – rail contact under contaminated conditions, 2011

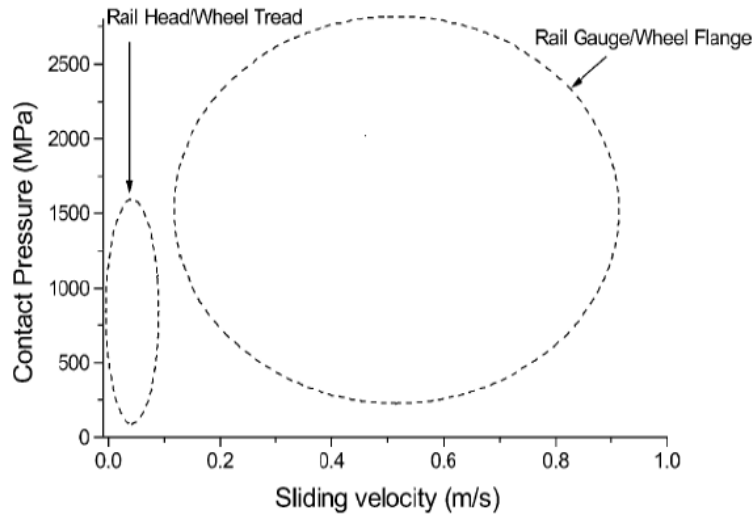


Figure 2.4: Contact conditions in the wheel-rail contact⁸

Due to the excessive contact pressure and sliding velocity in the contact area between the wheel flange and rail gauge, the former component is intentionally lubricated. This measure reduces the wear of the two parts. However, in case of a malfunction this lubricant can appear in the contact area between the wheel tread and rail head causing dramatic reduction of the adhesion coefficient. Since this contact area is responsible for transmitting the longitudinal force, this instance can highly influence the vehicle dynamics of the rolling stock. For more information about friction modifiers, see Chapter 2.2.

For adhesion research, thus in this thesis the wheel tread-railhead contact will be investigated exclusively. The huge amount of longitudinal force which is needed to accelerate and decelerate the rolling stock is applied on the small contact zones between the wheels and the rails. Higher adhesion coefficient between the two components results in higher transferable force. Excessively high adhesion, however, causes higher rolling resistance, hence higher energy consumption. Therefore, for the particular situation optimal adhesion coefficient has to be achieved. In case of adhesion loss which is mainly caused by contaminations, sanding is one of the most widespread method for increasing the adhesion coefficient. For more information about sanding see Chapter 3.

Furthermore, the high axle load of the rolling stocks causes very high contact pressure. In the literature a lot of information can be found about the contact mechanics of normal (Hertz contact theory) and tangential contact cases. However, this topic is in this thesis not further examined.

⁸ Lewis & Olofsson, 2004

2.2 CONTAMINATIONS AND FRICTION MODIFIERS

Adhesion loss between the wheel and the rail affects both safety and performance of the rolling stock. There is a clear distinction in the regulatory requirements for different operating conditions. Figure 2.5 shows the required adhesion coefficient in the Netherlands according to the operation categories, where the bar height is proportional to the maximum required adhesion coefficient.



Figure 2.5: Common adhesion requirements in railway transportation⁹

There are a lot of known reasons which cause low adhesion. One of the most severe problem is when leaves from the surrounding vegetation get in the contact area. They do not have to fall directly on the rail, the turbulence can lift them up and blow under the wheel. Due to the high contact pressure, the leaves are compressed and they cover the top of the rail. Especially in damp or wet weather a Teflon-like mulch layer will be created and the friction coefficient decreases tremendously.¹⁰

Furthermore, third-body layers can be created by different fluid and fine particulate contaminants as well which can have very disadvantageous effect on the adhesion. Among other things following substances can be present in the contact area: oil/grease, water, wear particles, iron oxid layer.

The above mentioned third bodies can be chemically bonded to the surfaces of the bulk materials. Therefore, the materials which are actually in contact can differ chemically from the base material of the wheel and rail.¹¹ This phenomenon is shown in Figure 2.6.

⁹ Arias-Cuevas, 2010, p. 9

¹⁰ Network Rail Limited, 2015

¹¹ Zhu, Adhesion in the wheel-rail contact, 2013, p. 11

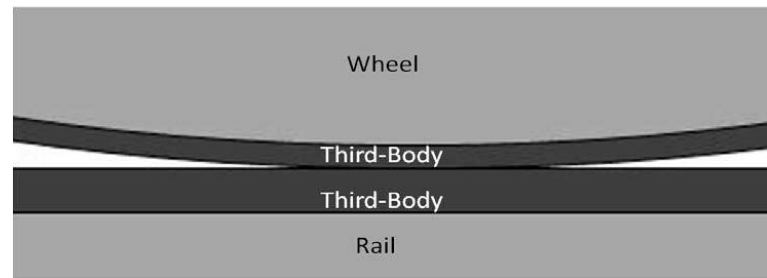


Figure 2.6: The third-body layer between the bulk materials in the wheel-rail contact¹²

Most of the contaminations are unintentionally present on the rail, like leaves or precipitation. These are called “natural third-body materials”. Nevertheless, there can be found on the rail so called “artificial third-body materials” as well. These are friction modifiers which are used, however, not exclusively for adhesion improvement. On the contrary, oil is intentionally applied on the rail flange as a lubricant to decrease friction in order to reduce wear and rolling resistance under severe contact conditions. The categorization of the friction modifiers is the following¹³:

- low-coefficient friction modifier (LCF)
- high-positive friction modifier (HPF)
- very-high-positive friction modifier (VHPF)

Sand is used as a very-high-positive friction modifier in order to improve the adhesion between the wheel and the rail. Further friction modifiers to improve adhesion are:

- Sandite – a mixture of sand and aluminium oxide particles¹⁴
- Ceramic particles – used in the network of high-speed railway lines in Japan (Shinkansen)¹⁵

Beside grit materials, there exists additional methods in order to improve the transmittable longitudinal force or to remove contaminations from the rail:

- Magnetic track brake¹⁶
- High-pressure water jetting¹⁷
- High-powered laser¹⁸

¹² Zhu, Adhesion in the wheel–rail contact, 2013, p. 11

¹³ Zhu, Adhesion in the wheel–rail contact, 2013, p. 14

¹⁴ Olofsson, Adhesion and friction modification, 2009, p. 522

¹⁵ Paces, 2013, p. 10

¹⁶ Arias-Cuevas & Li, 2011

¹⁷ Zhu, Adhesion in the wheel–rail contact, 2013, p. 15

¹⁸ Olofsson, 2007

2.3 SLIP

In vehicle dynamics wheel slip is the extent of the relative motion between the wheel and the ground. The basic formula of slip (s_t) is the following, where the single variables are illustrated in Figure 2.7:

$$s_t = \frac{v - r \cdot \omega}{v} \quad (1)$$

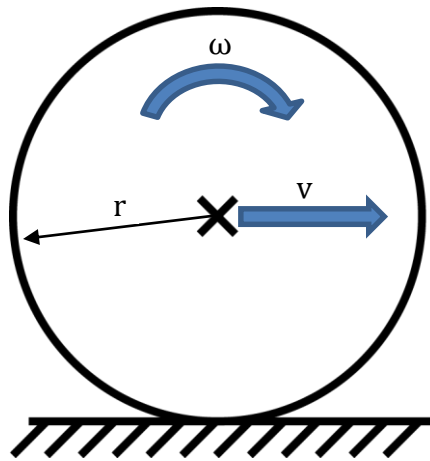


Figure 2.7: Rolling wheel

The case of zero slip is called pure rolling where the circumferential velocity and the velocity of motion are equal, hence the relative velocity between the two objects is zero:

$$v_{rel} = 0 = v - r \cdot \omega \quad (2)$$

If the relative velocity between the wheel and the ground is not zero, then four additional motion cases can be distinguished, which are listed in Table 1.

Motion case	Velocity relation
Pure rolling	$v = r \cdot \omega$
Traction	$v < r \cdot \omega$
Pure skidding	$v = 0 \quad r \cdot \omega \neq 0$
Braking	$v > r \cdot \omega$
Pure slipping	$v \neq 0 \quad r \cdot \omega = 0$

Table 1: Motion cases for diverse velocity relations

For more information about the way of calculation of the slip for the performed experiments, see Chapter 4.3.2.

In the literature the expression “creep” can be found frequently referring to the wheel slip. The reason for the different designation is that the term “slip” is also used for denoting the micro slip which is depicted in Figure 2.8, showing the stick-slip phenomenon in the contact area.

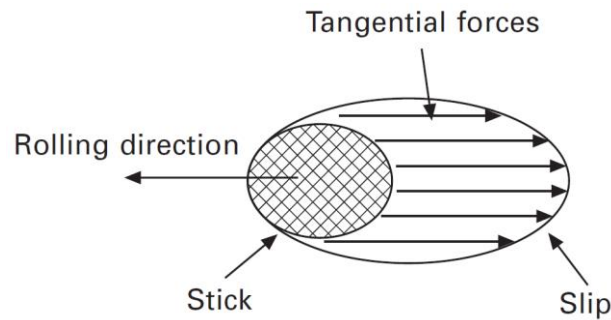


Figure 2.8: Stick-slip phenomenon¹⁹

In order to transmit force between the wheel and the rail (traction or braking), the circumferential velocity of the wheel has to differ from the velocity of motion, namely wheel slip has to be present. The wheel slip has a great importance in case of rolling movements because it influences the maximum amount of transmittable tangential force. Figure 2.9 is visualizing the interdependence between the wheel slip (creep) and the tangential force.

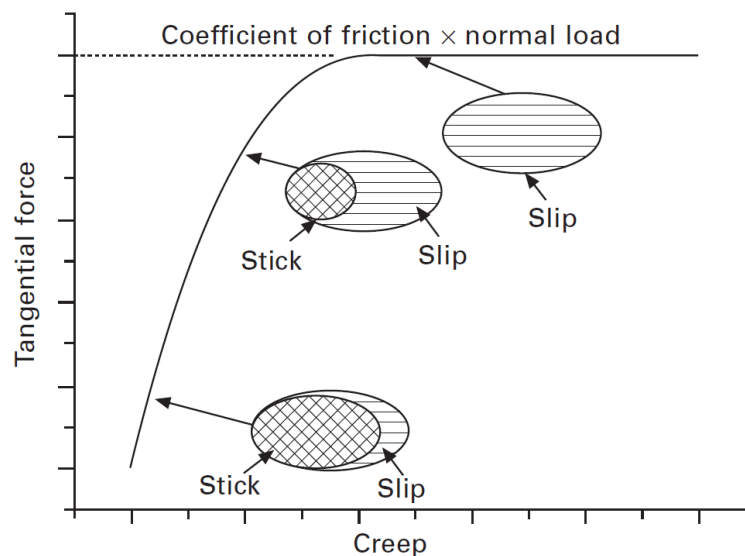


Figure 2.9: Relationship between tangential force and creep (slip) at the wheel-rail contact²⁰

¹⁹ Olofsson, Adhesion and friction modification, 2009, p. 515

²⁰ Olofsson, Adhesion and friction modification, 2009, p. 515

Slip occurs at the rear edge of contact area and it spreads forward as the wheel slip increases. The stick region decreases and the slip region increases until the saturation value of tangential force. From this point on the whole contact area is pure sliding.²¹

In the further terminology, the term “slip” will be used referring to the wheel slip exclusively.

2.4 COEFFICIENT OF ADHESION AND FRICTION

The friction between the wheel and the rail permits a tractive and brake force which is the result of the wheel load and the coefficient of adhesion.²² This relation is the base for the investigation of the wheel-rail contact in terms of vehicle dynamics. In this chapter the difference between adhesion and friction will be clarified.

Figure 2.10 shows the schematic of pure-sliding contact (“a”) and rolling-sliding contact (“b”).

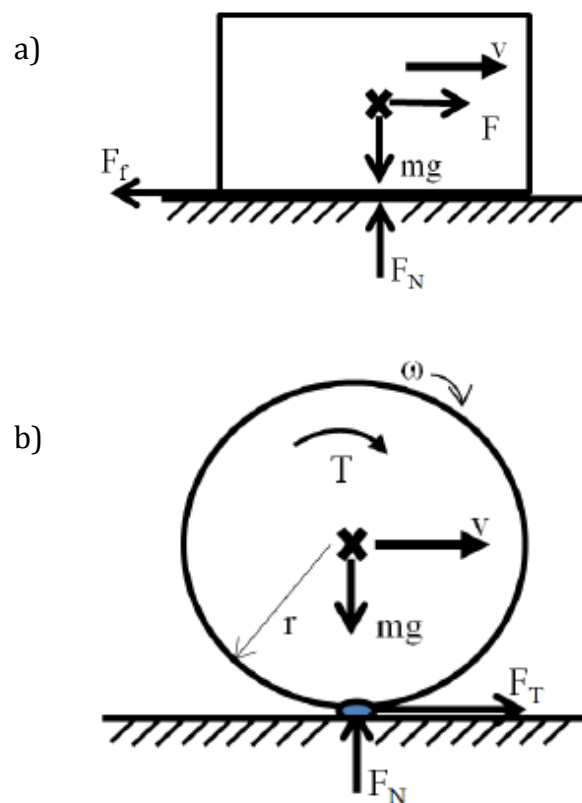


Figure 2.10: Schematic of a) a pure sliding contact and b) a rolling-sliding contact under acceleration (X is the gravity centre; all forces in the figure are acting on either the block or the wheel)²³

²¹ Zhu, Adhesion in the wheel-rail contact, 2013, p. 6

²² Prof. Gfatter & Lang, 2001, p. 10

²³ Zhu, Adhesion in the wheel-rail contact, 2013, p. 5

The model of static and kinetic friction, which is known as the Coulomb model of friction, can be seen in Figure 2.10 a). The static friction is opposing the start of the movement. After the block starts moving, the force opposing the sliding movement is called kinetic or dynamic friction.²⁴ The coefficient of friction is the ratio between the friction force and the normal force:

$$\mu_f = \frac{F_f}{F_N} \quad (3)$$

The coefficient of friction depends in a dry contact on the asperity ploughing (abrasion) and the atomic interaction (adhesion). Ploughing is caused by the interaction of surface asperities during the sliding movement. Furthermore, ploughing can be also affected by wear debris and hard particles. The adhesion force is generated by the attractive force between asperity contacts.²⁵

The model of rolling-sliding contact is illustrated in Figure 2.10 b). The rolling movement of a cylinder along a stationary plane surface is analogous to the case of a railway wheel is rolling along the rail. The tangential force in the longitudinal direction is referred to as adhesion. This is valid for both acceleration and deceleration. However, the available adhesion force is limited by the coefficient of friction.²⁶ The coefficient of adhesion is the ratio between the tangential (adhesion) force and the normal force:²⁷

$$\mu = \frac{F_T}{F_N} \leq \mu_f \quad (4)$$

Adhesion can be characterized as the friction in the function of slip. The friction and adhesion coefficients are schematically depicted in Figure 2.11, where the solid lines indicate the coefficient of adhesion while the dashed lines indicate the coefficient of friction.

²⁴ Arias-Cuevas, 2010, p. 2

²⁵ Hutchings, 1992

²⁶ Olofsson, Adhesion and friction modification, 2009, p. 514

²⁷ Zhu, Adhesion in the wheel – rail contact under contaminated conditions, 2011, p. 5

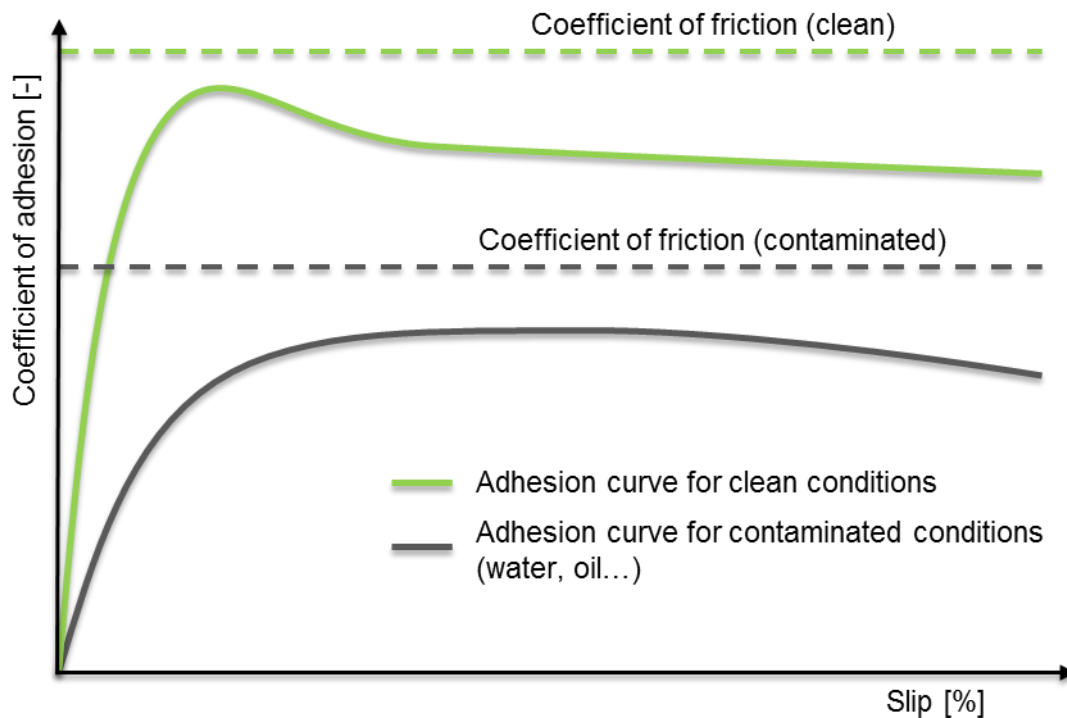


Figure 2.11: Schematic of the adhesion curve and coefficient of friction under clean and contaminated conditions (modified from Zhu)²⁸

The coefficient of adhesion is larger than the coefficient of friction for both (clean and contaminated) depicted conditions. The adhesion, or limiting friction, in the longitudinal direction is less than the total friction because a part of the friction is utilised by lateral and spin forces.

From the characteristic of the adhesion curve the conclusion can be derived that the maximum adhesion can be achieved with an accurate slip control. The adhesion maximum is approximately at 1-2 % slip.²⁹ However, if the actual slip differs slightly from this point to a smaller value (to the left on the adhesion curve), a remarkable drop of the adhesion occurs. In the reality this would mean poor braking/traction performance. Furthermore, heavy stick-slip oscillation would occur which results in high vibration and increased wear. Therefore, the modern wheel slide protection systems on rolling stocks are operating between 10 % and 20 % slip.

Note that in Figure 2.11 the coefficient of friction is shown as a constant value because of the better illustration, however, in reality it is influenced by many factors.

²⁸ Zhu, Adhesion in the wheel-rail contact, 2013, p. 7

²⁹ Polach, 2005

In Table 2 typical coefficient of friction values are presented under different conditions. The data was measured using a hand-pushed tribometer by Olofsson.

Condition	Coefficient of friction
Sunshine dry rail, 19°C	0.6-0.7
Recent rain, 5°C	0.2-0.3
With a lot of grease on rail, 8°C	0.05-0.1
Damp leaf film on rail, 8°C	0.05-0.1

Table 2: Friction coefficients measured with a salient system tribometer³⁰

According to Moore, the available friction in the form of the adhesion coefficient is listed in Table 3 for a wide range of conditions.

Condition of rail surface	Adhesion coefficient
Dry rail (clean)	0.25-0.30
Dry rail (with sand)	0.25-0.33
Wet rail (clean)	0.18-0.20
Wet rail (with sand)	0.22-0.25
Greasy rail	0.15-0.18
Moisture on rail	0.09-0.15
Light snow on rail	0.10
Light snow on rail (sand)	0.15
Wet leaves on rail	0.07

Table 3: Examples of wheel-rail adhesion coefficients³¹

³⁰ Olofsson, Adhesion and friction modification, 2009, p. 516

³¹ Moore, 1998

3 SANDING

3.1 THE OBJECTIVE OF SANDING

In the most frequent cases low adhesion causes severe damage on the rail and the wheels of the rolling stock. Wheel spin during traction and wheel slide during braking leads to an early wear of the parts. Braking is more critical because wheel slide can result in wheel flat which can be even recognized by the passengers as an uncomfortable rattling. In severe cases low adhesion can result in delays of the trains but it can even lead to a safety related issue.

Sanding can successfully prevent the above mentioned adverse effects of low adhesion. Sand is used as an artificial third-body material in order to overcome the harmful impact on the surface condition of diverse substances (see Chapter 2.2) by increasing the adhesion coefficient in a targeted manner. It is applied in front of the wheels and due to its physical properties it has an immediate impact on the adhesion.

3.2 HISTORY OF THE TECHNOLOGY

Already in the 19th century sand was used as a grit material. In that time trains were not equipped with electropneumatic wheel slide protection systems which hinders a harmful excessive relative speed difference between the wheel and the rail during traction and braking process. Therefore, acceleration and deceleration caused some difficulties even with the significantly lower speed compared to existing railway vehicles. Skidding and gliding happened frequently, causing severe surface damages both to the wheels and the rails.

At least since 1847 sanding devices are used as a common method for adhesion improvement. It became widespread mainly due to its low operating costs and easy accessibility to the grit material. The sand however, has some basic requirements which has to be fulfilled. It was found out in the early times that in order to ensure an optimal operation, the sand has to be dry and must not contain any loamy components. Therefore, on steam locomotives the sandbox was mounted on the steam dome of the boiler. The dry sand was transmitted by manually operated gears and valves to tubes which ended at the sand pipe and the grit was finally outputted on the rail. Later conveyor spirals were used which transmitted the sand more reliable. During the evolution of technology, sanding devices have undergone considerable development. In Chapter 3.3 the basic structure and the operating principles of a state of the art sanding device will be described.

3.3 SANDING SYSTEMS

In Figure 3.1 the schematic diagram of a modern sanding system can be seen. The sand is stored in a pressure sealed box. The filling level can be continuously monitored by sensors. The sanding device is equipped with a dryer unit because it has to be prevented that sand gets stuck in the device caused by condensation humidity. During operation, sand is outputted by pressured air through the sand pipe. The exit velocity of the sand can reach 10 m/s. The sand pipe heater is used to prevent the sand tube outlet from freezing. This solution ensures a safe function of the sanding system throughout the year.

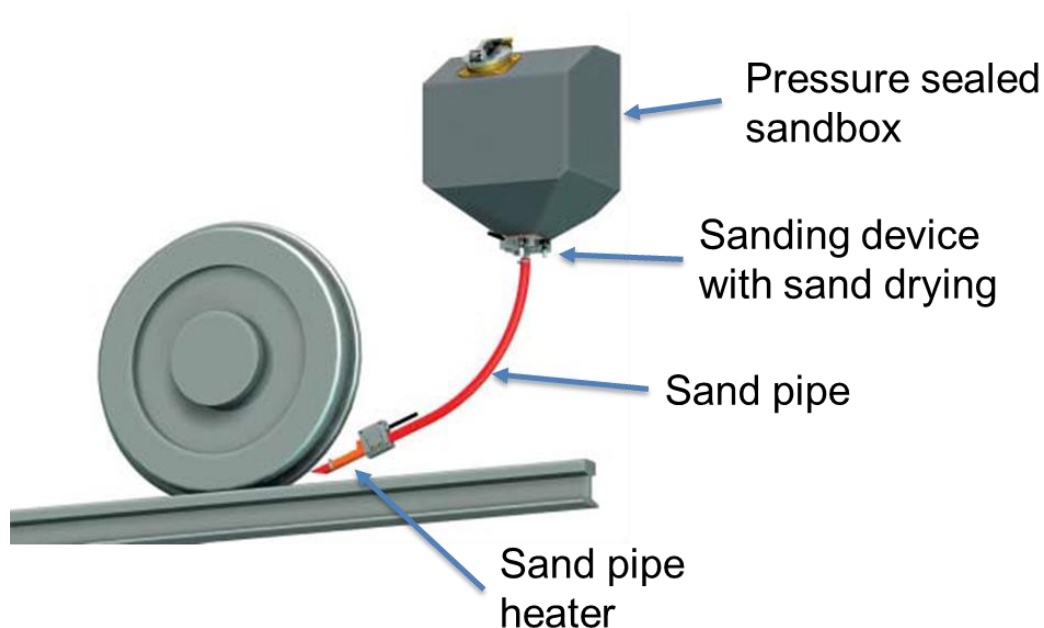


Figure 3.1: Schematic diagram of a sanding system³²

3.4 OPERATION AND EFFECTS OF SANDING

The activation of sanding can happen manually by the driver or automatically by a signal from the wheel slide protection unit. The way of operation depends on the type of the rolling stock and the circumstances of activation. The microprocessor controlled wheel slide protection can detect low adhesion state by the differences in the speed of the train's movement and the rotational speed of the wheel. In this case quickly applying and releasing the brake pressure prevents the wheel from locking up and avoids skidding. If the wheel slide protection alone cannot achieve the desired

³² Prof. Gfatter & Lang, 2001, p. 17

acceleration/deceleration, it can give a signal to activate the sanding system. Figure 3.2 shows the sanding system in operation.



Figure 3.2: Sanding system in operation³³

Eventually, sand is used to increase the adhesion and it enables to reach the desired amount of traction/braking force. Figure 3.3 shows the effect of sanding on the braking deceleration and on the brake cylinder pressure.

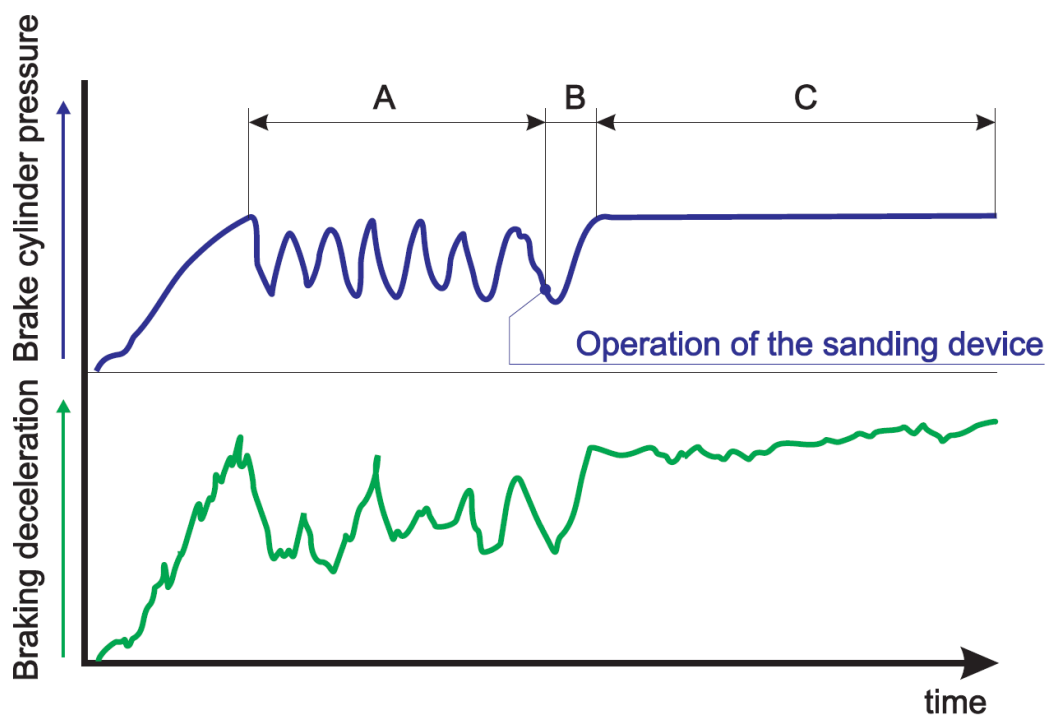


Figure 3.3: Effect of sanding³⁴

³³ Knorr-Bremse GmbH

³⁴ Prof. Gfatter & Lang, 2001, p. 22

Prior to the activation of the sanding system (timespan “A”), the brake cylinder pressure oscillates heavily because the wheel slide protection is in use. This phenomenon has an effect of irregular deceleration values. After the sanding system is operated, the cylinder pressure increases and remains steady because the wheel slide protection is no longer in use. Furthermore, the deceleration of the train gets higher as well which results in a shorter braking distance.

The precondition for the above described process is an increased adhesion coefficient between the wheel and the rail which is achieved with the sand. One of the reasons for the adhesion improvement is that the grinded sand grains have a high ability to absorb moisture due to the increased surface. Furthermore, the sand has a remarkable impact on the surface structure as well. It induces plastic deformation and abrasion of the asperities, which finally results in roughening of the contact surfaces.

3.5 SANDING PARAMETERS

3.5.1 Amount of sand and regulations

The most important sanding parameter is the outputted amount of sand. Too little amount has no significant effect on the adhesion improvement. Too much of sand, however, can increase the impedance between the wheel and the rail excessively. In this case the track signalling can indicate clear line signal falsely in the presence of a rolling stock. Therefore, directives exist for the maximum allowed impedance and sand amount. The TSI (Technical specification for interoperability relating to the subsystem “Control-Command and Signalling” of the trans-European conventional rail) document of the European Union contains all the current regulations, which are described in the followings.

The operative regulation for the impedance of a wheelset:

“Electrical resistance between the running surfaces of the opposite wheels of a wheelset shall not exceed:

- 0.01 Ohm for new or reassembled wheelsets
- 0.05 Ohm after overhaul of wheel sets

The resistance is measured by a measuring voltage that is between 1.8 VDC and 2.0 VDC (Open voltage)”³⁵

³⁵ Official Journal of the European Union, 2006

The operative regulation for the sanding systems:

“For improving braking and traction performances, it is permissible to apply sand on the tracks. The allowed amount of sand per sanding device within 30s is

- for speeds of $V < 140$ km/h: 400 g + 100 g
- for speeds of $V \geq 140$ km/h: 650 g + 150 g

The number of active sanding devices shall not exceed the following:

- For multiple units with distributed sanding devices: first and last car and intermediate cars with a minimum of 7 intermediate axles, between two sanding devices that are not sanded. It is permissible to couple such multiple units and to operate all sanding devices at the coupled ends.
- For loco-hauled trains
- For emergency and full service braking: all available sanding devices
- In all other cases: a maximum of 4 sanding devices per rail³⁶

The tested sand amounts in the experiments (see Chapter 5) are based on the values in the regulation. However, it has to be noted that for the experiments the effective sand amount has been used. According to empirical observations only 50 % of the actual outputted sand gets into the contact area between the wheel and the rail. The other half of the sand does not get into the contact area among others because of crosswind or turbulence by the moving rolling stock.

A modern speed-dependent sanding system is able to output a permanent amount of sand for the whole velocity field.

3.5.2 Properties of sand

There are some specified and standardized parameters of the sand which has to be fulfilled by the manufacturer of the sand and the operator of the rolling stock in order to maintain the optimal and permanent operating condition of the sanding systems. These main parameters are:

- Grain size
- Composition
- Physical properties
- Flow property

³⁶ Official Journal of the European Union, 2006

Figure 3.4 shows some commonly used sand types with different grain size and composition.



Figure 3.4: Different types of sand

For the experiments two types of sand were used. Both sand types consist of quartz and differ in terms of grain size only. Table 4 lists the main properties of the investigated sand types.

Sand type	Fine (0.1 - 0.4 mm)	Coarse (1.4 - 2.2 mm)
Chemical composition	SiO ₂ (> 96 %)	
Crude grain density	2.65 t/m ³	
Hardness	7 Mohs	
Residual moisture content	< 0.2 %	

Table 4: Sand properties

The coarse grain size roughly represents the upper limit of what is currently used as grit in railway vehicles.

3.6 DRAWBACKS OF SANDING

3.6.1 Isolation

One of the most crucial disadvantage of sanding is a safety related issue. The rail signalling safety systems use electric currents in the track to locate trains. In case of a malfunction of the sanding system the detection signals can be blocked by an excessive sand output which creates an electrically insulating layer between the wheel and the rail.

3.6.2 Increased wear

Because of the increased adhesion, the wheel and the rail are exposed to an increased wear. Furthermore, small sand grains can get between the crushed stone under the rail and it can lead to loosening of the track ballast.

3.6.3 Need for maintenance

On the one hand, sanding causes residual damages on the wheel surface. On the other hand, it prevents the formation of wheel flats, so ultimately sanding can even help to extend the time period for overhauling/changing the wheel unit.

However, the sanding system has some maintenance needs. The sanding device has to work properly and the sand needs to be kept dry and clean, otherwise it can stuck in the sandbox. The sand level has to be checked regularly as well.

3.6.4 Environmental impact

The application of sand by trams results in dirt in the cities. Special cleaning vehicles are needed to remove the residues of the mixture of sand and contaminants.

A more severe problem of sanding is the formation of fine airborne particles which has a very harmful effect on the human health. This kind of pollution is called PM₁₀, which stands for the polluting particles which has an aerodynamic diameter smaller than 10 µm. PM₁₀ is considered as the most important air pollutant worldwide. Contrary to other air contaminants like CO₂ or NO_x which are pure substances, PM₁₀ is a mixture of particles of different size and composition.³⁷

³⁷ Nesaratnam & Taherzadeh, 2014, p. 64

PM₁₀ originates from a wide variety of sources. According to a research in Switzerland (between 2003 and 2004), the railway industry is responsible for 11 % of the particulate emission. The amount and proportion of the yearly PM₁₀ emission caused by different sources by the railway industry in Austria is presented in Table 5.³⁸

Source	[t]	[%]
Brakes	936	58.1
Rails	474.5	29.4
Wheels	108	6.7
Pantographs	0.5	0
Overhead lines	13	0.8
Grit material	80	5
Total amount	1612	100

Table 5: Yearly PM₁₀ emission of the ÖBB³⁹

³⁸ Schamberger, 2012, p. 34

³⁹ Schamberger, 2012, p. 38

4 TESTING FACILITY AT KNORR-BREMSE AUSTRIA

4.1 CONSTRUCTION

All the experiments described in this thesis were conducted with the wheel-rail test rig of Knorr-Bremse Austria. The arrangement of the test rig consists of a rail unit with rack and pinion drive and a vertically adjustable wheel unit, see Figure 4.1 and Figure 4.2. Wheel and rail have its own electric drive, which allows them to be moved independently of each other. In this way arbitrary slip parameters are possible to set.

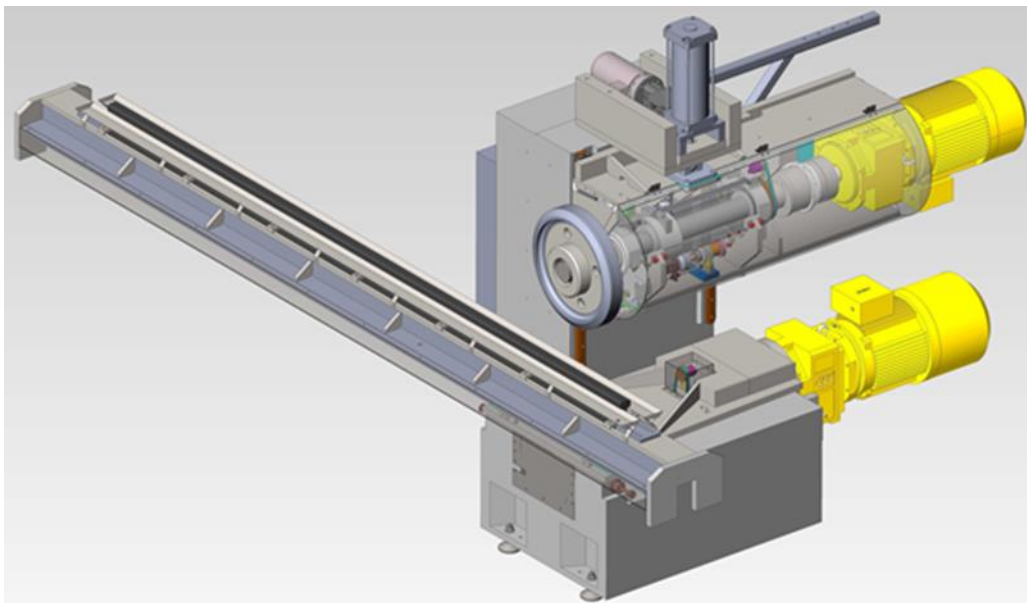


Figure 4.1: CAD-model of the test rig⁴⁰

Basic parameters of the test rig:

- Rail type: S49
- Usable rail length: 3290 mm
- Wheel type: cylindrical (without flange)
- Wheel diameter: 624 mm
- Max. wheel load: 40 kN

Furthermore, the test rig contains following auxiliary equipment which are used for conditioning and cleaning purposes: fluid pump, vibrating conveyor and high pressure nozzles.

⁴⁰ Knorr-Bremse GmbH



Figure 4.2: Photo of the test rig⁴¹

4.2 MEASURING DEVICES, SENSORS, SOFTWARE

The test rig is equipped with several sensors in order to be able to measure the required variables. Following devices are mounted on the test rig and used during the measurements:

- Rotary encoders
- Torque sensor
- Conductivity sensor

The encoders are needed to calculate the velocity of the rail and the angular velocity of the wheel. The torque sensor is used to obtain the adhesion coefficient between the rail and the wheel. Further details and the calculated variables from the measured values are outlined in Chapter 4.3.3. The measurement signals are processed by two QuantumX amplifiers and forwarded over an Ethernet port to a PC.

Various software are used to process the measurement data. First, catmanAP is utilized to record and save the predefined variables into an .xlsb (Excel Binary Workbook Format) file. Next, the files are imported into MATLAB and using various scripts they can be processed and evaluated in many different ways depending on the objectives of the current experiment. In this step the raw data are filtered, stacked and used to calculate the desired variables. Finally, with MATLAB, MS Excel or other tools plots can be created in order to visualize the results.

Figure 4.3 shows the sequence of the data acquisition and processing. For more detail about the evaluation of the results for a specific experiment, see Chapter 5.4.

⁴¹ Knorr-Bremse GmbH

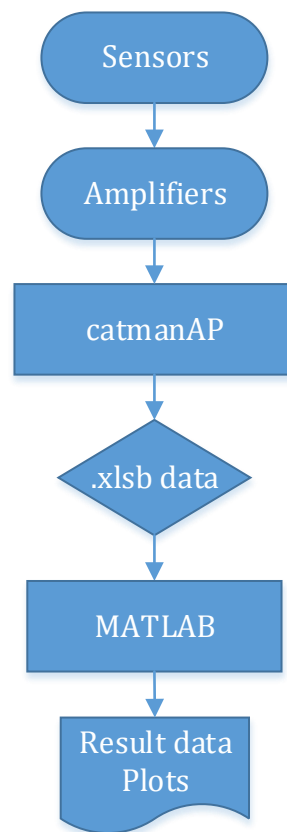


Figure 4.3: Data acquisition and processing

4.3 INPUT-, OUTPUT PARAMETERS

4.3.1 Amount of sand

For an automatic spreading of the sand a Retsch DR100 (see Figure 4.4) vibrating conveyor is used. The adjustable delivery rate of this unit allows to deploy the desired sand amount accurately. However, the set value on the vibrating conveyor does not directly stands for the amount of outputted sand. The actual feed rate has to be measured prior to experiments as it is strongly influenced by many parameters, like the operating temperature, fill level and even the y-position of the conveyor.

Previous field tests have shown that in reality only 50 % of the ejected sand gets into the contact area between the wheel and rail.⁴² Therefore, all the set values at the test rig correspond to the half of the amount which is used in railway vehicles.

For simplicity reasons the unit of measurement for the sand amount is [g/m].

⁴² Knorr-Bremse GmbH

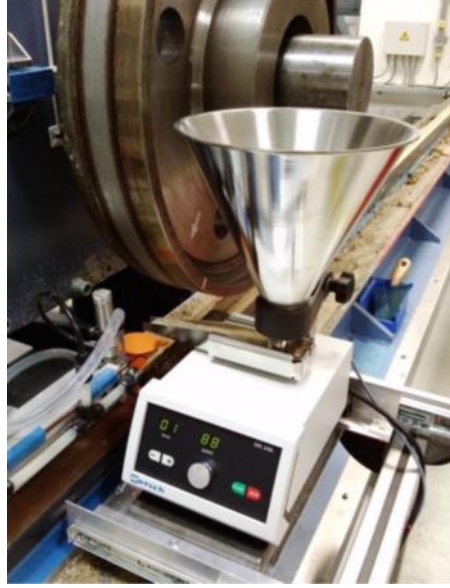


Figure 4.4: Spreading of the sand with the vibrating conveyor

4.3.2 Slip

The slip value on the test rig (s_t) can be adjusted as the speed ratio of the wheel and the rail.

$$\varphi = \frac{v_{wheel}}{v_{rail}} = \frac{r \cdot \omega_{wheel}}{v_{rail}} \quad (5)$$

$$s_t = 1 - \varphi \quad (6)$$

The speed of the rail is considered as master, if the φ ratio is bigger or smaller than one, traction or brake slip can be defined respectively.

The slip value in the evaluation of the results (s) however is referred according to Kalker's definition, which is a more widespread formula within the railway industry:

$$s = 2 \cdot \frac{v_{rail} - r \cdot \omega_{wheel}}{v_{rail} + r \cdot \omega_{wheel}} \quad (7)$$

Because the deviation between the two definitions in the range of the investigated slip values is very small, in the denomination of the slip values in the experiments, the following simplification was used:

$$s_t \approx s \quad (8)$$

4.3.3 Test rig output variables

Using the sensors which were presented in Chapter 4.2, several variables can be recorded and used during the evaluation. The following values are saved during the experiments:

- speed of the rail → needed for slip calculation
- speed of the wheel → needed for slip calculation
- torque on the wheel → longitudinal tangential force is calculated; needed for coefficient of adhesion
- electrical resistance between wheel and rail → needed for isolation

5 EXPERIMENTS

5.1 GOAL OF THE EXPERIMENTS

The aim of the series of experiments is to simulate the adhesion and isolation behaviour of an entire railway vehicle on the wheel-rail test rig of Knorr-Bremse Austria.

Using the test rig with different amount of sand and target slip values various surface characteristics can be investigated over multiple axles. Goal of the experiment is to perform a parameter study for all combination of the defined input variables. In the end, the correlation between these parameters is searched.

The experiment results are needed for the research and development of new generation sanding systems and for the optimization of the sanding strategy for current devices in operation.

5.2 GENERAL WORKFLOW

5.2.1 Multi-axle measurements

The goal of the multi-axle measurements is to simulate several consecutive axles of a railway vehicle. It is done by repeatedly rolling over the same rail section. Within the series of experiments always 20 axles were measured. Limitations during this experiment procedure:

- The first simulated axle corresponds to the first turn of the wheel on the freshly conditioned rail. During the subsequent axles however, the surface of both the wheel and rail already contains sand debris from previous overrollings. This kind of sand summation effect will not be considered. During the evaluation special attention should be paid to the first axle.
- The speed of the overrollings is low (1 m/s). Therefore, it comes on the test rig barely to turbulence or wind effects that could result in a reduction of the remaining amount of sand for the subsequent axles.

5.2.2 Repetition runs

Every measurement with the same settings (slip and amount of sand) was carried out four times. It is needed to ensure the required precision of the whole experiment.

5.2.3 Conditioning with Socolub

Socolub is a liquid, water-soluble lubricant, which is used to lowering the friction. It behaves similar to liquid soap and causes low adhesion coefficient of about 0.05 to 0.07. The low friction on the test rig simulates a slippery track and is used as a basis for the adhesion increasing effect of the sand. During the experiments an aqueous solution with a mass concentration of 4 % was used. A submersible pump was used to spill the solution on the rail. The fluid flow was regulated to 0.5 l/min.

5.2.4 Reference run

Reference runs are needed to determine the adhesion increasing effect of the sand. For the reference run the above described Socolub solution is used. During an overrolling the lubricant is pressed and stuck in the surface of the wheel and rail. Multiple overrollings are needed to achieve the desired low coefficient of adhesion (~0.08). However, during an overrolling with sand, this lubricant layer will be removed. In order to achieve a reproducible experiment, a measurable initial condition is needed. It can be achieved with conditioning runs between every experiment.

However, it is a difficult process to achieve a reproducible and reliable reference condition prior to measurement. The main problem is that both the reference runs and the experiments with sand change the surface condition. Generally, overrollings with Socolub decrease, overrollings with sand increase the adhesion coefficient for the subsequent overrolling, see Figure 5.1. Higher slip and higher amount of sand has a stronger effect on changing the surface condition.

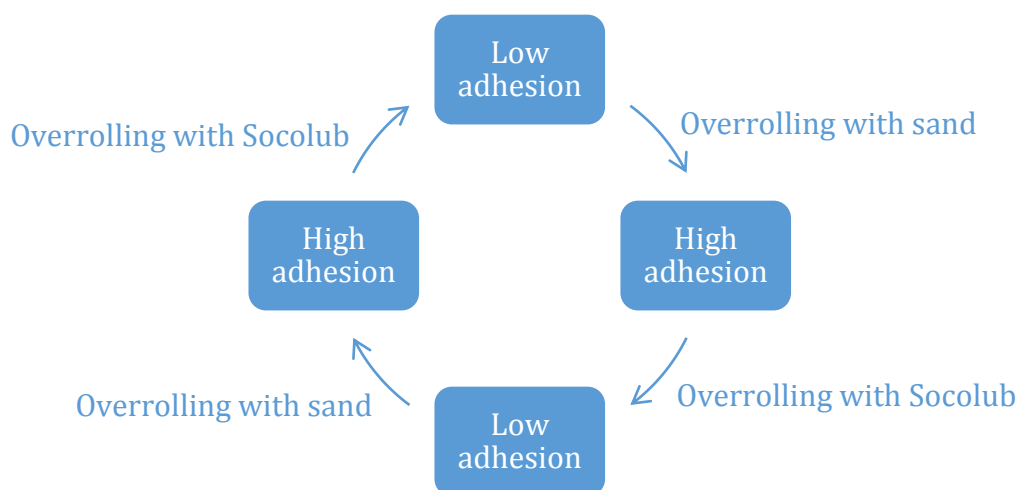


Figure 5.1: Effect of sand and Socolub on the surface condition (adhesion coefficient)

This issue arose during the execution of the experiments. Therefore the reference condition was achieved different ways:

- 0 % slip: no reference run needed (only test runs were made between the experiments).
- 2 % slip: one reference run with 20 axles was made before the experiments. Before every measurement, reference checks were made in order to verify the reference condition.
- 5 % and 10 % slip: before every single measurement a reference run was made with 5 axles. It allowed to compare the results of the measurements with the actual surface condition. Based on experience, it is enough to measure 5 axles as a reference, see Figure 5.2. After the 5th axle the further decrease of the adhesion coefficient is not significant. The reference value is simplified as a constant between the 5th and 20th axle.

The reason for changing the method is that it did not perform well with higher slip values. In order to ensure the plausibility of the experiment, the reference for the 2 % slip was evaluated the same way as for the 5 % and 10 %.

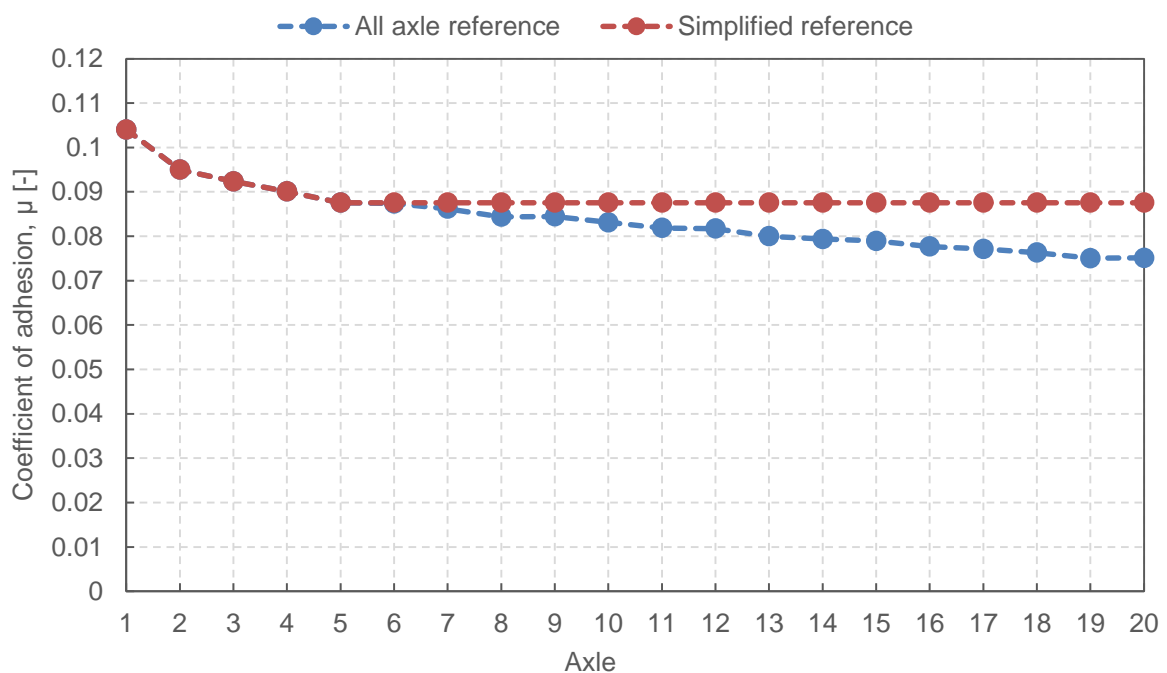


Figure 5.2: Simplified reference run

5.2.5 Sequence of actions

The experiments with all the necessary auxiliary activities were performed in the following sequence:

- 1 Test rig initialization
- 2 Measurement software zero point calibration
- 3 Reference check with Socolub: usually multiple overrollings are needed in order to lower the coefficient of adhesion
- 4 Reference run
- 5 Setting the amount of sand at the vibrating conveyor
- 6 Starting the measurement software
- 7 **Experiment** (21 “back and forth” movement of the rail in total)
 - a. 1st movement: Conditioning with lubricant and sand without wheel load, see Figure 5.3
 - b. 20 overrollings without further sand and lubricant output
- 8 Stopping the measurement software and saving the data
- 9 Cleaning the wheel and the rail

} Only after switching-on the test rig



Figure 5.3: Conditioning with lubricant and sand without wheel load⁴³

⁴³ Knorr-Bremse GmbH

5.3 PARAMETERS FOR THE EXPERIMENTS

5.3.1 Sand

For the main part of the series of experiments the fine sand was used. With the coarse sand, only the 0 % slip was investigated (for isolation issues). For the properties of the sand qualities, see Chapter 3.5.2.

Four different sand amounts were tested: 0.5 g/m, 1 g/m, 2 g/m and 4 g/m. These amounts are visualized for the fine sand on Figure 5.4.



Figure 5.4: 0.5 g; 1 g; 2 g; 4 g fine sand

In addition, previous studies have shown that not all of the, by the vibrating conveyor applied sand gets into the contact area during the overrolling. Some of the sand falls off the rail or remains lying on the side of the rail head, where it does not come into contact with the wheel. Therefore an increased sand amount by 10 % was used.⁴⁴ The sand amounts indicated in this thesis denote a target value, assuming it is the actually amount which gets into the wheel-rail contact. Figure 5.5 shows the dispersion density of the fine sand for all four tested sand amounts.

⁴⁴ Knorr-Bremse GmbH

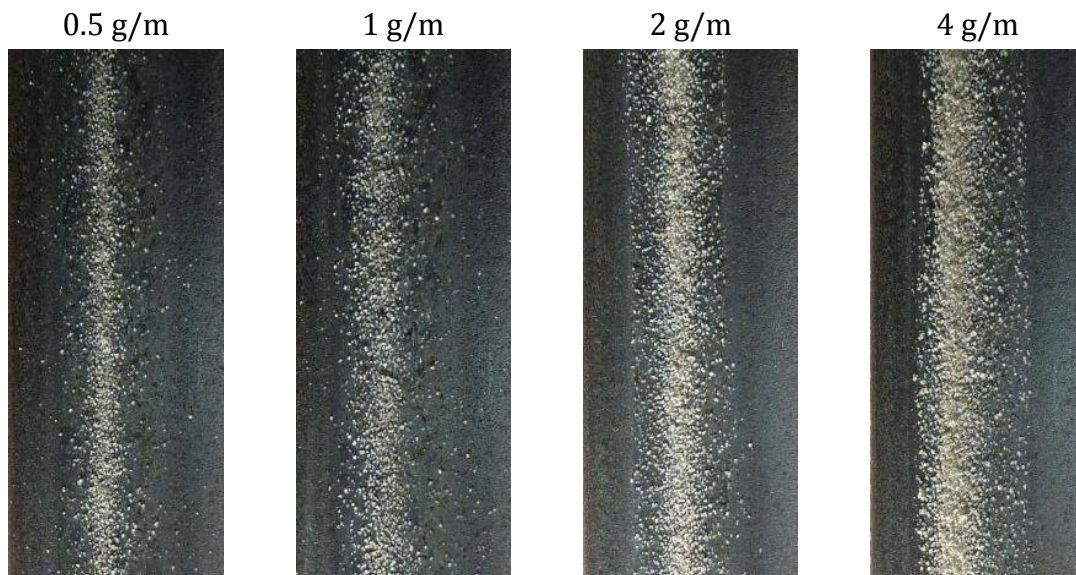


Figure 5.5: Overview of the dispersion density of the fine sand depending on the amount of sand⁴⁵

5.3.2 Slip

The experiments with the fine sand were carried out with four different slip values: 0 %, 2 %, 5 %, 10 %. The experiments with the coarse sand were carried out only with 0 % slip. All the used slip settings are corresponding to brake slip.

It should be noted that the actual slip value is not constant during an overrolling. It differs under some conditions considerably from the target value. Reasons are, for example, vibrations in the driveline and the limits of the controller accuracy under highly dynamic load cases. Therefore it is necessary to create intervals around the target slip value. The width of these intervals can be defined after examining the dispersion of the actual slip values of the measurements.

For the evaluation of the results the following intervals of slip values were used:

Target value	2 %	5 %	10 %
Interval for the measured values	1-3 %	4-6 %	9-12 %

Table 6: Slip intervals for the evaluation

⁴⁵ Knorr-Bremse GmbH

5.3.3 Further parameters and overview

The following test rig related parameters were used during the experiments:

- Wheel load: 40 kN
- Speed of the rail: 1 m/s

Since the temperature and humidity affects the surface condition in terms of friction, they were measured every day and were varying in the following range:

- Room temperature: 19-25 °C
- Humidity: 29-32 %rH

Table 7 shows the summary of the input parameters.

Sand type	Fine (0.1 - 0.4 mm)	Coarse (1.4 - 2.2 mm)
Slip [%]	0 / 2 / 5 / 10	0
Adhesion reducer	Socolub	
Amount of sand [g/m]	0.5 / 1 / 2 / 4	
Axles	1 - 20	
Repetition	4	

Table 7: Summary of the input parameters

5.4 EVALUATION OF THE RESULTS

5.4.1 Introduction

The evaluation of the measurement results is a very important part of the experiments. Since the output of the measurement software is a huge amount of raw data, it has to be filtered and processed in a reasonable way in order to receive valuable results. In this chapter the whole evaluation process will be shown by an example.

5.4.2 Single overrollings

After starting to record the data, the measurement software is collecting all the predefined variables continuously. One single overrolling with all preliminary activities takes about 1 minute. For the evaluation however, only a few seconds of the

recording are needed when the real measurement happens. With a MATLAB script it is possible to automatically acquire the dataset of the actual overrolling. But this contains unusable information as well because of the need to start and stop the device. The controller needs some time to ramp up and ramp down the target value of the slip. Therefore the measured adhesion coefficient needs to be considered only in a specified section of the whole overrolling. Figure 5.6 shows the measured adhesion coefficient in the total length of the rail and a section between 600 mm and 2200 mm, where the data was chosen to cut out and use for the evaluation.

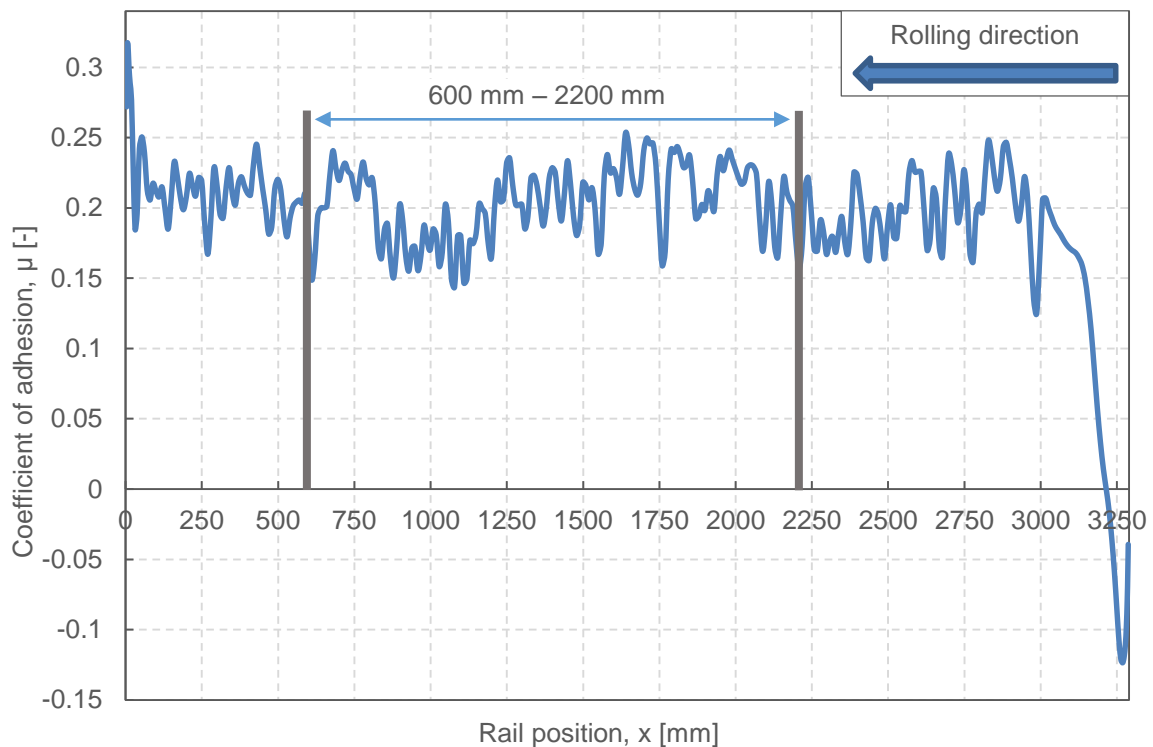


Figure 5.6: Adhesion coefficient over rail position

The above figure shows the result of the 10th axle with 2 g/m fine sand and 5 % slip. In this specific case the interval could have been wider, but there are some results with different settings where this is not possible. Therefore, the above defined interval was chosen to be the same for all measurement results.

5.4.3 Repetition runs

After all repetition measurements were made, the results were inspected manually to verify them. During the conducted series of experiment there were two cases, which needed some investigation. Because of the heavy air circulation around the test rig (which caused a remarkably sooner drying), two repetition runs were not used during the evaluation in the following cases:

- Run Nr. 4 with 1 g/m fine sand and 10 % slip
- Run Nr. 1 with 2 g/m fine sand and 10 % slip

After the check, the results were added together which can be seen on Figure 5.7 which depicts the adhesion coefficient in the function of the slip.

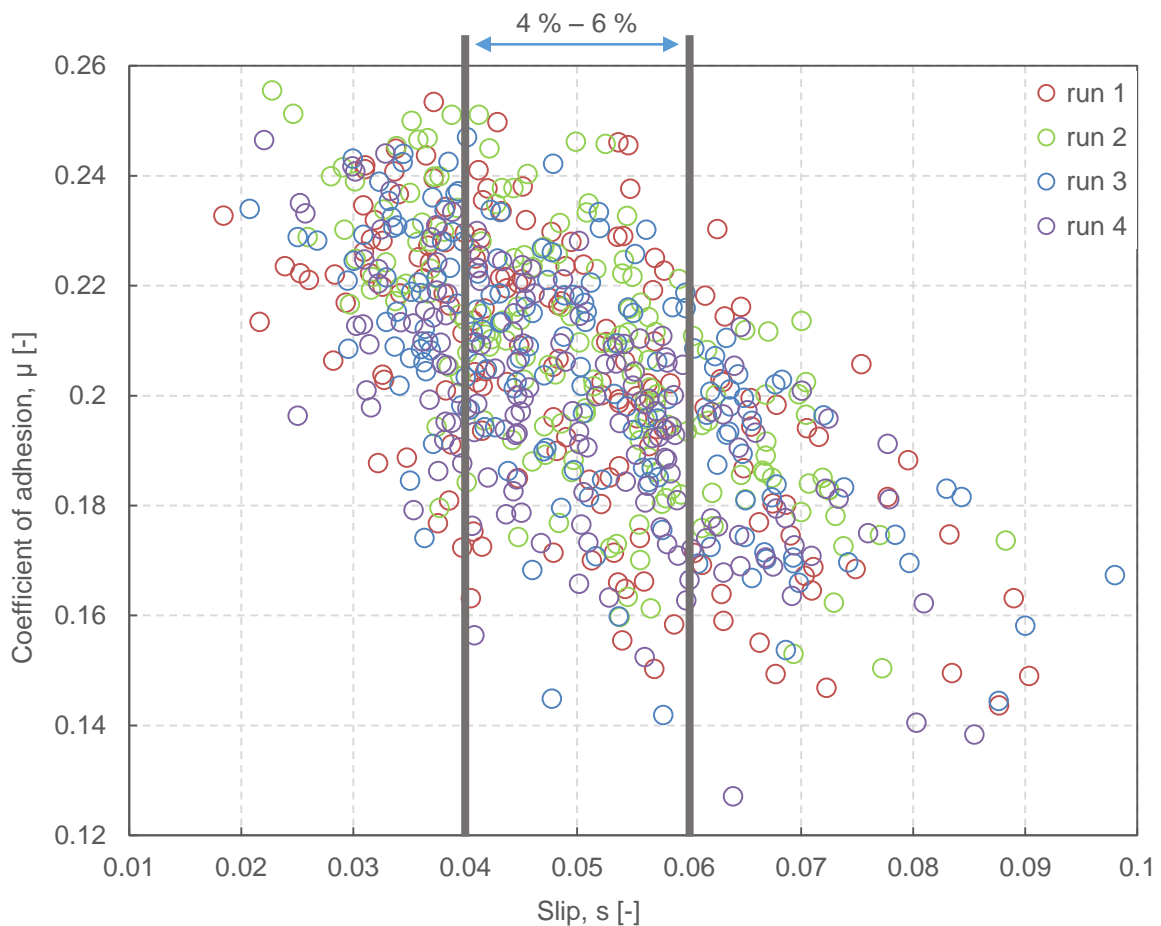


Figure 5.7: Combination of repetition runs and creation of slip interval

In this case all four measurements were used and the results are overlapping each other in a large extent. Though, despite the predefined 5 % slip setting, the real slip values are scattered in a wide range. The reason for this phenomenon is the test rig controller, which cannot keep the slip on the exact value. Therefore slip intervals are needed to define in order to ensure a true comparison of the results.

5.4.4 Multi-axle results

After completing the procedure described in Chapter 5.4.2 and Chapter 5.4.3 for all 20 axles of a measurement, the long lasting effect of the sand can be investigated. Figure 5.8 shows this trend for a specific slip and sand amount. The bars are meaning the range between the 10th and 90th percentiles, while the red markers are showing the arithmetic mean values.

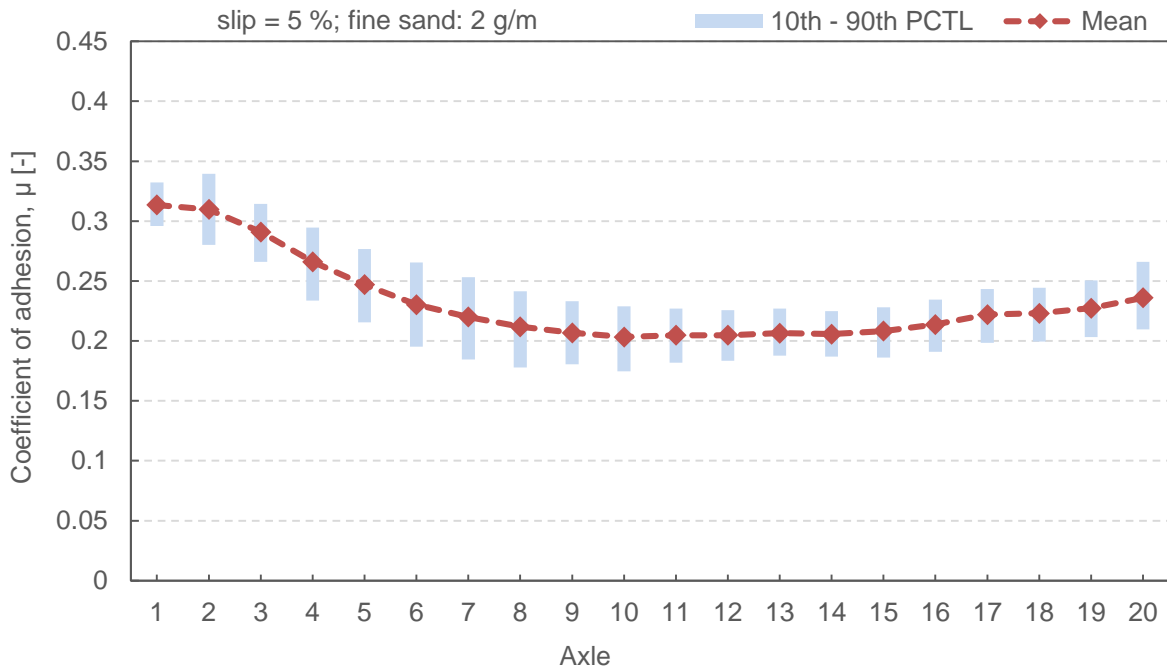


Figure 5.8: Mean values and dispersion of adhesion coefficient

Basically each bar represents the middle 80 % of the data between the interval borders on Figure 5.7.

For averaging the results, simply the arithmetic mean was used. Preliminary tests have shown that there is a negligible difference between other methods, like median, harmonic mean and geometric mean.

5.4.5 Adhesion curve

After finishing the experiments for all slip values and performing the above described evaluation process for each result, the adhesion curve can be created, see Figure 5.9. It shows the correlation between the slip and the adhesion coefficient which is the most desired result data of the experiments. Furthermore, the effect of the sand for subsequent axles can be extrapolated as well.

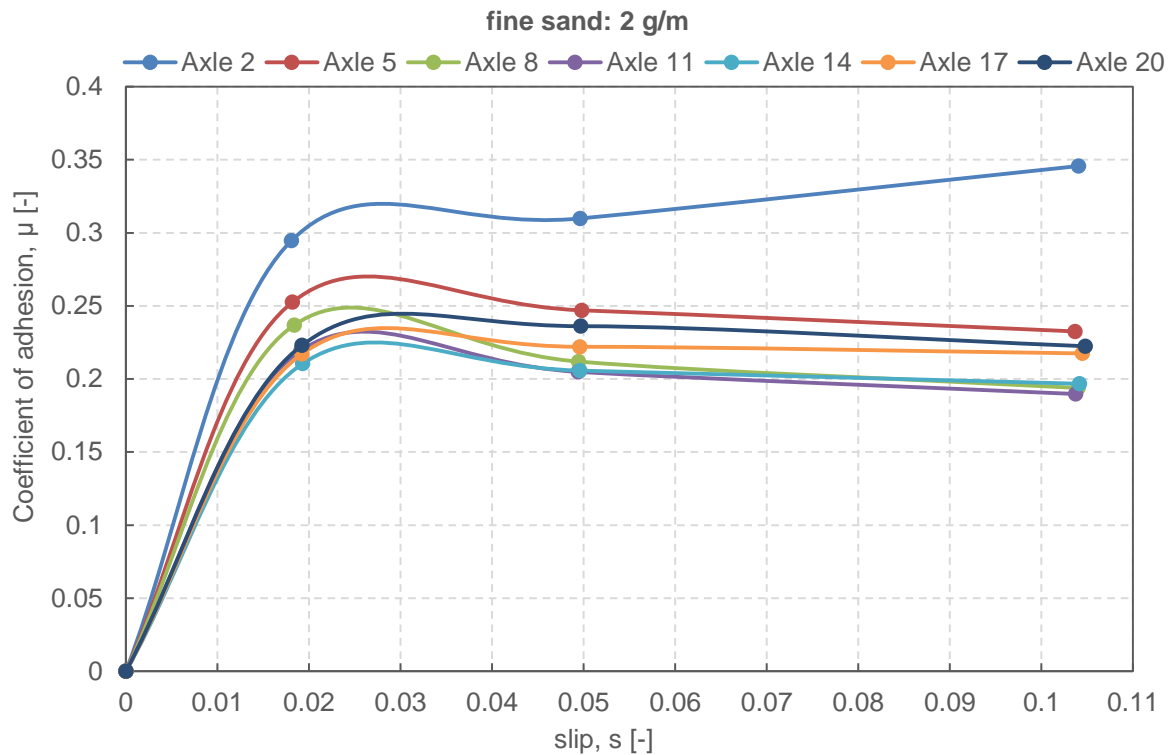


Figure 5.9: Adhesion curve

5.4.6 Reference and adhesion improvement

In order to investigate the effect of the sand on the adhesion improvement, the results of the reference measurement has to be subtracted. The parameters and limitations of the reference runs are outlined in Chapter 5.2.4. During the evaluation the mean reference value was subtracted from the corresponding measurement result, thus the difference is the adhesion improvement by the sand.

5.4.7 Isolation

The result of the electrical resistance is used for the determination of the isolated time period. Isolation was defined as present if the measured resistance exceeded a threshold value of 20 Ohm. In this case the isolated time amount of the single experiments was averaged for the repetition runs, thus a time proportion of isolation was calculated which was given as a number between 0 and 1.

5.5 PRELIMINARY EXPERIMENTS

5.5.1 Introduction

Prior to the series of experiments several test runs and preliminary experiments were performed. The goal of these trials was to reveal correlation between diverse phenomena and to test the new workflow.

5.5.2 20 % slip

From the practical point of view, experiments with 20 % slip would be very important. However, it is not possible because of the physical limits of the test rig. Two test runs were made with the following settings:

- Slip: 20 %
- Sand type: fine
- Amount of sand: 2 g/m

Figure 5.10 shows the dispersion of the slip in the function of time. It is clearly visible that the controller was not able to keep the slip in the proximity to the target value ($s = 22.2\%$). The actual slip suffered very high and rapid fluctuations.

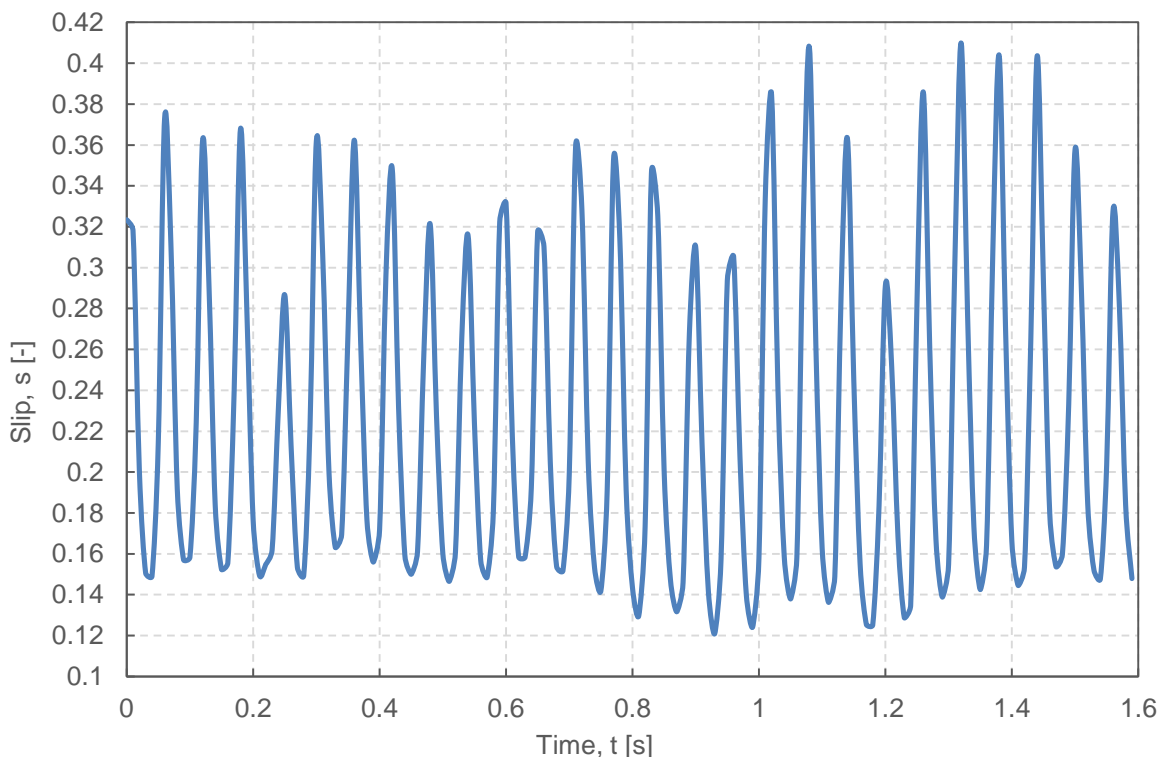


Figure 5.10: Slip fluctuation at 20 % target slip

The bigger problem with the 20 % slip is that the two performed overrollings caused serious damage to the rail. Figure 5.11 shows the 20-30 mm long strips which were caused by the stick-slip oscillation. The middle of these strips are corresponding to the peak slip values in Figure 5.10. Furthermore, these strips caused a long lasting damage of the surface structure, on Figure 5.12 the place of the strips are still visible after more than 500 overrollings.



Figure 5.11: Strips on the rail caused by the stick-slip oscillation

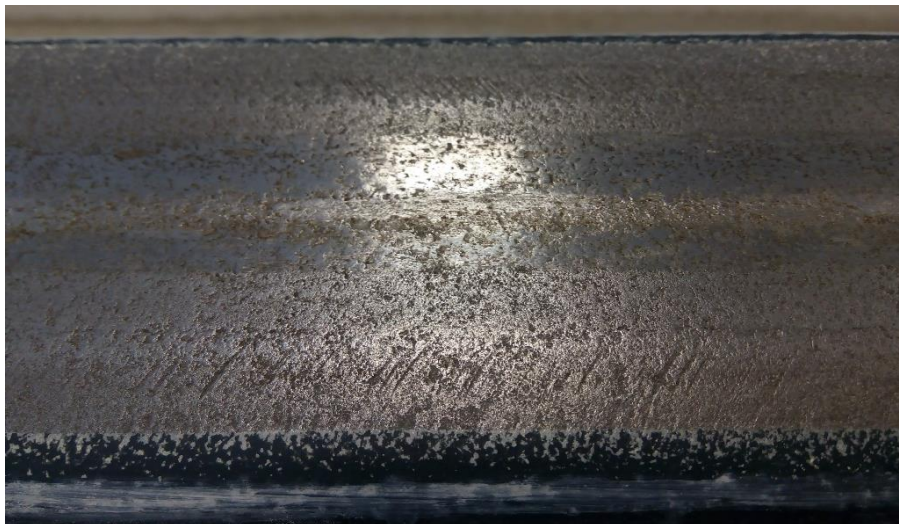


Figure 5.12: Long lasting effect of two overrollings with 20 % slip

5.5.3 Modification of the surface condition

5.5.3.1 General influence on the surface condition of sand and Socolub

As it was mentioned before, both the overrollings with Socolub and with sand are modifying the surface condition. Figure 5.13 and Figure 5.14 are showing this phenomenon caused by the sand and the Socolub respectively.

The circumstances and settings for the measurement on Figure 5.13:

- Initial situation: after 30 overrollings with Socolub
- Slip: 5 %
- Surface condition: Socolub + fine sand: 4 g/m
- Execution process: identical experiments were carried out four times successively (wiping the wheel and rail between them)

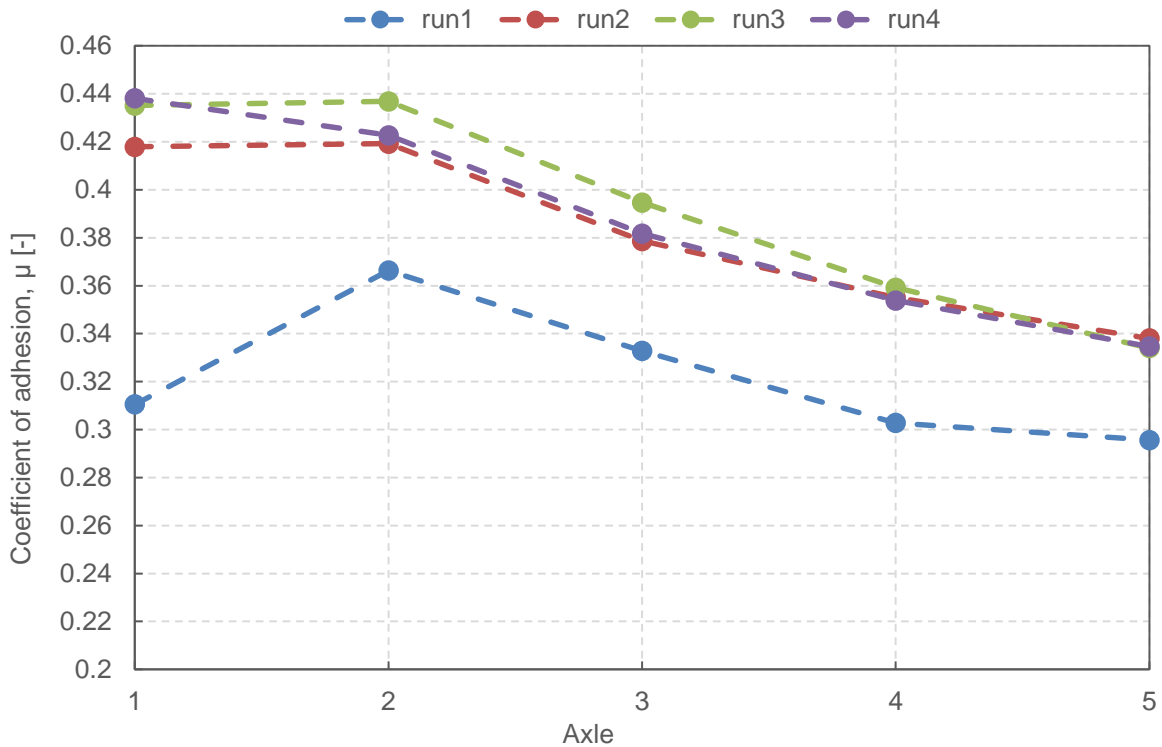


Figure 5.13: Modification of the surface condition caused by the sand

The results show that it is very important to include overrollings with Socolub between every experiment with sand in order to ensure an equal initial condition.

The circumstances and settings for the measurement on Figure 5.14:

- Initial situation: after approx. 100 overrollings with sand
- Slip: 5 %
- Surface condition: Socolub
- Execution process: identical experiments were carried out four times successively (wiping the wheel and rail between them)

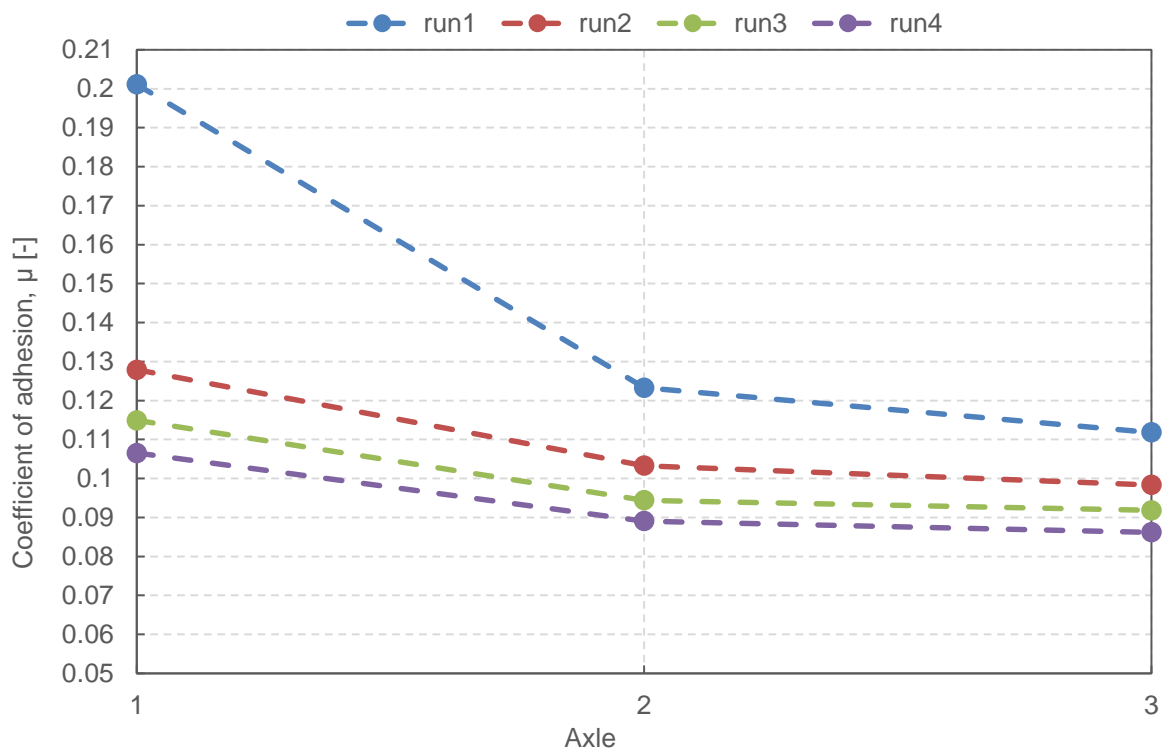


Figure 5.14: Modification of the surface condition caused by the Socolub

The results show the importance of reference-checks because after overrollings with sand the coefficient of adhesion is very high due to the removed Socolub layer.

5.5.3.2 Socolub increases the dry adhesion coefficient

Figure 5.15 shows the dry adhesion coefficient before and after Socolub was applied. Between the two experiments approx. 180 overrollings were performed with Socolub. It has increased the dry adhesion coefficient by 64 % in average.

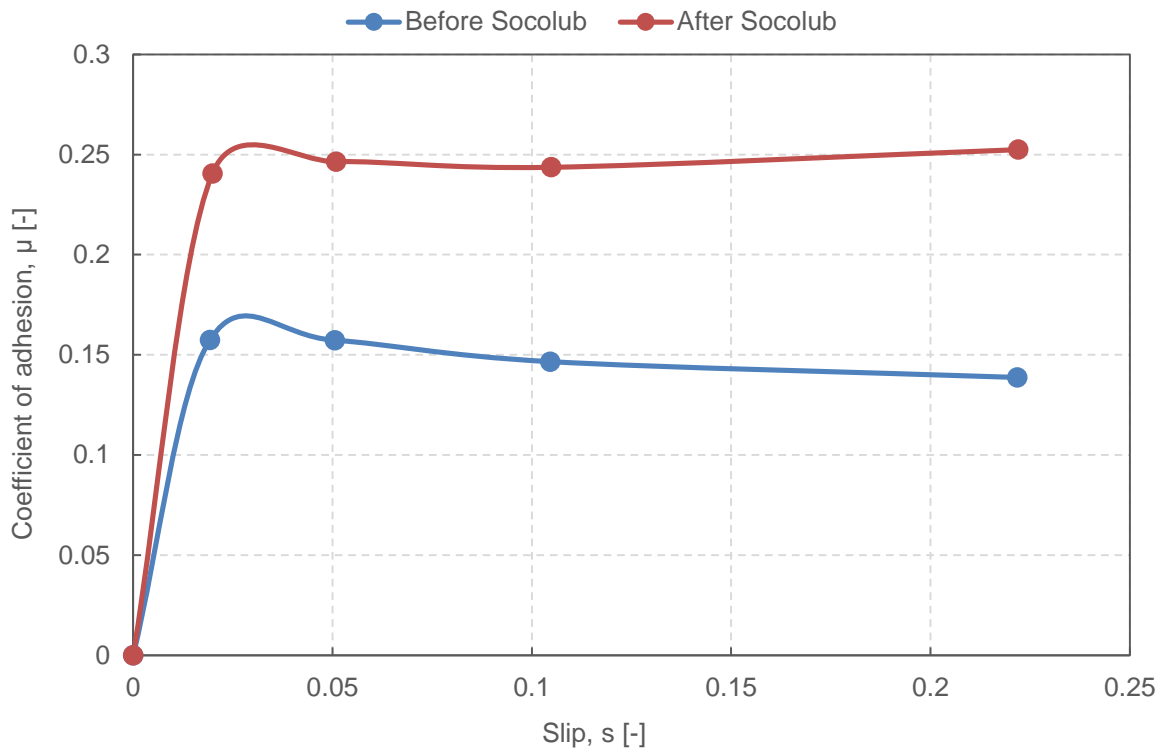


Figure 5.15: Difference in the dry adhesion coefficient before and after Socolub was applied

During overrollings with Socolub the changes in the surface topography causes an alteration in the adhesion coefficient. There are multiple reasons for this phenomenon. The modification in the surface topography is not exclusively a change in the asperities by the plastic deformation and wear debris of the steel. The dry Socolub creates a third body layer between the steel surfaces and acts as a friction modifier.

5.5.3.3 Oversaturation of Socolub

Although Socolub is used for reducing the coefficient of adhesion, it turned out that after some point it loses this property. It is slippery only in the presence of water. After too much overrollings with Socolub (without sand), the contact surfaces become dry faster. The coefficient of adhesion of the remaining sticky surfaces increases immediately, which can be seen in Figure 5.16.

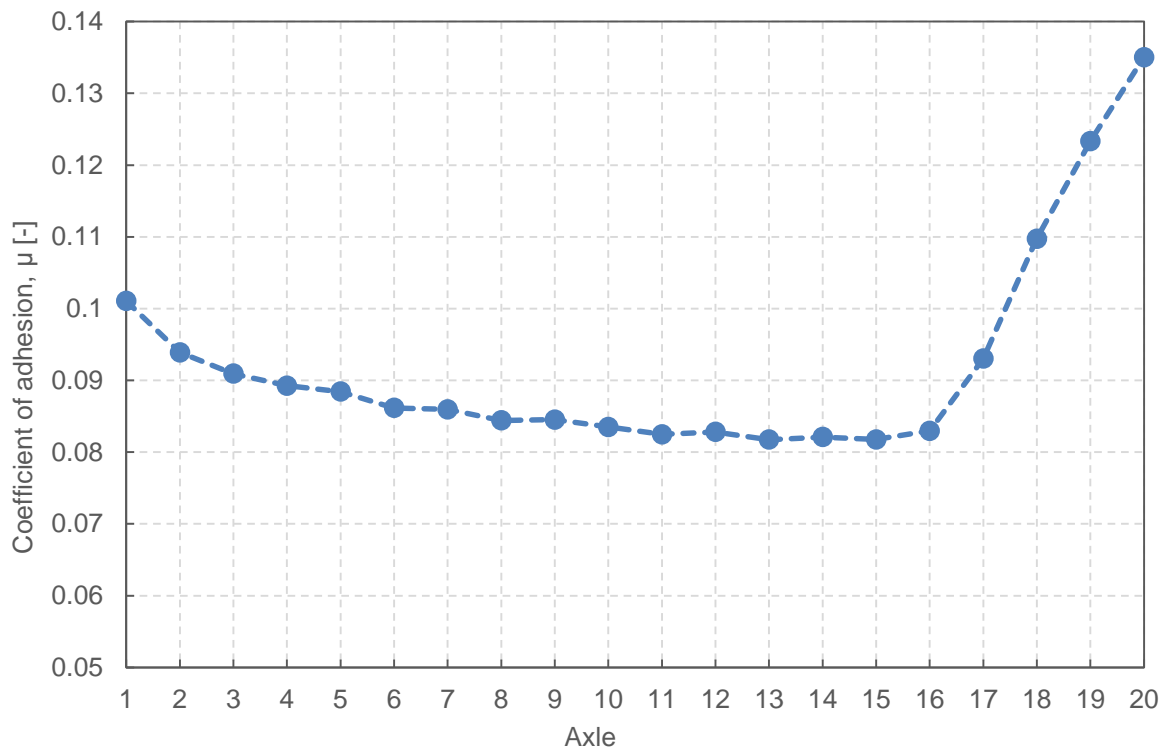


Figure 5.16: The increased coefficient of adhesion after drying up

This adverse phenomenon of Socolub becomes visible, which is shown in Figure 5.17. Socolub is pressed in the microscopic structure of the surface. If it happens, it hinders the liquid solution to stay in the microstructure. The Socolub creates a topcoat on the surface which leads to an earlier drying of the lubricant. The most effective way to remove the Socolub from the surface is to perform overrollings with sand. Figure 5.17 shows the efficiency of this method.

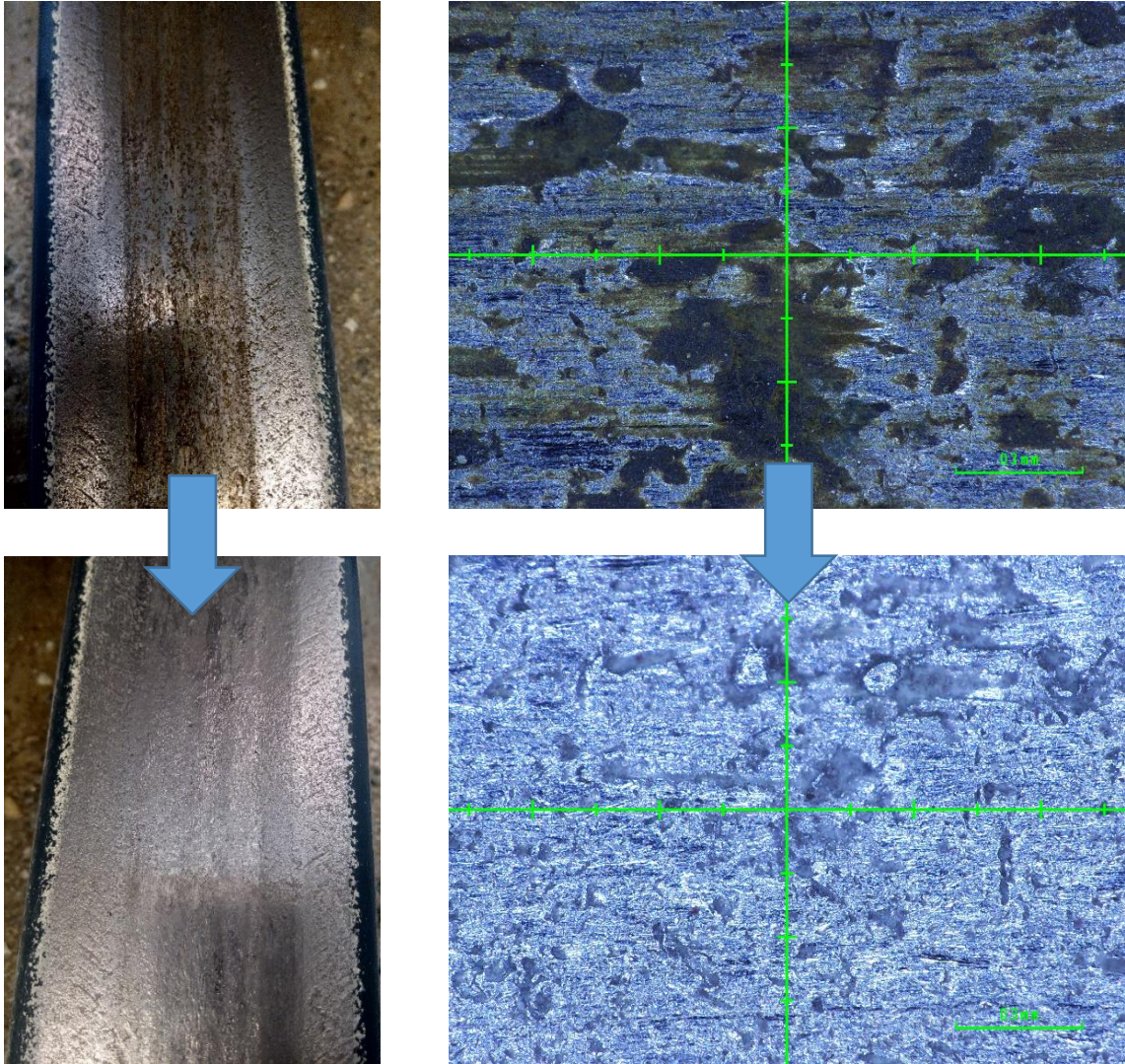


Figure 5.17: Socolub layer and the effect of the surface cleaning with sand

5.6 RESULTS OF THE EXPERIMENTS

5.6.1 Rail at the end of the experiments

Figure 5.18 shows the rail at the end of each experiment (after the 20th axle, one of the 4 repetition runs) with the fine sand.

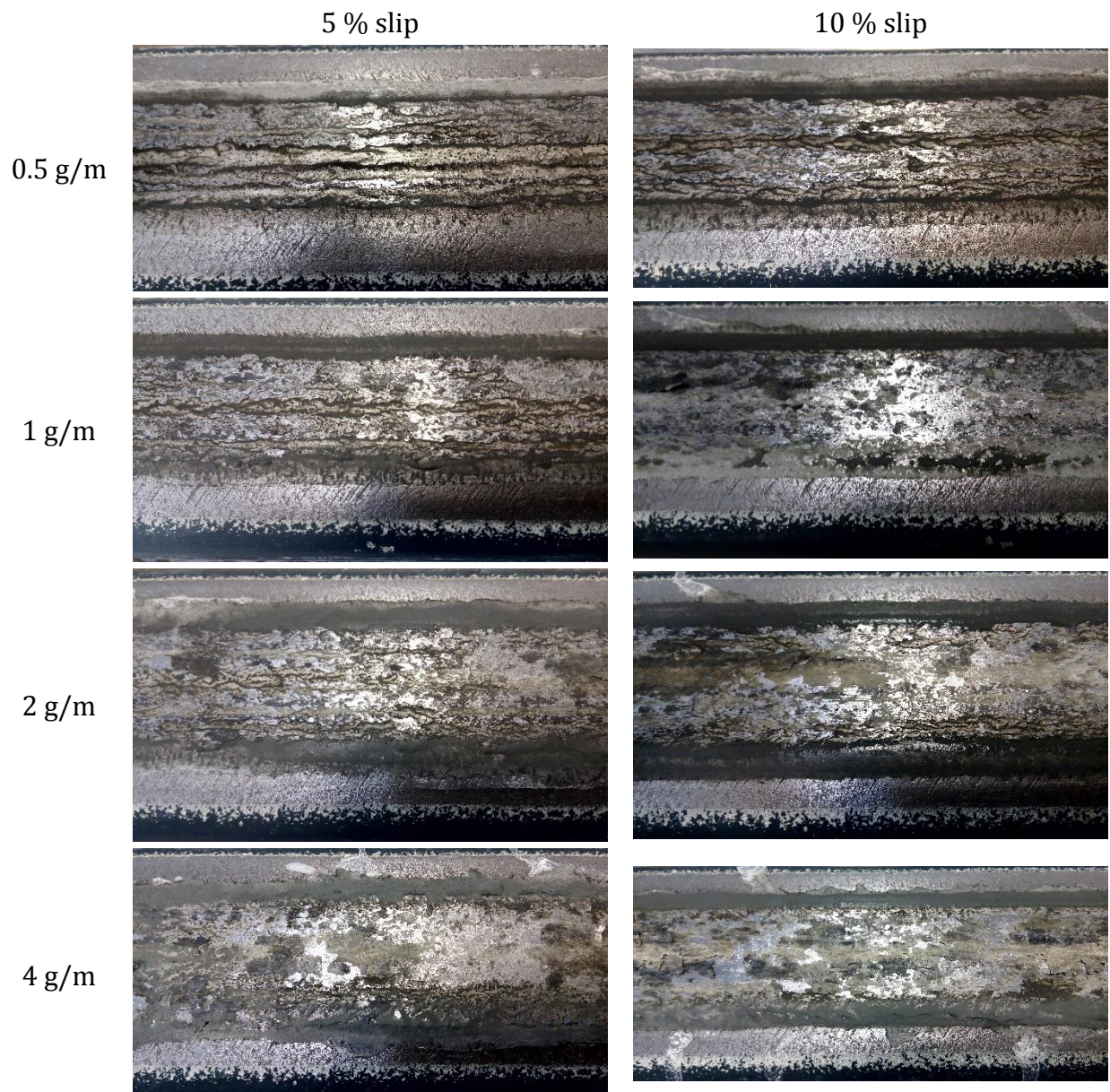


Figure 5.18: Photo of the rail at the end of the experiments

There is a clear correlation between the surface condition and the input parameter of slip and sand amount. At higher slip values and higher sand amounts the surface dries faster. This phenomenon causes higher amount and dispersion of the adhesion coefficient.

5.6.2 Comparison of the sand amount

The following figures show the comparison of the sand amount. The coefficient of adhesion and its increase (reference subtraction) is displayed for each slip value.

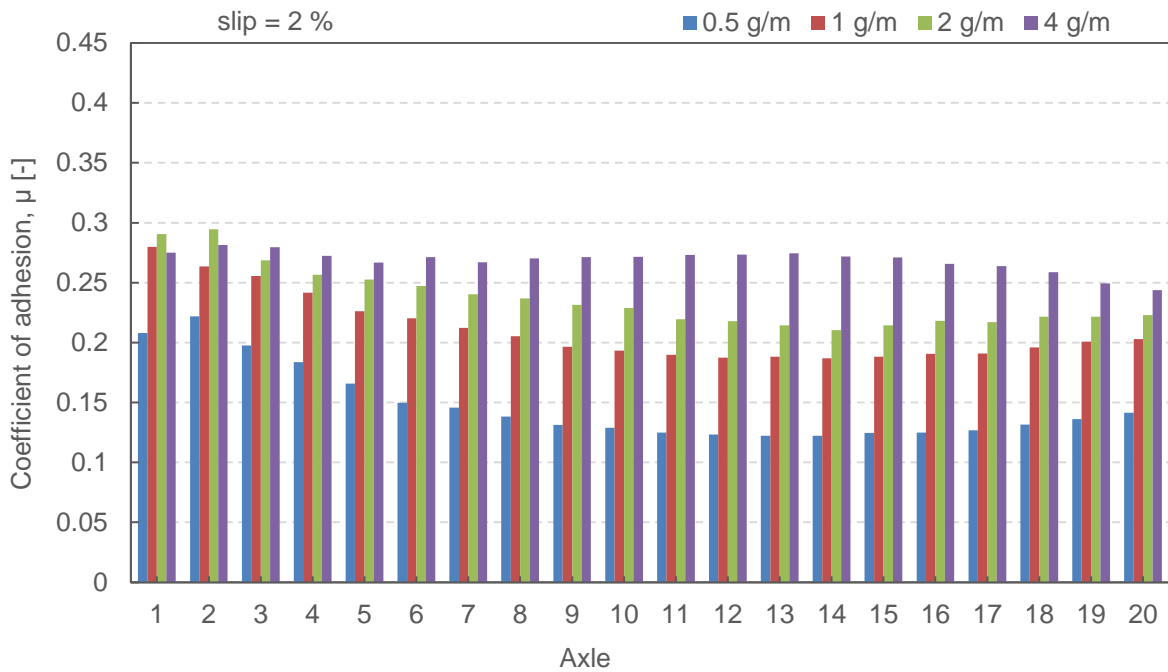


Figure 5.19: Coefficient of adhesion, comparison of the sand amount at 2 % slip

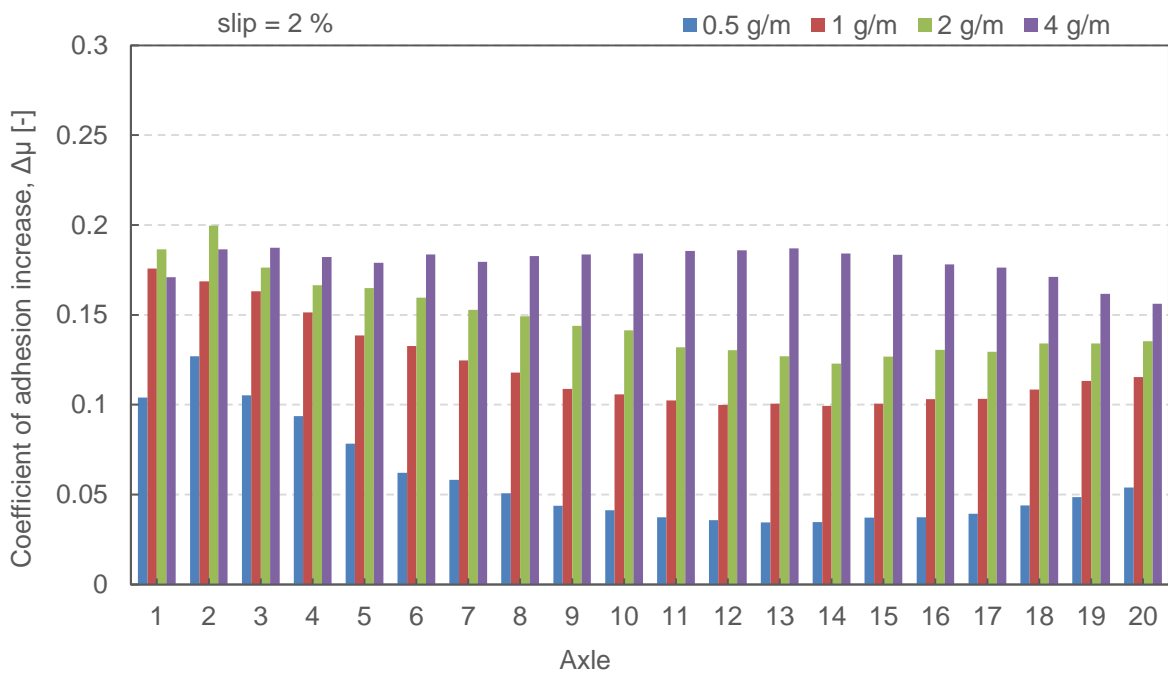


Figure 5.20: Coefficient of adhesion increase, comparison of the sand amount at 2 % slip

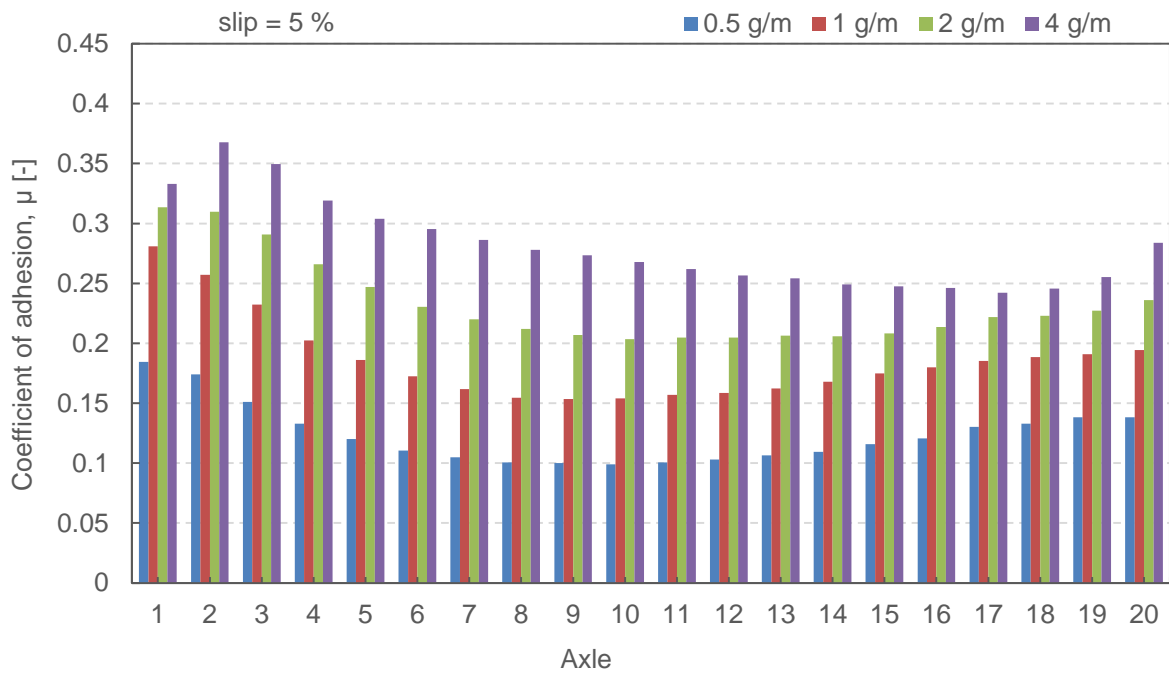


Figure 5.21: Coefficient of adhesion, comparison of the sand amount at 5 % slip

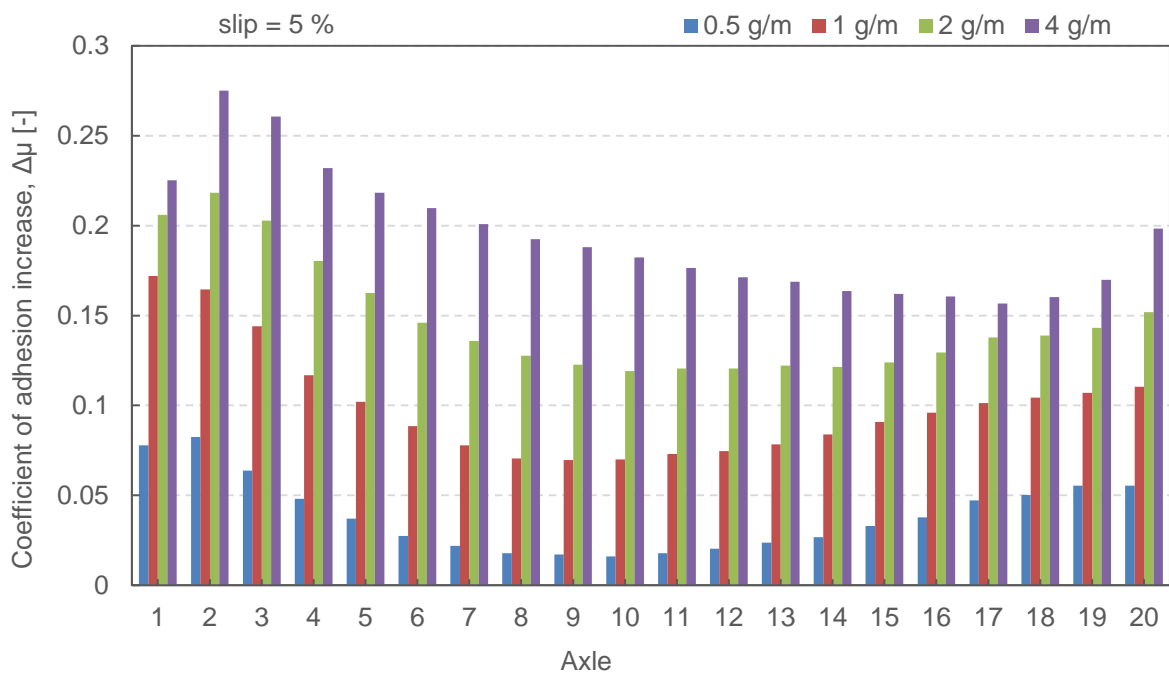


Figure 5.22: Coefficient of adhesion increase, comparison of the sand amount at 5 % slip

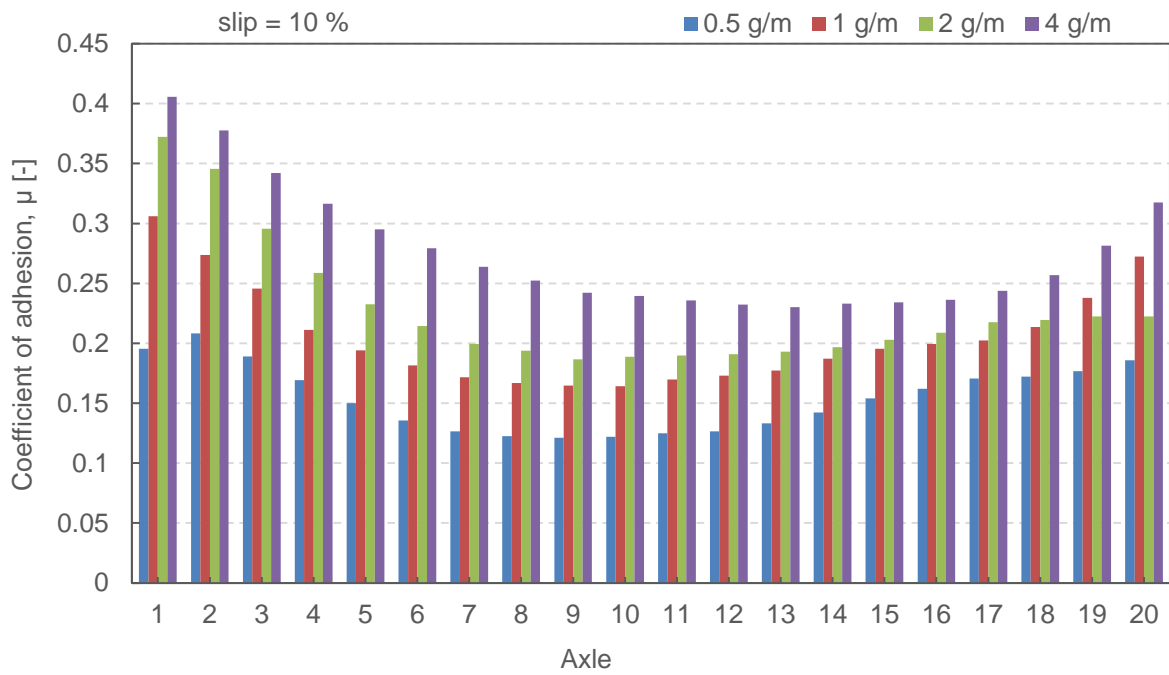


Figure 5.23: Coefficient of adhesion, comparison of the sand amount at 10 % slip

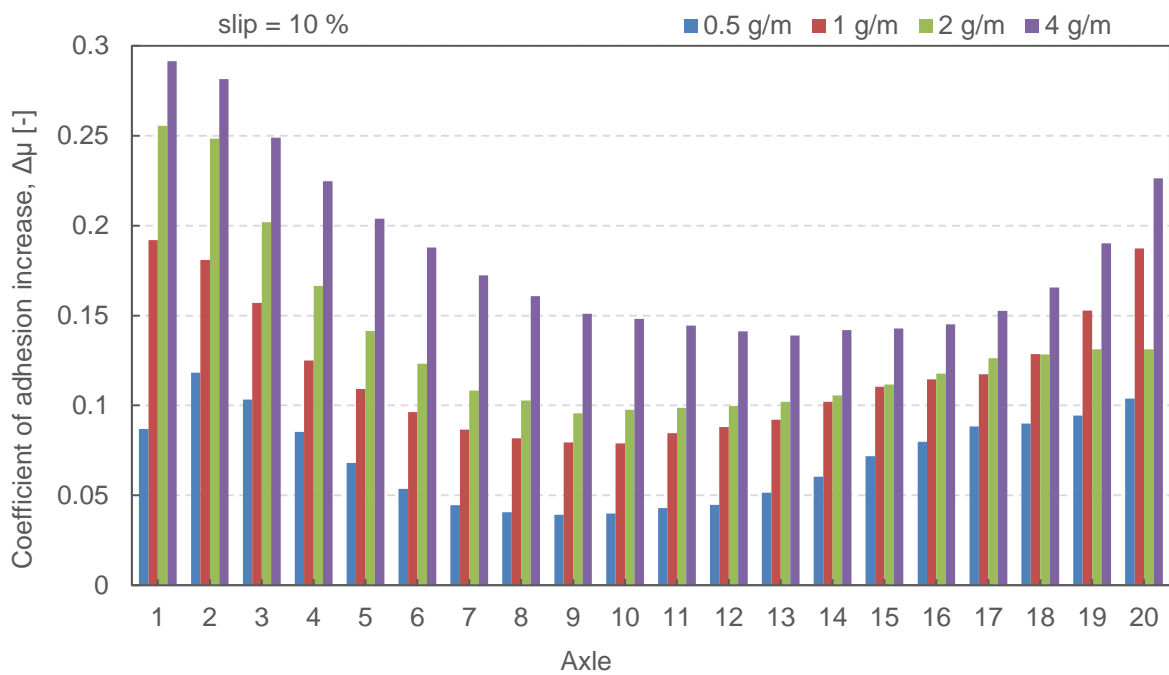


Figure 5.24: Coefficient of adhesion increase, comparison of the sand amount at 10 % slip

5.6.3 Comparison of the slip values

The following figures show the comparison of the slip values. The coefficient of adhesion is displayed for each sand amount.

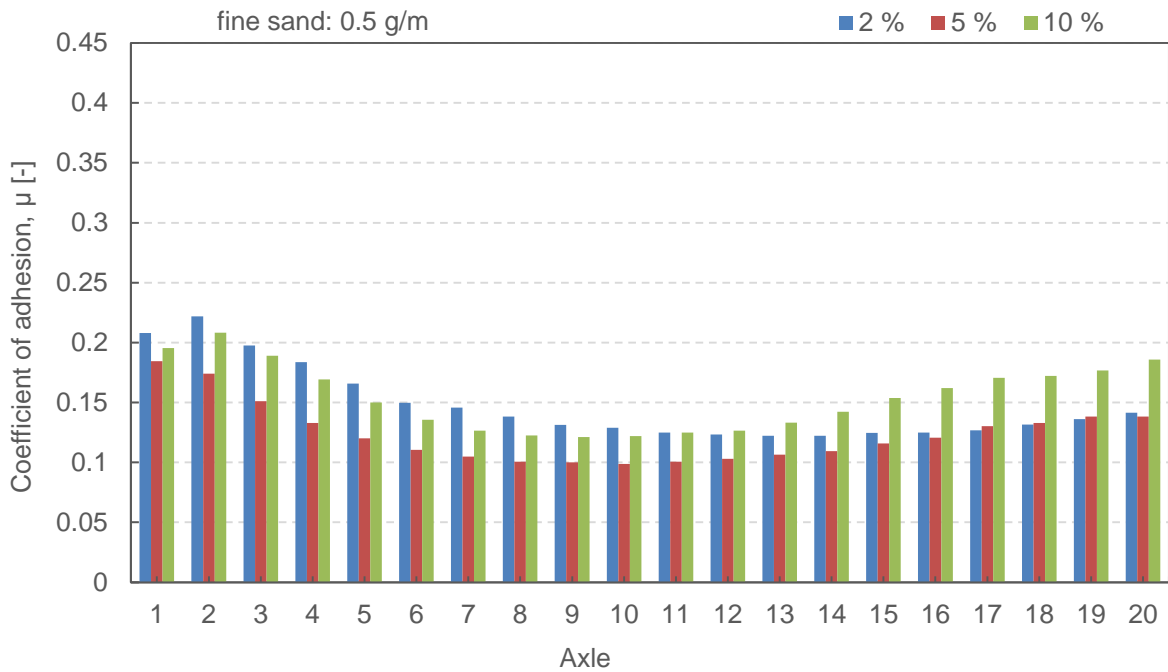


Figure 5.25: Coefficient of adhesion, comparison of the slip values at 0.5 g/m fine sand

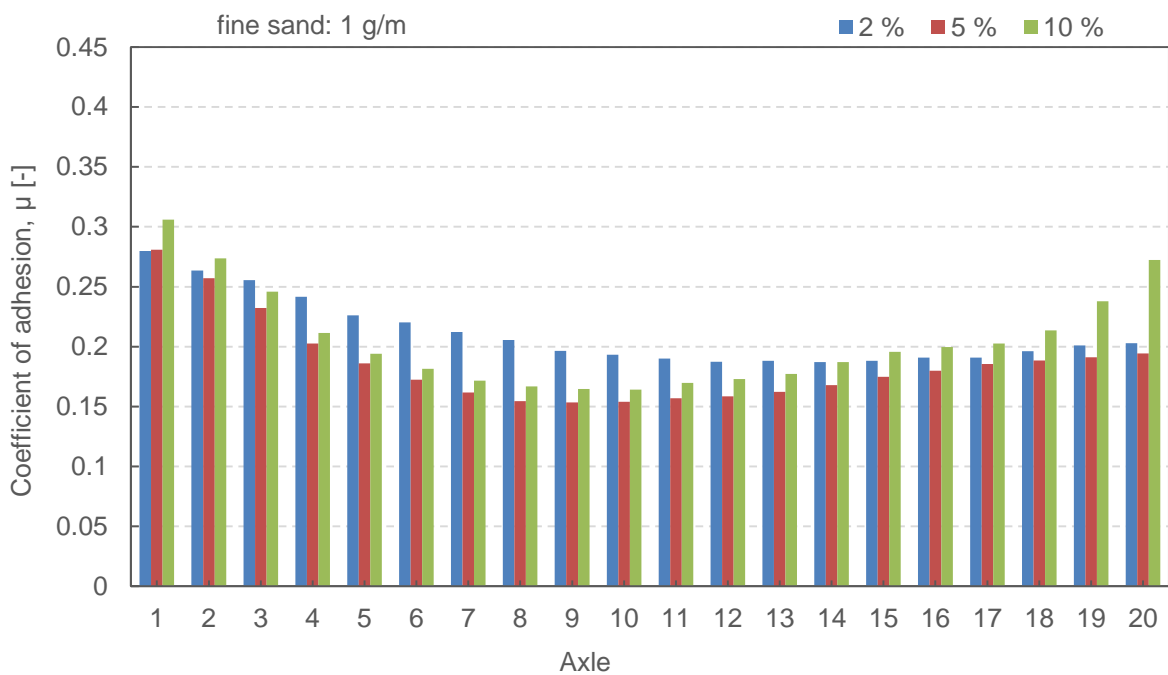


Figure 5.26: Coefficient of adhesion, comparison of the slip values at 1 g/m fine sand

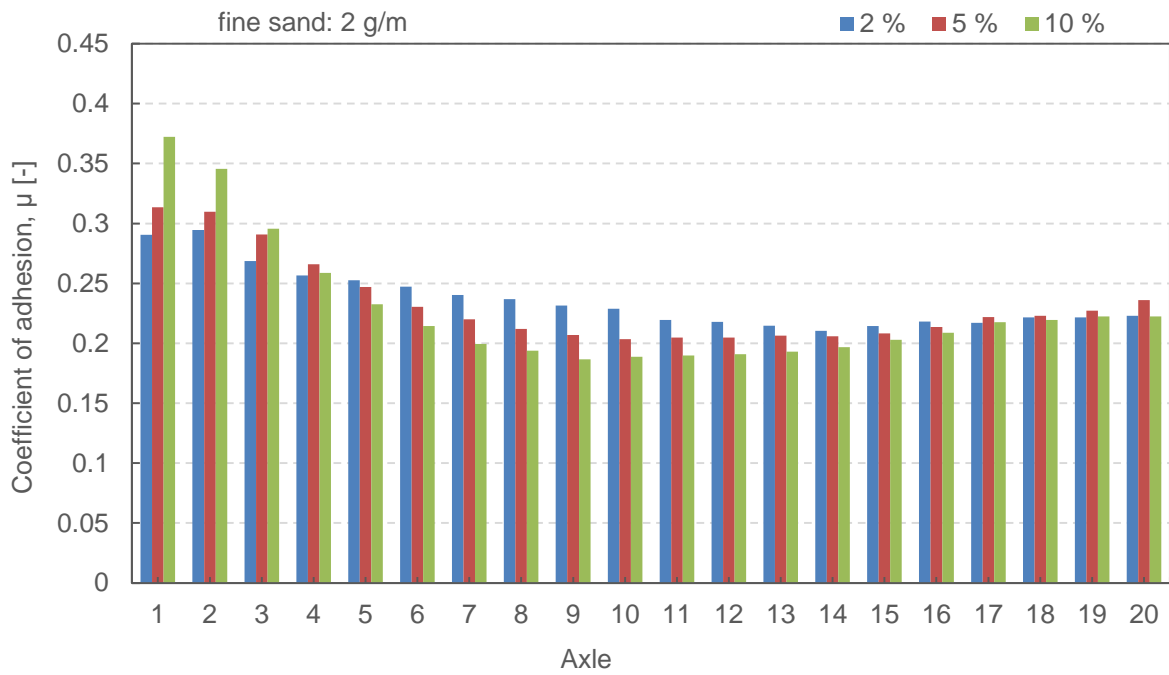


Figure 5.27: Coefficient of adhesion, comparison of the slip values at 2 g/m fine sand

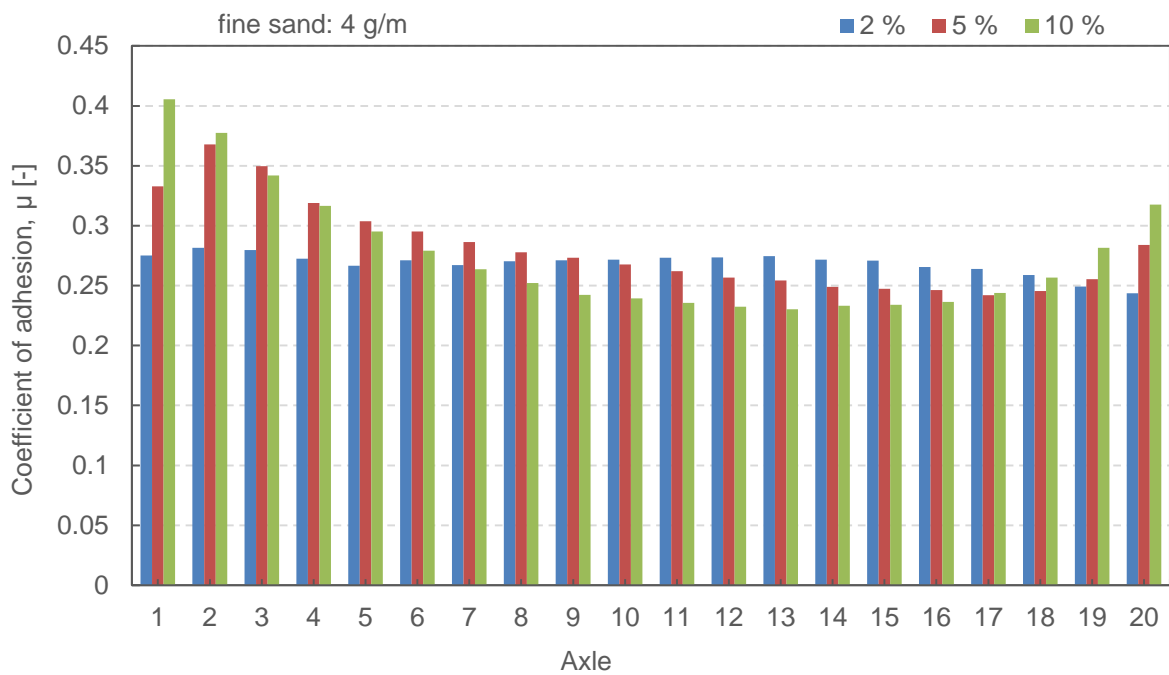


Figure 5.28: Coefficient of adhesion, comparison of the slip values at 4 g/m fine sand

5.6.4 Adhesion curve

The following figures show the adhesion curve for each sand amount.

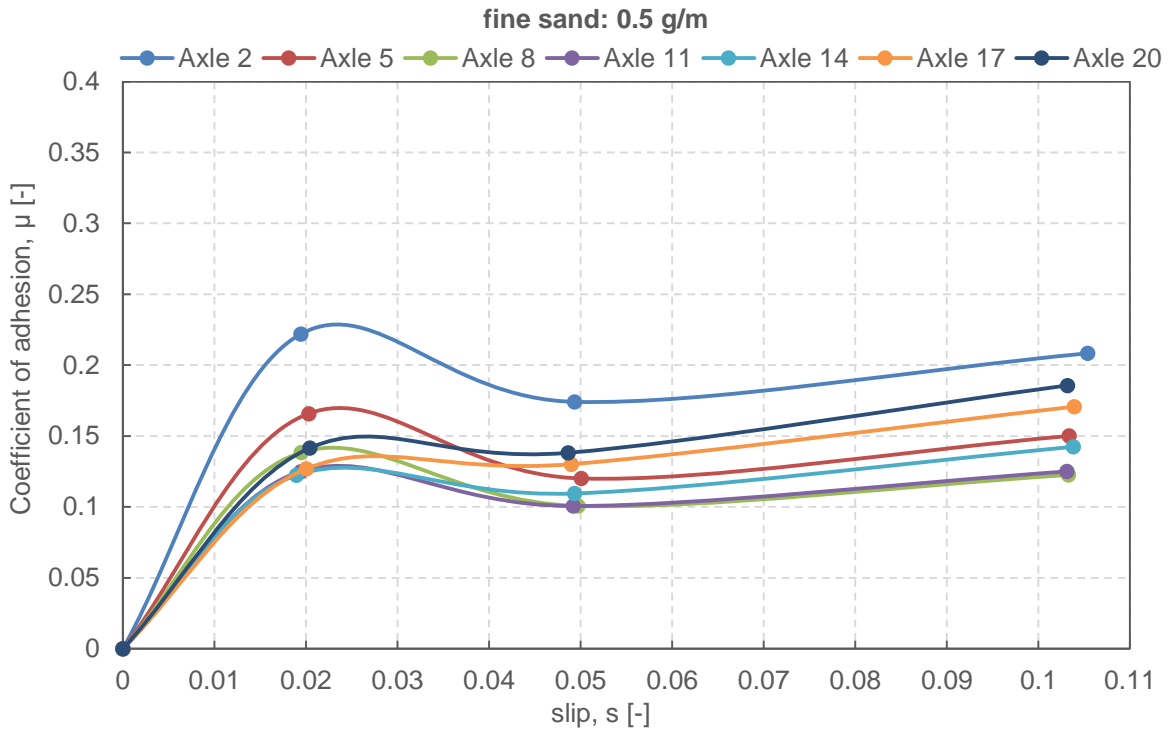


Figure 5.29: Adhesion curve at 0.5 g/m fine sand

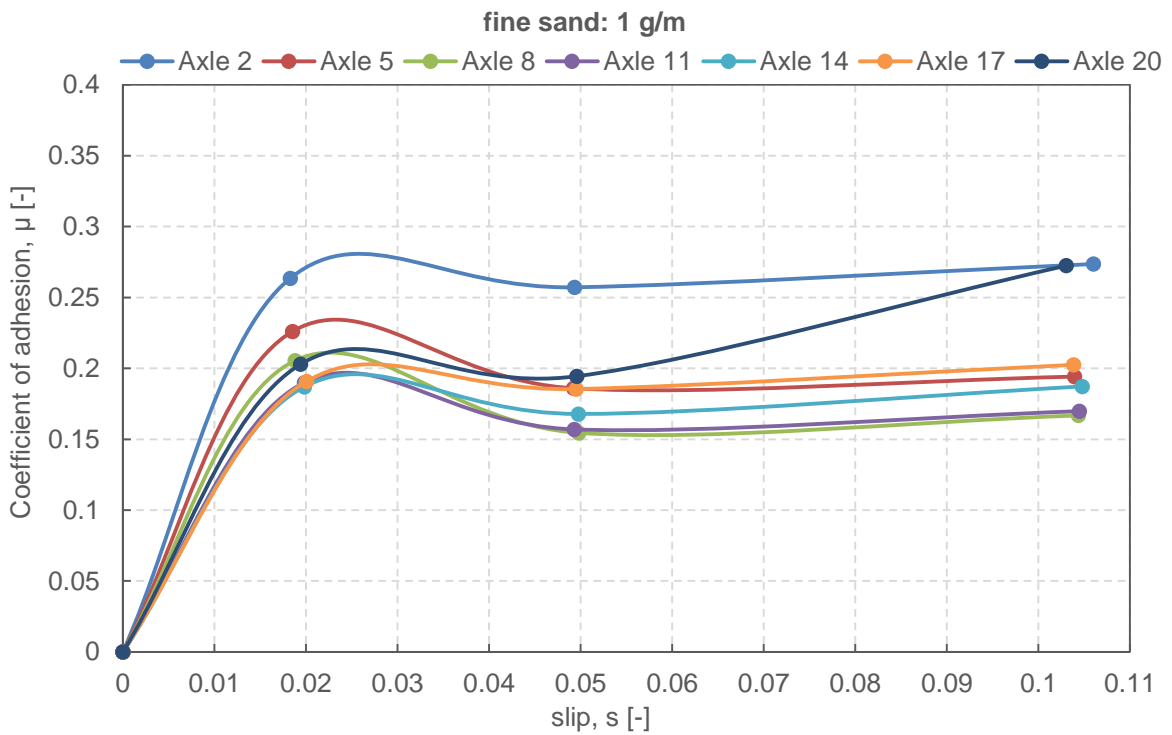


Figure 5.30: Adhesion curve at 1 g/m fine sand

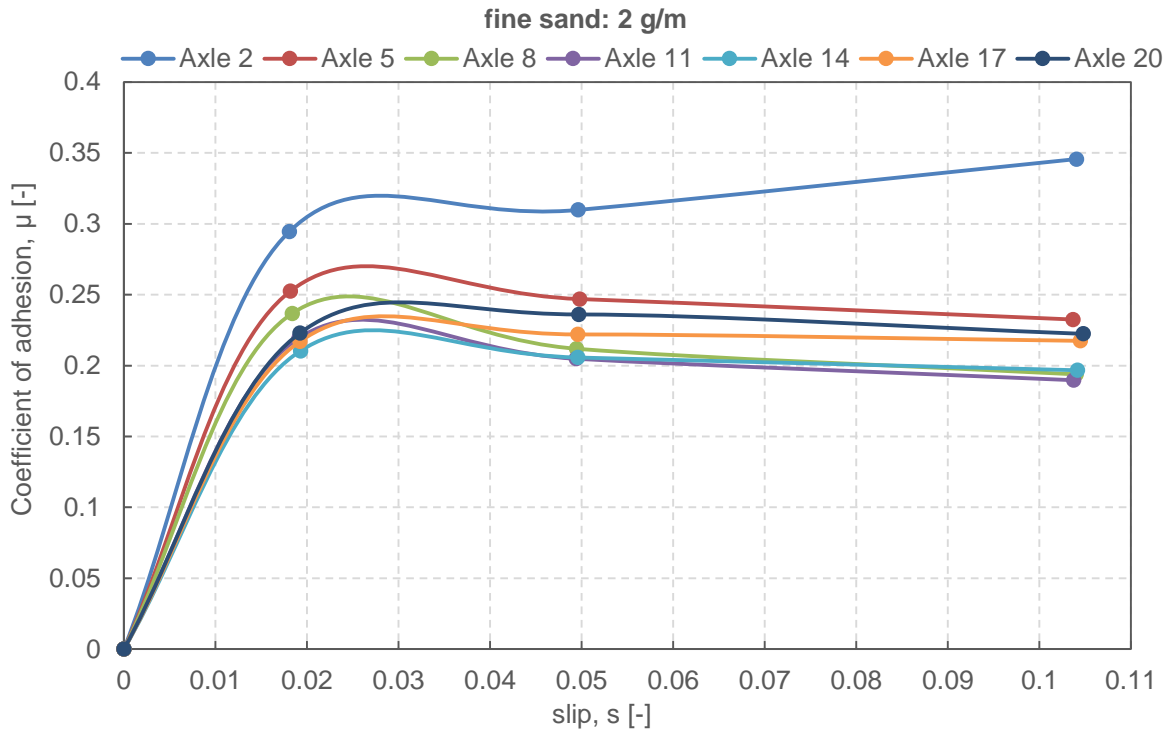


Figure 5.31: Adhesion curve at 2 g/m fine sand

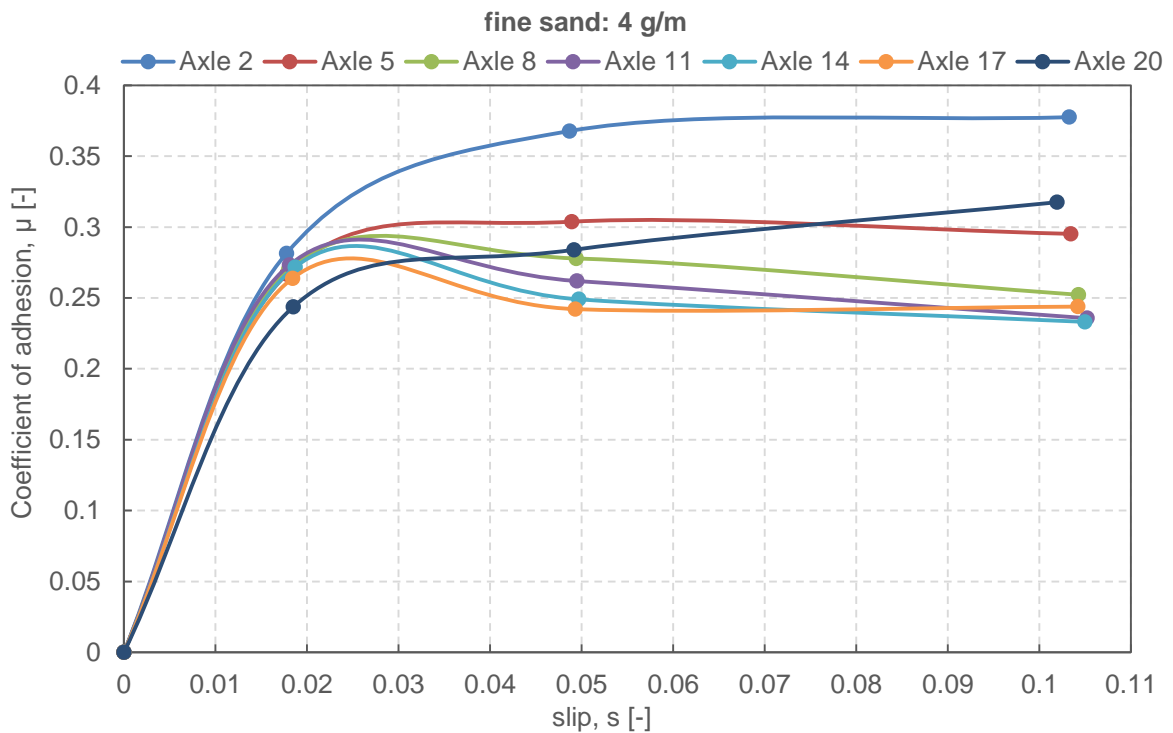


Figure 5.32: Adhesion curve at 4 g/m fine sand

The 1st axle is not shown on purpose, because its result is not realistic (the wheel is dry for the 1st roll). Every 3rd subsequent axle is shown in order to maintain a good transparency.

5.6.5 Isolation

The following figures show the electrical isolation caused by the fine sand. The time proportion of the isolation (1 means 100 % isolation, namely sand creates an isolating layer for the entire overrolling) is displayed for each sand amount. At 0.5 g/m sand amount did not happen any isolation at all. It was only present in case of more sand.

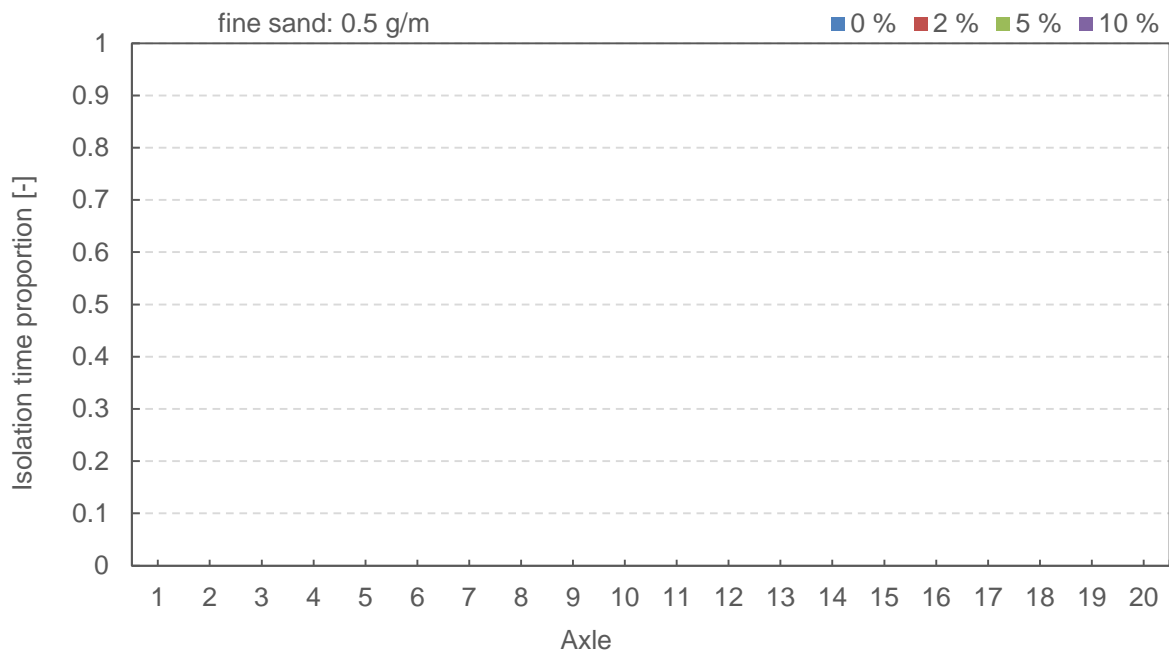


Figure 5.33: Electrical isolation of the fine sand at 0.5 g/m

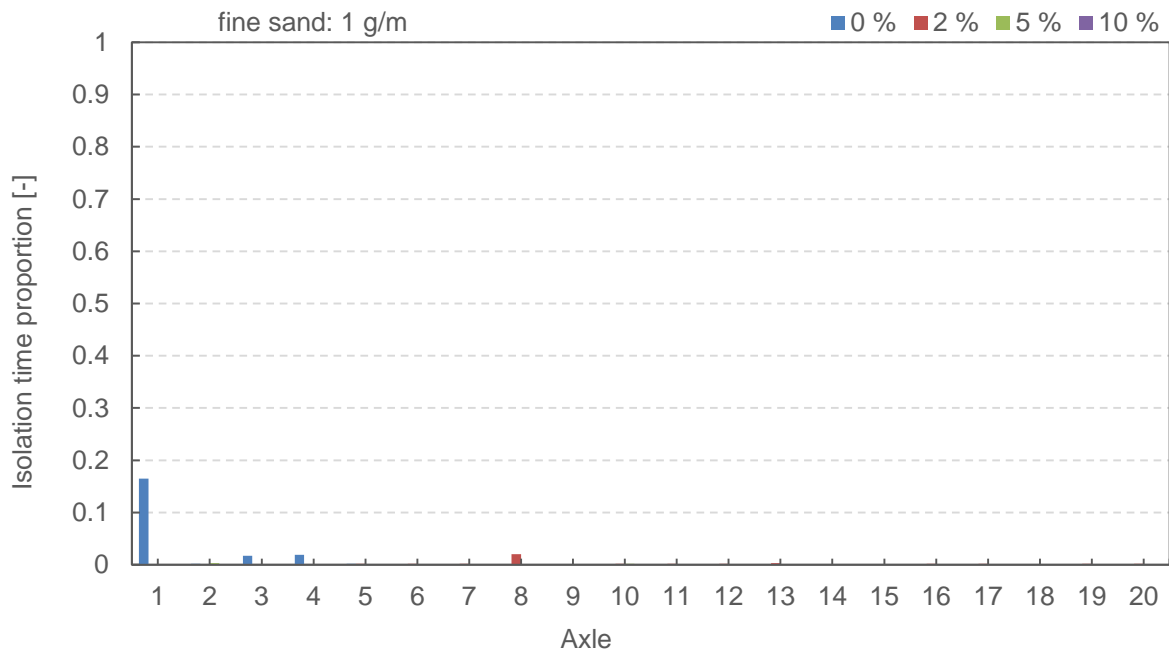


Figure 5.34: Electrical isolation of the fine sand at 1 g/m

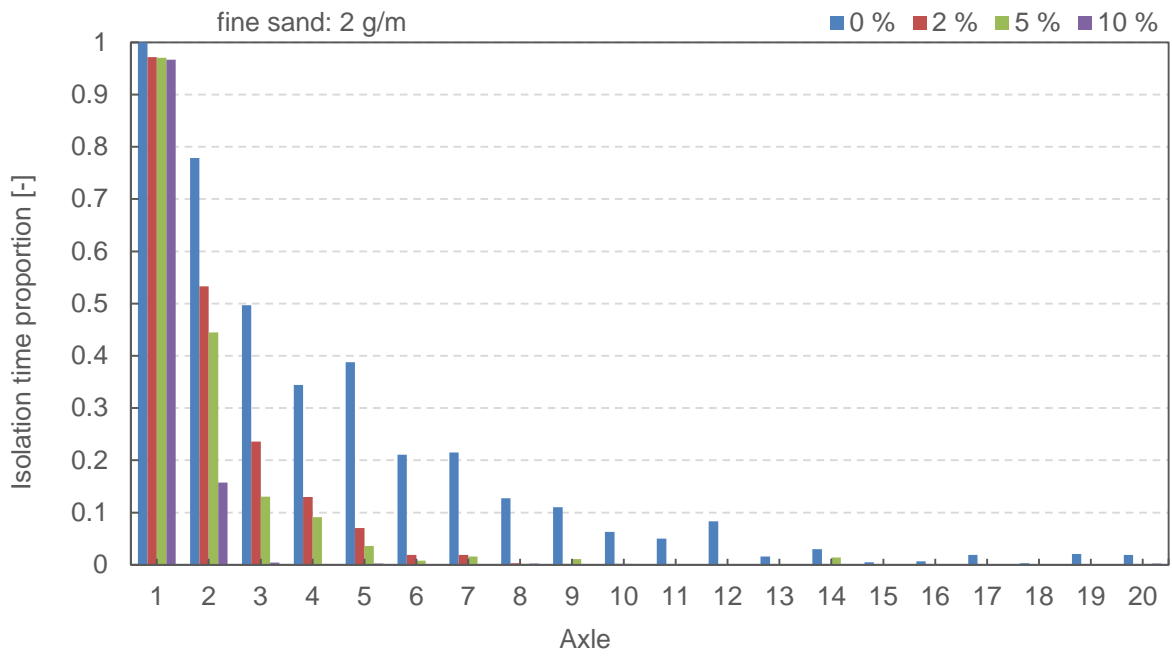


Figure 5.35: Electrical isolation of the fine sand at 2 g/m

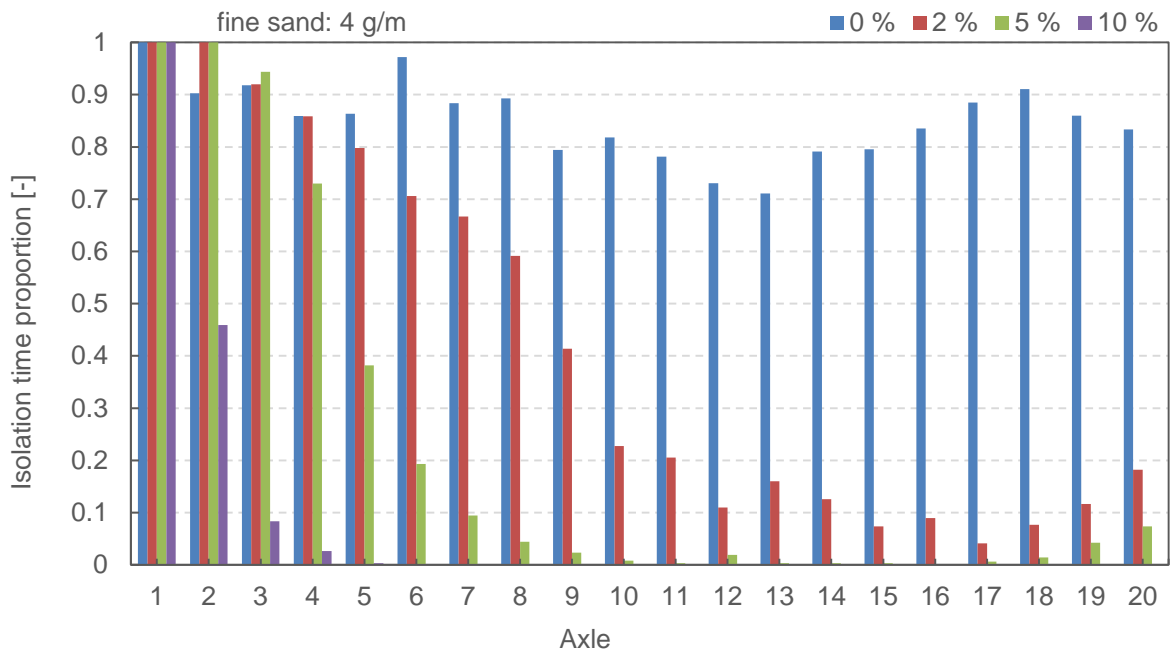


Figure 5.36: Electrical isolation of the fine sand at 4 g/m

Figure 5.37 shows the isolation of the coarse sand at 0 % slip for all examined sand amounts.

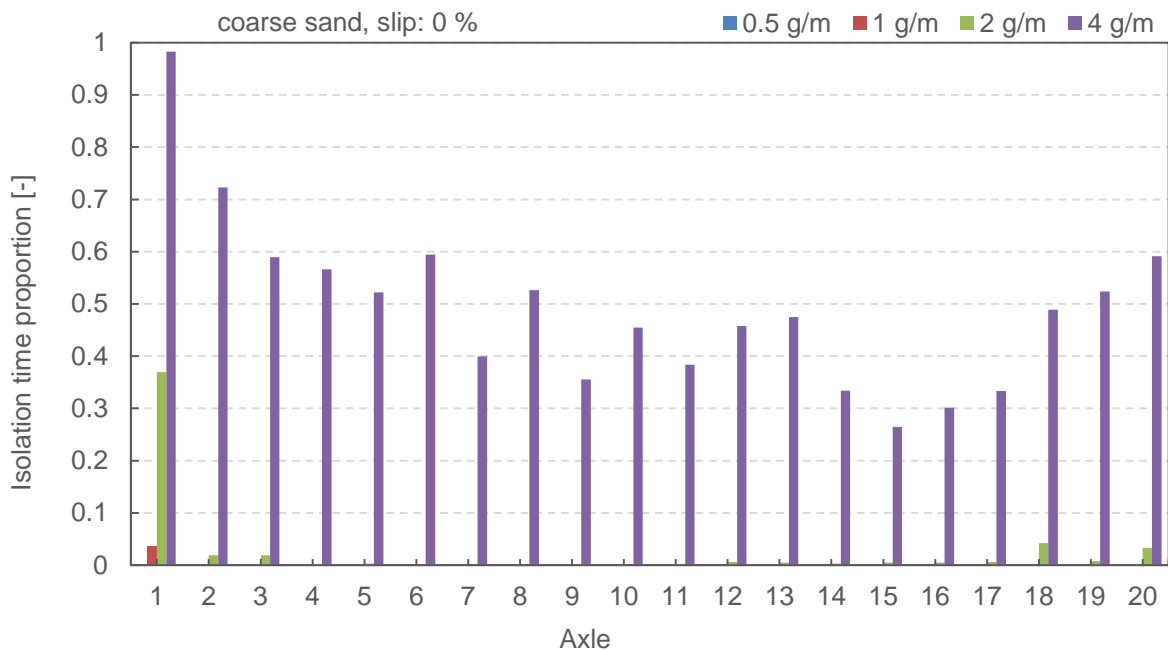


Figure 5.37: Electrical isolation of the coarse sand

5.7 CONCLUSION

Generally, in the experiments turned out that more sand results in higher level of adhesion improvement. However, the adhesion curve shows that the difference between the various sand amounts is getting smaller with increasing slip values. Although the adhesion curve is only an automatically generated spline function by MS Excel, it shows a decisive correlation between sand amount and coefficient of adhesion. Therefore, it is very probable that this falling trend would follow between 10 % and 20 % slip (the operating interval of wheel slide protection systems on rolling stocks).

The isolation for the fine sand is not an issue for 0.5 g/m and 1 g/m. At 2 g/m the first few axles are affected and at 4 g/m occurred a remarkable isolation. Less slip causes definitely more isolation. The coarse sand causes less isolation than the fine sand. The reason is probably the bigger grain size, thus it cannot create a contiguous isolating sand layer. Furthermore, the coarse sand is more problematic because it jumps off the rail because of its greater mass. Therefore, the actual sand amount for the coarse sand has to be set more accurately.

The amount of dispersion of the slip and the coefficient of adhesion is very diverse for different target slip values and sand amounts. The following experimental observation has been made:

- The test rig can control the slip better for more sand
- At low sand amount the control accuracy is better for higher slip values
- At high sand amount the control accuracy is better for lower slip values
- Worst case for the controller was 0.5 g/m sand at 2 % slip (and 20 % slip in the preliminary experiments)

Furthermore, there is a significant deviation of the dispersion among the axles. It is unavoidable that the conditions will vary during the experiment progress. It was observed that the results of the first 5 and the last 5 axles suffered higher dispersion than the axles in the middle.

Reason for the dispersion of the first 5 axles: the sand grains are being shattered under the wheel load and this process leads to higher fluctuations of the surface condition until a quasi-steady condition is achieved.

Reason for the dispersion of the last 5 axles: after a certain amount of time the contact surface starts to dry up gradually. Drier spots have higher coefficient of adhesion and it leads to an overall higher dispersion of the results. Furthermore, the airflow around the test rig has a significant effect on this phenomenon.

More figures about detailed results can be found in the Appendix.

5.8 OUTLOOK

For a more comprehensive analysis of the surface relationships in the future, there are some suggestions which can help to understand the processes taking place during the test rig experiments. A complete investigation of the adhesion between the wheel and rail requires a tribological approach. Therefore, measuring the surface topography, namely the surface roughness would be of great importance. Additionally, monitoring third-body layers, like the residual Socolub or the oxide layer on the surfaces could give further information for understanding the processes which take place during overrollings.

6 WORKFLOW OPTIMIZATION

6.1 INTRODUCTION

Before carrying out the experiments, several test runs and preliminary experiments were made. During these investigations and trials a lot of experience were collected which enabled to optimize the workflow. A previous series of experiments is taken as a base for the improvement which was conducted with the same test rig and with very similar objectives and input parameters.

The major differences are outlined in Chapter 6.2. The effect of these changes altogether is shown in Chapter 6.3. The result shows a remarkable improvement which leads to a more accurate and more reproducible way to carry out the experiments.

6.2 IMPROVEMENTS

6.2.1 Conditioning

6.2.1.1 Description of the problem

Vibration of the test rig during an overrolling has a huge influence on the sand output of the vibrating conveyor. The increased vibration can increase the amount of sand by as high as 100 % which hinders an accurate adjustment of the sand output. Furthermore, the increased amount of sand varies in a wide range because it depends strongly on the target value of the sand and the slip.

6.2.1.2 Execution method

Old method: during the first overrolling (with full wheel load, active measurement).

New method: first horizontal movement (back and forth) of the rail without wheel load (without contact). This movement is used only to apply the lubricant and sand on the rail. With this method an accurate setting of the targeted sand amount is possible. It has to be mentioned that with the new method the increased time between conditioning and first overrolling may causes a sooner drying (which causes an increased coefficient of adhesion).

6.2.1.3 Comparison of the sand output

During testing and comparing the two methods several experiments were made. Table 8 shows the sequence and settings of these experiments. The target value is 0.5 g/s. The green marked rows are showing the settings for the new method.

	Sand [g/s]	Deviation		Wheel load	Surface condition	Slip
1	0.56	0.06	11.55 %	yes	Socolub	5 %
2	0.50	0.00	0.28 %	no	-	-
3	0.51	0.01	2.54 %	no	-	-
4	0.54	0.04	8.89 %	yes	Socolub	5 %
5	0.64	0.14	27.32 %	yes	dry	5 %
6	0.52	0.02	3.66 %	no	-	-
7	0.50	0.00	0.28 %	no	-	-
8	0.81	0.31	62.82 %	yes	Socolub + sand	5 %
9	0.70	0.20	39.72 %	yes	Socolub + sand	5 %
10	0.65	0.15	29.58 %	yes	Socolub + sand	5 %
11	0.65	0.15	29.58 %	yes	Socolub + sand	5 %
12	0.81	0.31	62.25 %	yes	Socolub + sand	5 %
13	0.96	0.46	92.68 %	yes	Socolub + sand	10 %
14	0.54	0.04	7.04 %	no	-	-

Table 8: Settings for the comparative measurements

Figure 6.1 shows the outputted amount of sand, where the target value is 0.5 g/s.

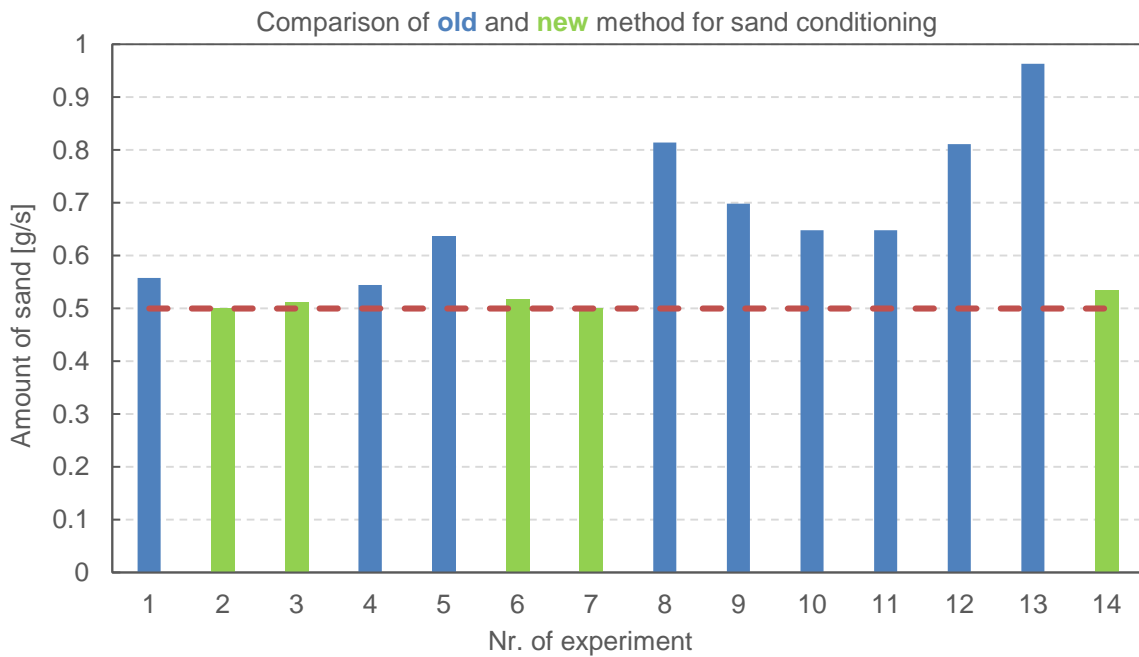


Figure 6.1: Outputted amount of sand

Figure 6.2 shows the deviation from the target value.

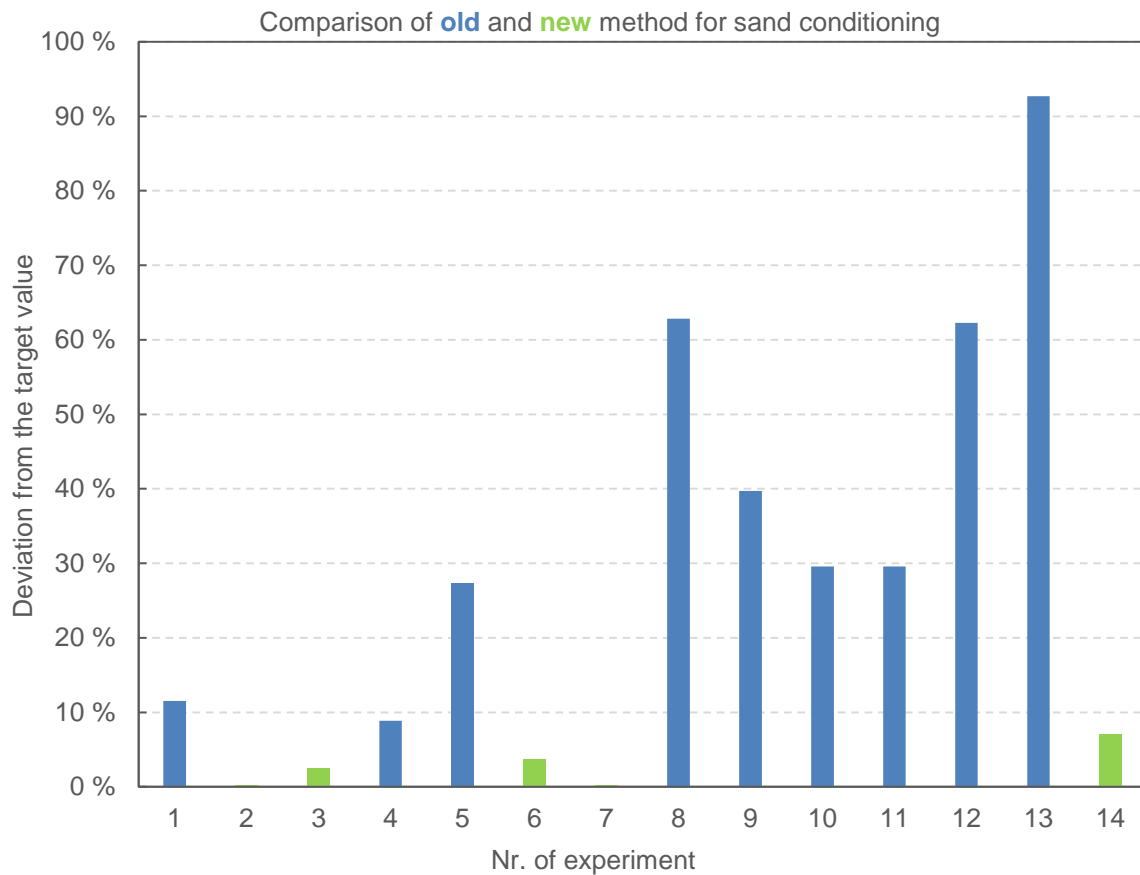


Figure 6.2: Deviation from the target value

6.2.1.4 Conclusion

The new method shows only a negligible dispersion which makes it more suitable for accurate and reproducible experiments. During a test measurement the difference in the coefficient of adhesion between the two methods was higher than 10 %. It was carried out with 1 g/m sand at 5 % slip. The difference would be much higher with 0.5 g/m sand and 10 % slip.

However, it has to be noted that during the old series of experiments paper was used as well for simulating a slippery surface. For that kind of experiments it is vital to start with the first overrolling after conditioning as fast as possible. Hence, the above described new method is valid for experiments with Socolub exclusively.

6.2.2 Sequence of actions and reference runs

6.2.2.1 Description of the problem

The initial condition for the experiment is to have a reference run with a desired low coefficient of adhesion. After the experiment it is used to determine the adhesion increasing effect of the sand. For the reference run a lubricant (4 % Socolub solution) is used. During an overrolling the lubricant is pressed and stuck in the surface of the wheel and rail. Multiple overrollings are needed to achieve the desired low coefficient of adhesion. However, during an overrolling with sand, this lubricant layer will be removed. In order to achieve a reproducible experiment, a measurable initial condition is needed. The problem is, that even the reference run is modifying the surface condition.

6.2.2.2 Execution method

Old method: At the beginning of the series of experiments all the reference runs were made. Between the experiments, runs with the lubricant were made only occasionally. This method has failed to have a measured initial condition.

New method: Between every experiment several conditioning runs took place. Furthermore, each reference run was performed directly before the experiment. With this method the adverse modification effect on the surface condition of the lubricant and the sand has been minimized. The new method requires a slightly different evaluation process as well. In order to define the adhesion increasing effect of the sand, from every measurement result the matching reference run has to be subtracted.

6.2.2.3 Conclusion

With the new method the desired repeatability of the experiments has been achieved. It enables to start every measurement run with nearly the same surface condition.

6.2.3 Evaluation

6.2.3.1 Description of the problem

After combining the results of the repetition runs, the next step in the evaluation process is to define slip intervals. It is needed because of the extensive dispersion of the actual slip values caused by the insufficient precision of the controller. This phenomenon is clearly visible in Figure 6.3 (sand: 2 g/m, 10th axle), where the actual slip values are exceeding the target values significantly. There are multiple ways to create these intervals.

6.2.3.2 Execution method

Old method: The intervals were defined using all result data from measurements with all target slip values. Figure 6.3 shows the interval generation for the 5 % slip. It can be seen that this interval contains data even from the 2 % slip as well.

New method: The intervals are defined separately for all target slip values, as it is showed for the 5 % slip in Figure 6.4. There is no data in these intervals originating from other target slip settings.

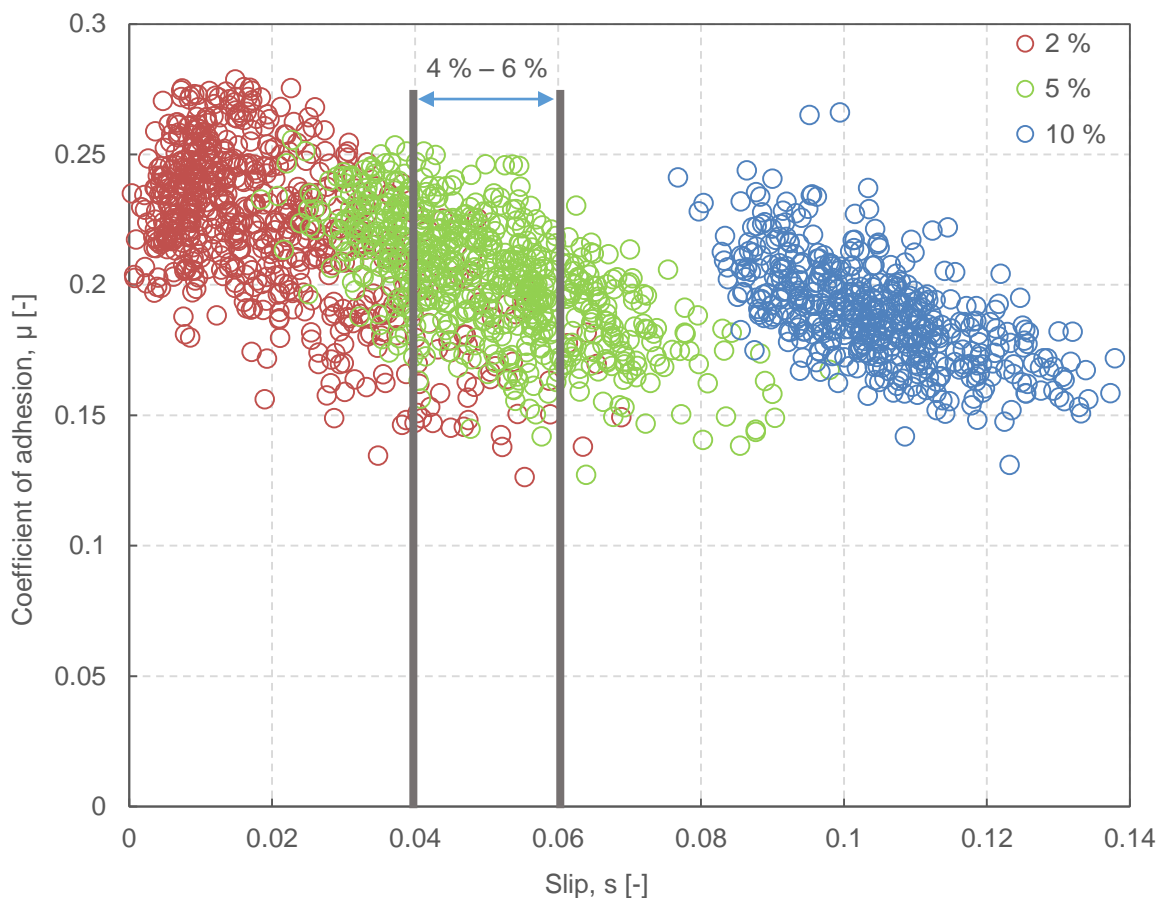


Figure 6.3: Slip intervals with the old method

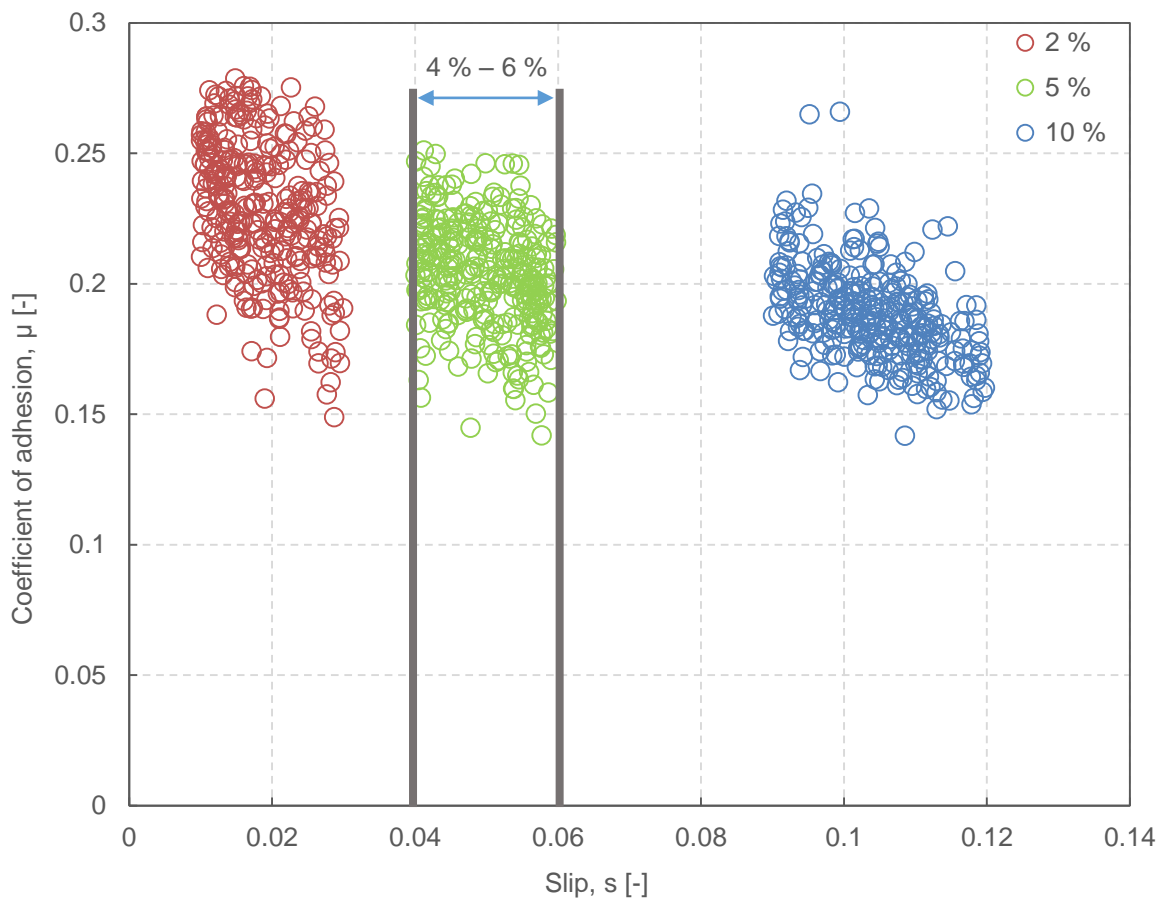


Figure 6.4: Slip intervals with the new method

6.2.3.3 Conclusion

The usage of inaccurate data from separate measurements with different slip settings is prevented with the new method. This action increases the accuracy of the overall experiment.

Furthermore, the evaluation of the isolation was changed as well. Since there is a strong correlation between slip and isolation, it is vital to evaluate isolation separately for all slip values.

6.3 PERFORMANCE OF THE NEW WORKFLOW

For comparing the performance of the old and new workflow, the dispersion of the adhesion coefficient was used. Not the specific adhesion coefficient values though, because not the exact results are compared here, but rather the repeatability of the experiment.

For the comparison, the results of the 5 % slip from the new experiment and 6 % from the old experiment were used. Although it was not exactly the same target value,

but the deviation is negligible. The differences between the circumstances of the two experiments were described in Chapter 6.2. The disparity in the dispersion origin from the combined effect of the modified sub-processes. One further big difference is that in the old series of experiments only two repetition runs were made, whereas in the new it was four. It requires much more workflow accuracy to achieve at least the same level of dispersion with four repetition runs.

The following figures are showing the difference between the 90th and 10th percentile for every 20 axle. Basically the range of the measurement data without the upper and lower 10 % is compared. It is important to note, that the dispersion of the adhesion coefficient has two reasons:

- 1) Dispersion during a single overrolling (test rig specific issue)
- 2) Dispersion due to the repetition runs (workflow specific issue)

Reason Nr. 1 is not directly connected to the workflow, it is caused by the accuracy limit of the controller. But reason Nr. 2 is caused by the measurement error between the repetition runs. Therefore, if the dispersion of the results is higher, it means that the workflow's repeatability is lower. And inversely, lower dispersion means higher repeatability.

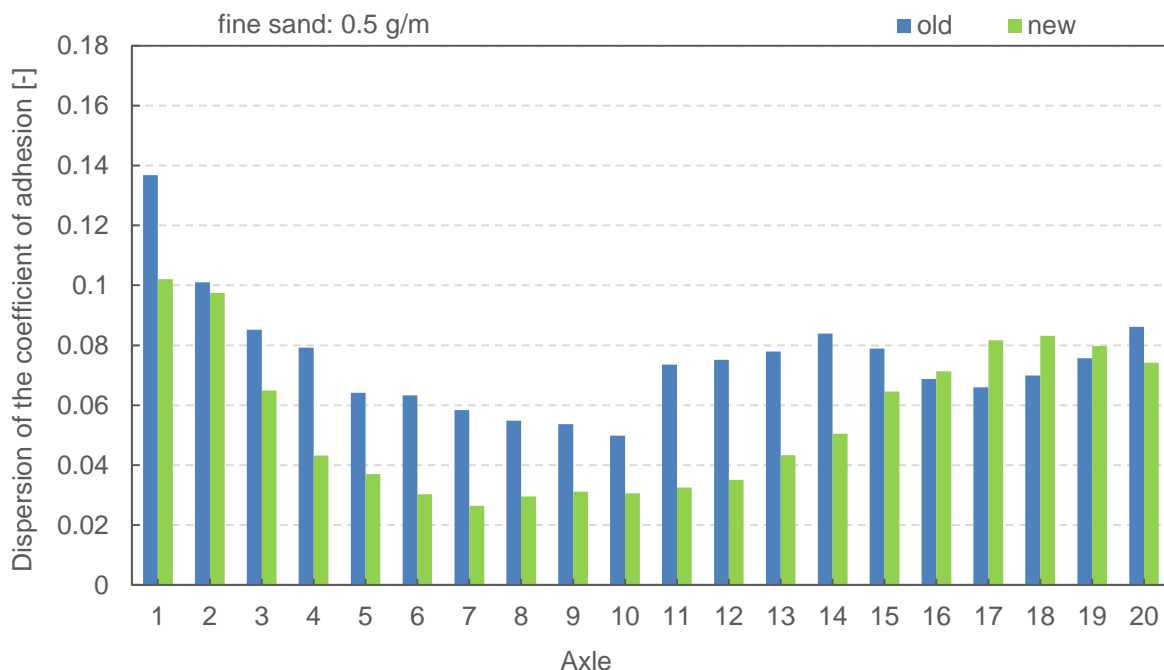


Figure 6.5: Workflow comparison, fine sand: 0.5 g/m

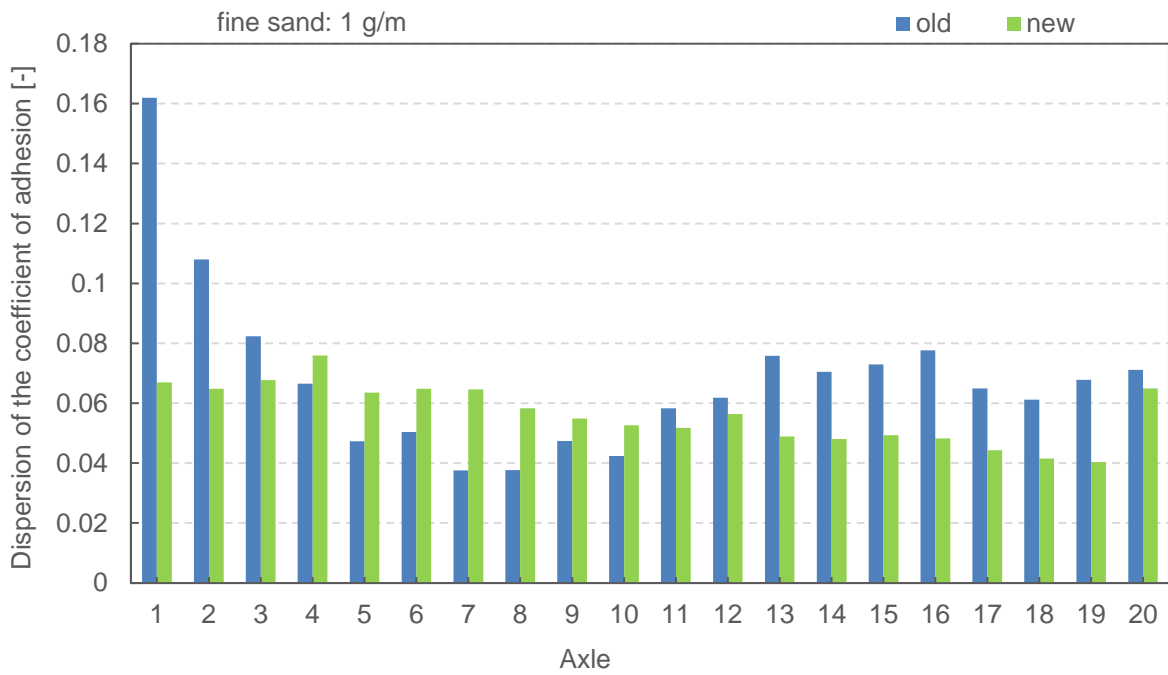


Figure 6.6: Workflow comparison, fine sand: 1 g/m

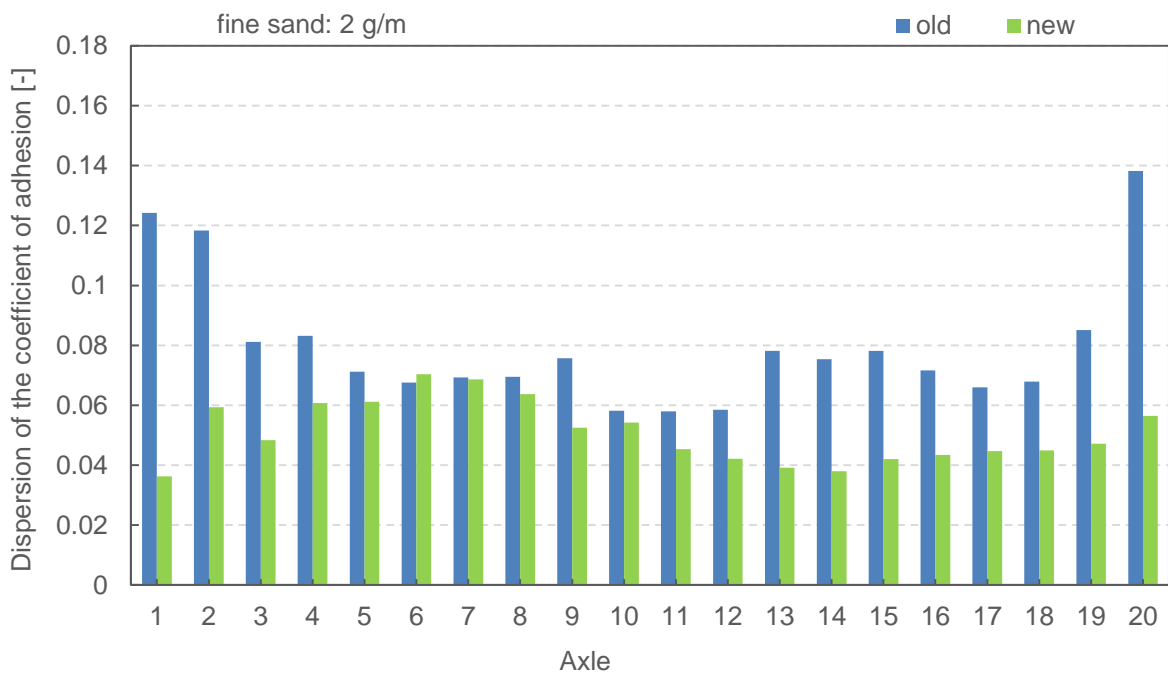


Figure 6.7: Workflow comparison, fine sand: 2 g/m

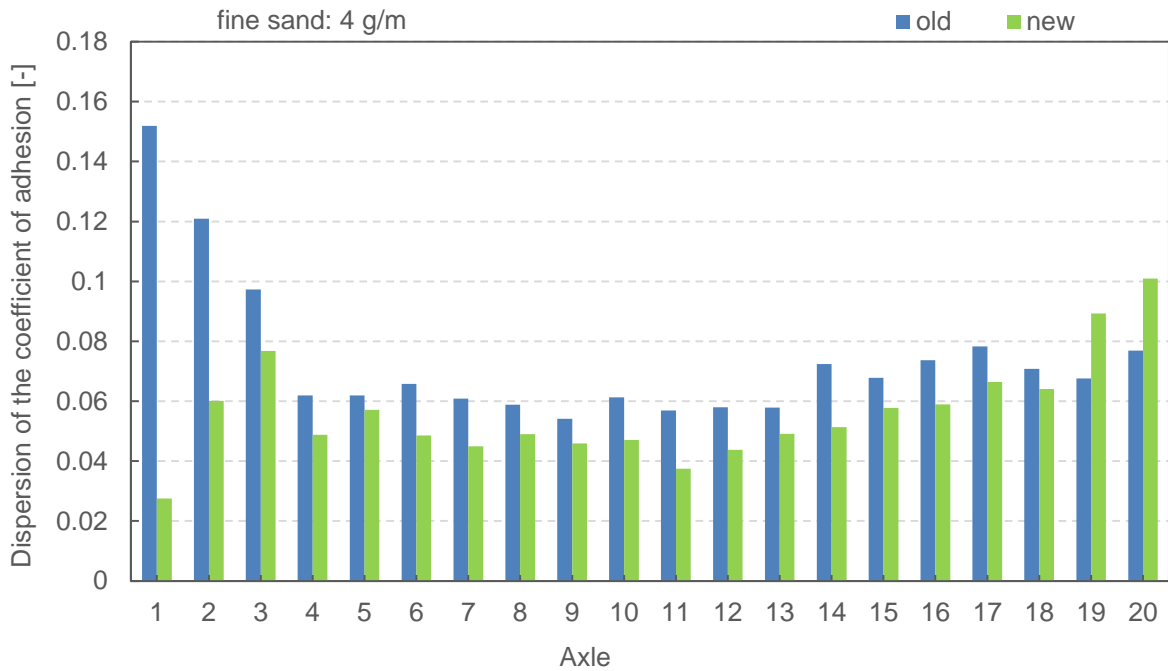


Figure 6.8: Workflow comparison, fine sand: 4 g/m

With the new workflow the dispersion decreased an average of 26 %. It means that the new workflow has a remarkable advantage in reproducibility despite the fact that more repetition runs were made.

6.4 COMPARISON OF THE RESULTS

The next figures show the comparison of the adhesion coefficient between the old and the new workflow. There is a significant difference, which is mainly caused by the different sequence of actions, particularly the more frequent reference runs. Namely, this is responsible for lowering the friction prior to measurement.

Furthermore, the changed way of sand conditioning plays an important role as well. The effective sand amount is lower because of the smaller vibration during sand output.

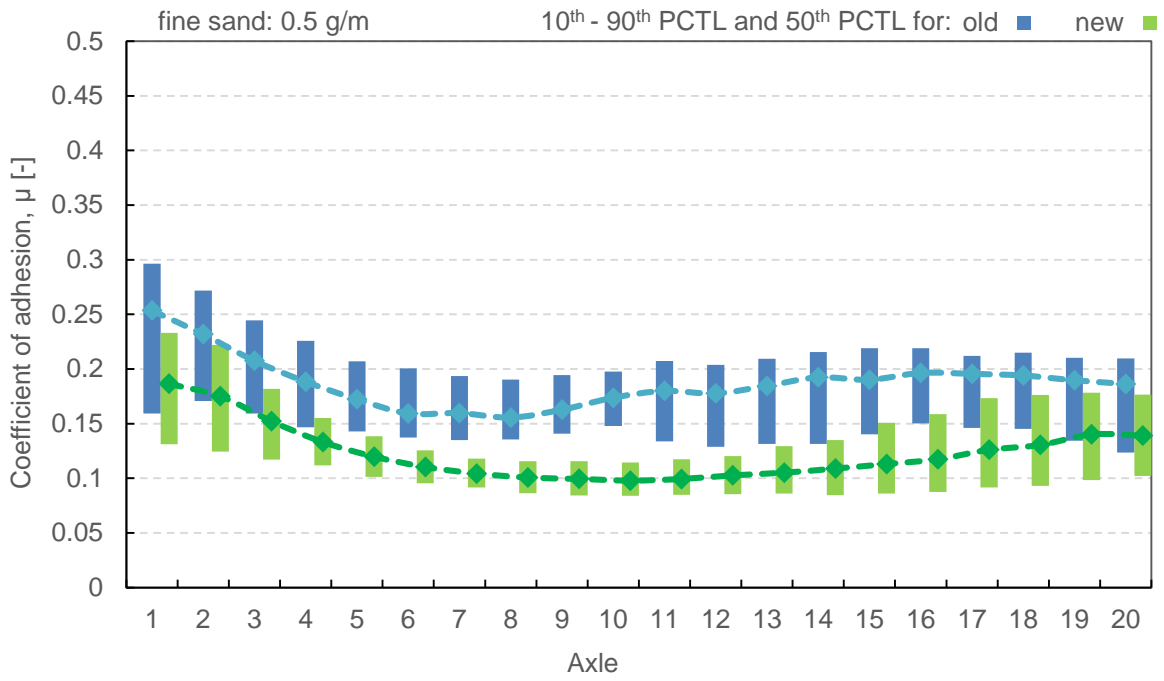


Figure 6.9: Comparison of the adhesion coefficient, fine sand: 0.5 g/m

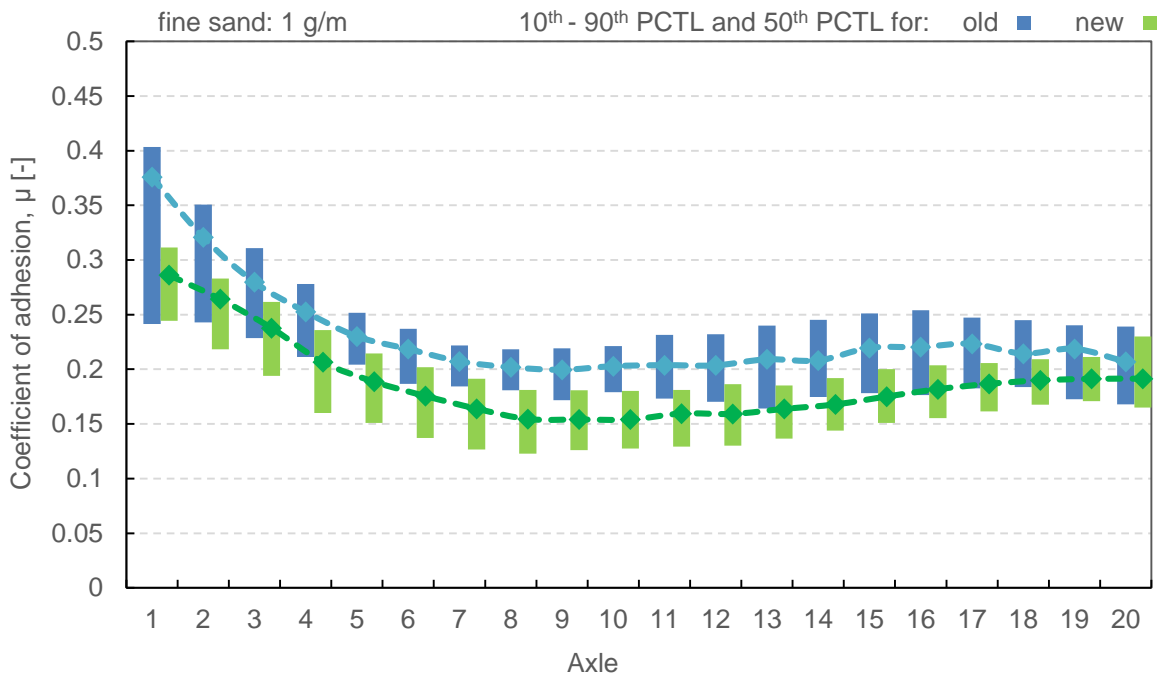


Figure 6.10: Comparison of the adhesion coefficient, fine sand: 1 g/m

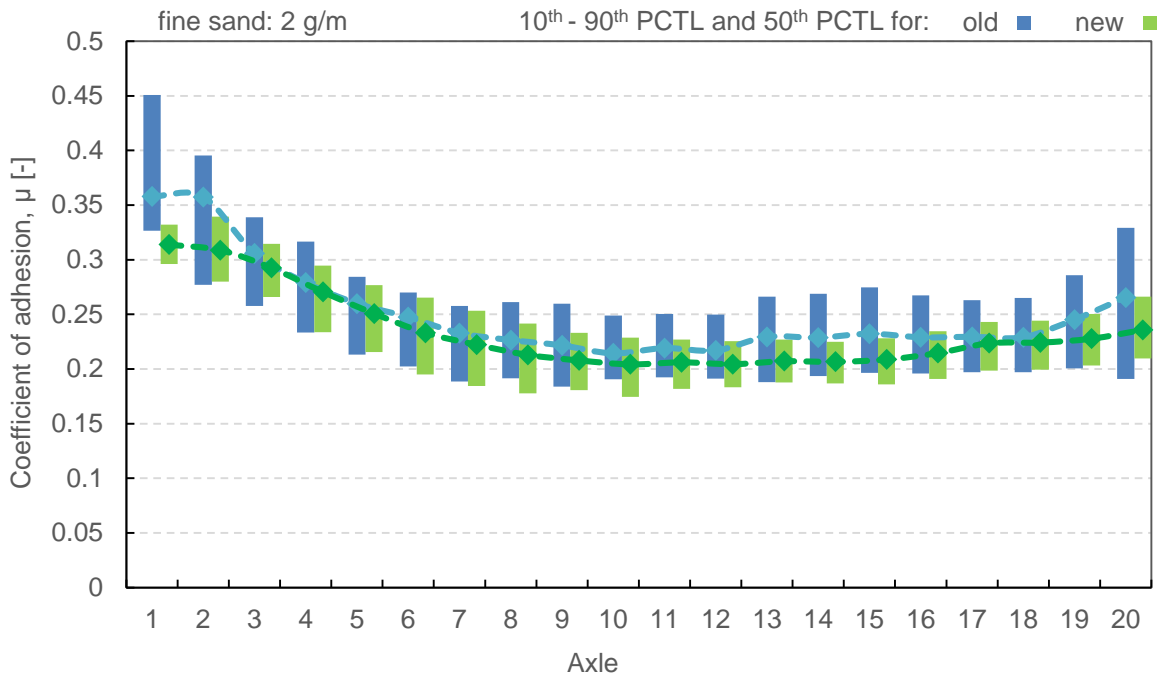


Figure 6.11: Comparison of the adhesion coefficient, fine sand: 2 g/m

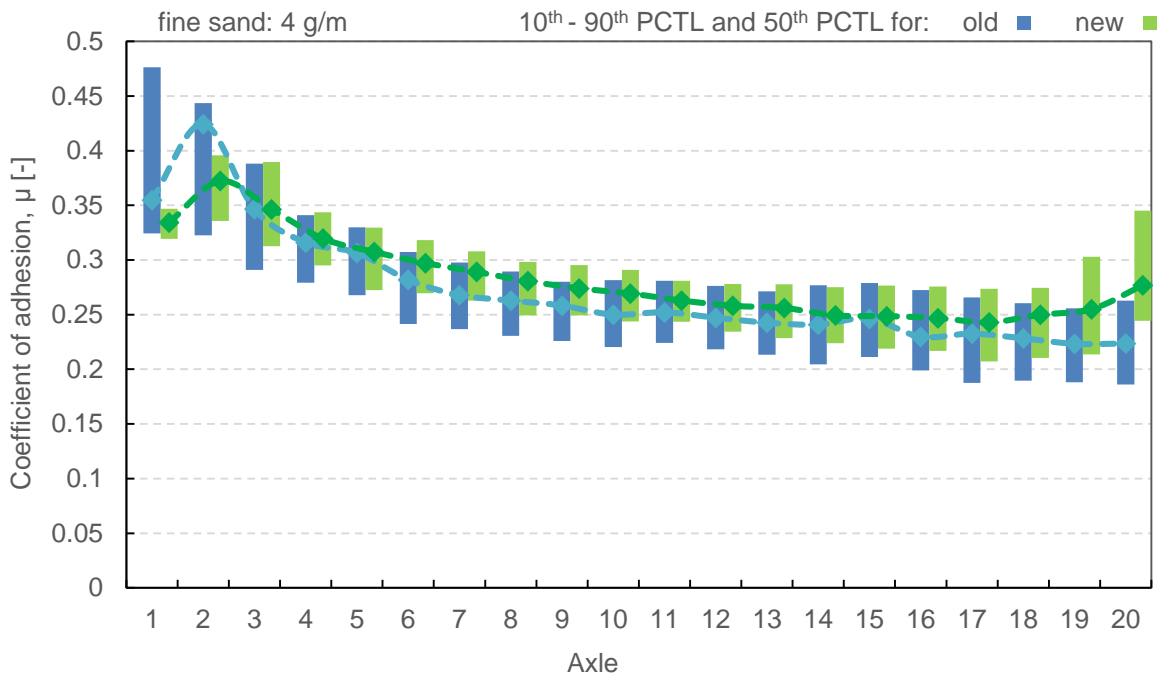


Figure 6.12: Comparison of the adhesion coefficient, fine sand: 4 g/m

For 0.5 g/m and 1 g/m sand amount the coefficient of adhesion is considerably lower for the new workflow. At 2 g/m there is only a slight difference and at 4 g/m the results are higher for the new workflow, but the difference is very small.

7 SUMMARY

The goal of the thesis was to carry out the experiments and to make a profound analysis on its workflow optimization. Furthermore, a thorough analysis of the scientific literature has been completed in order to be able to investigate properly the main research topic of the thesis.

The planned series of experiments have been accomplished, which results are containing valuable information about the adhesion improvement with sand. The experiments have been carried out using different sanding parameters and finally the comparison of the effect of the input variables has been made. The conclusion is that a close correlation exists between the wheel slip and the resulted coefficient of adhesion. Furthermore, the isolation behaviour was investigated as well, where the critical case of 0 % slip has been stated.

The optimization of the experiment workflow had a huge effect on the repeatability of the experiments. Introducing several measures both for the preliminary actions and the evaluation process, the dispersion of the results has been minimized which will enable a high accuracy for experiments in the future, even with different input settings (e.g. different sand type).

Both of the targeted objectives of the thesis have been achieved, the outcome will greatly contribute to future product developments at Knorr-Bremse GmbH which will make railway transport safer and more reliable.

LIST OF REFERENCES

- Andersson, E., Berg, M., & Stichel, S. (2007). Rail Vehicle Dynamics. Stockholm, Sweden.
- Arias-Cuevas, O. (2010). Low Adhesion in the Wheel-Rail Contact. Delft, Netherlands.
- Arias-Cuevas, O., & Li, Z. (2011). Field investigations into the performance of magnetic track brakes of an electrical multiple unit against slippery tracks. Part 1: Adhesion improvement. *Proceedings of the Institution of Mechanical Engineers, Part F: Journal of Rail and Rapid Transit*.
- German National Standard. (2001). DIN 25003.
- Hutchings, I. (1992). Tribology: friction and wear of engineering materials.
- Knorr-Bremse GmbH. (n.d.).
- Lewis, R., & Olofsson, U. (2004). Mapping rail wear regimes and transitions. *Wear*.
- Lundén, R., & Paulsson, B. (2009). Introduction to wheel-rail interface research. *Wheel-rail interface handbook*. Sweden: Woodhead Publishing Limited and CRC Press LLC.
- Moore, D. F. (1998). Principles and Applications of Tribology. Amsterdam, Netherlands: Elsevier.
- Nesaratnam, S. T., & Taherzadeh, S. (2014). Air quality management. Milton Keynes, United Kingdom: John Wiley & Sons Ltd.
- Network Rail Limited. (2015). *Network Rail*. Retrieved from <http://www.networkrail.co.uk/timetables-and-travel/delays-explained/autumn/>
- Official Journal of the European Union. (2006). Technical specification for interoperability relating to the subsystem "Control-Command and Signalling" of the trans-European conventional rail. Brussels, Belgium.
- Olofsson, U. (2007). A multi-layer model of low adhesion between railway wheel and rail. *Proceedings of the Institution of Mechanical Engineers, Part F: Journal of Rail and Rapid Transit*.
- Olofsson, U. (2009). Adhesion and friction modification. *Wheel-rail interface handbook*. Sweden: Woodhead Publishing Limited and CRC Press LLC.
- Paces, M. (2013). Sand im Rad/Schiene-Kontakt. Vienna, Austria.
- Polach, O. (2005). Creep forces in simulations of traction vehicles running on adhesion limit. *Wear*.
- Prof. Gfatter, G., & Lang, D. (2001). Sanding Systems. Mödling, Austria: KNORR-BREMSE GmbH.
- Schamberger, S. (2012). Die Wirkung von Sand auf den Reibwert zwischen Rad und Schiene. Vienna, Austria.

- Wang, W., Zhang, H., Wang, H., Liu, Q., & Zhu, M. (2010). Study on the adhesion behavior of wheel/rail under oil, water and sanding conditions. *Wear*. Chengdu, China: Elsevier.
- Zhu, Y. (2011). Adhesion in the wheel – rail contact under contaminated conditions. KTH Royal Institute of Technology.
- Zhu, Y. (2013). Adhesion in the wheel–rail contact. Stockholm, Sweden: KTH Royal Institute of Technology.

LIST OF ABBREVIATIONS

DIN	German Institute for Standardization
e.g.	for example
ÖBB	Austrian Federal Railways
PCTL	percentile
pm	particulate matter
TU Graz	Graz University of Technology
UIC	International Union of Railways

LIST OF FIGURES

Figure 1.1: The typical damages of wheel/rail under low adhesion, (a) skidding marks on the rail surface; (b) wheel flats on the tread.....	1
Figure 2.1: Classification of rolling stocks	4
Figure 2.2: Sketch of bogie with primary suspension and wheelset in contact with rails on railpads, sleepers and ballast.....	5
Figure 2.3: Schematic of wheel-rail contact positions.....	6
Figure 2.4: Contact conditions in the wheel-rail contact	7
Figure 2.5: Common adhesion requirements in railway transportation	8
Figure 2.6: The third-body layer between the bulk materials in the wheel-rail contact.....	9
Figure 2.7: Rolling wheel.....	10
Figure 2.8: Stick-slip phenomenon	11
Figure 2.9: Relationship between tangential force and creep (slip) at the wheel-rail contact.....	11
Figure 2.10: Schematic of a) a pure sliding contact and b) a rolling-sliding contact under acceleration (X is the gravity centre; all forces in the figure are acting on either the block or the wheel).....	12
Figure 2.11: Schematic of the adhesion curve and coefficient of friction under clean and contaminated conditions (modified from Zhu)	14
Figure 3.1: Schematic diagram of a sanding system	17
Figure 3.2: Sanding system in operation.....	18
Figure 3.3: Effect of sanding.....	18
Figure 3.4: Different types of sand.....	21
Figure 4.1: CAD-model of the test rig.....	24
Figure 4.2: Photo of the test rig	25
Figure 4.3: Data acquisition and processing.....	26
Figure 4.4: Spreading of the sand with the vibrating conveyor	27
Figure 5.1: Effect of sand and Socolub on the surface condition (adhesion coefficient)	30
Figure 5.2: Simplified reference run.....	31
Figure 5.3: Conditioning with lubricant and sand without wheel load	32
Figure 5.4: 0.5 g; 1 g; 2 g; 4 g fine sand.....	33
Figure 5.5: Overview of the dispersion density of the fine sand depending on the amount of sand	34
Figure 5.6: Adhesion coefficient over rail position.....	36
Figure 5.7: Combination of repetition runs and creation of slip interval.....	37
Figure 5.8: Mean values and dispersion of adhesion coefficient	38
Figure 5.9: Adhesion curve.....	39
Figure 5.10: Slip fluctuation at 20 % target slip.....	40
Figure 5.11: Strips on the rail caused by the stick-slip oscillation	41
Figure 5.12: Long lasting effect of two overrollings with 20 % slip.....	41
Figure 5.13: Modification of the surface condition caused by the sand	42
Figure 5.14: Modification of the surface condition caused by the Socolub.....	43
Figure 5.15: Difference in the dry adhesion coefficient before and after Socolub was applied	44
Figure 5.16: The increased coefficient of adhesion after drying up.....	45
Figure 5.17: Socolub layer and the effect of the surface cleaning with sand	46
Figure 5.18: Photo of the rail at the end of the experiments.....	47

Figure 5.19: Coefficient of adhesion, comparison of the sand amount at 2 % slip	48
Figure 5.20: Coefficient of adhesion increase, comparison of the sand amount at 2 % slip	48
Figure 5.21: Coefficient of adhesion, comparison of the sand amount at 5 % slip	49
Figure 5.22: Coefficient of adhesion increase, comparison of the sand amount at 5 % slip	49
Figure 5.23: Coefficient of adhesion, comparison of the sand amount at 10 % slip	50
Figure 5.24: Coefficient of adhesion increase, comparison of the sand amount at 10 % slip.....	50
Figure 5.25: Coefficient of adhesion, comparison of the slip values at 0.5 g/m fine sand	51
Figure 5.26: Coefficient of adhesion, comparison of the slip values at 1 g/m fine sand	51
Figure 5.27: Coefficient of adhesion, comparison of the slip values at 2 g/m fine sand	52
Figure 5.28: Coefficient of adhesion, comparison of the slip values at 4 g/m fine sand	52
Figure 5.29: Adhesion curve at 0.5 g/m fine sand	53
Figure 5.30: Adhesion curve at 1 g/m fine sand	53
Figure 5.31: Adhesion curve at 2 g/m fine sand	54
Figure 5.32: Adhesion curve at 4 g/m fine sand	54
Figure 5.33: Electrical isolation of the fine sand at 0.5 g/m	55
Figure 5.34: Electrical isolation of the fine sand at 1 g/m.....	55
Figure 5.35: Electrical isolation of the fine sand at 2 g/m.....	56
Figure 5.36: Electrical isolation of the fine sand at 4 g/m.....	56
Figure 5.37: Electrical isolation of the coarse sand	57
Figure 6.1: Outputted amount of sand.....	60
Figure 6.2: Deviation from the target value	61
Figure 6.3: Slip intervals with the old method.....	63
Figure 6.4: Slip intervals with the new method	64
Figure 6.5: Workflow comparison, fine sand: 0.5 g/m.....	65
Figure 6.6: Workflow comparison, fine sand: 1 g/m	66
Figure 6.7: Workflow comparison, fine sand: 2 g/m	66
Figure 6.8: Workflow comparison, fine sand: 4 g/m	67
Figure 6.9: Comparison of the adhesion coefficient, fine sand: 0.5 g/m	68
Figure 6.10: Comparison of the adhesion coefficient, fine sand: 1 g/m	68
Figure 6.11: Comparison of the adhesion coefficient, fine sand: 2 g/m	69
Figure 6.12: Comparison of the adhesion coefficient, fine sand: 4 g/m	69

LIST OF TABLES

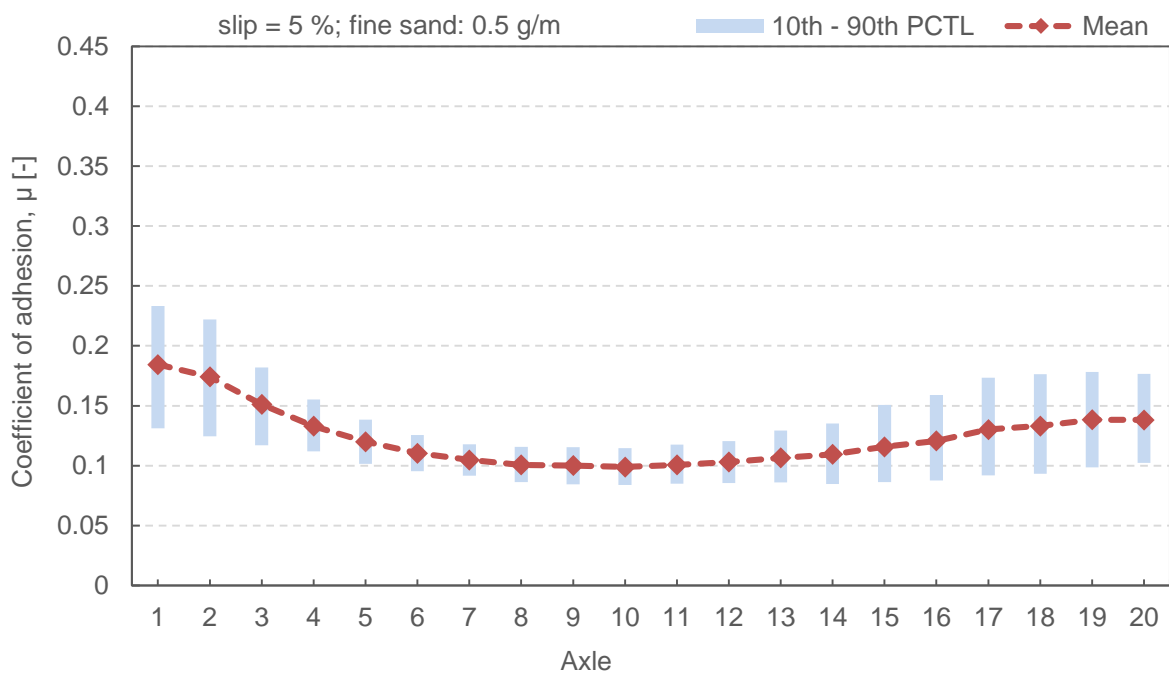
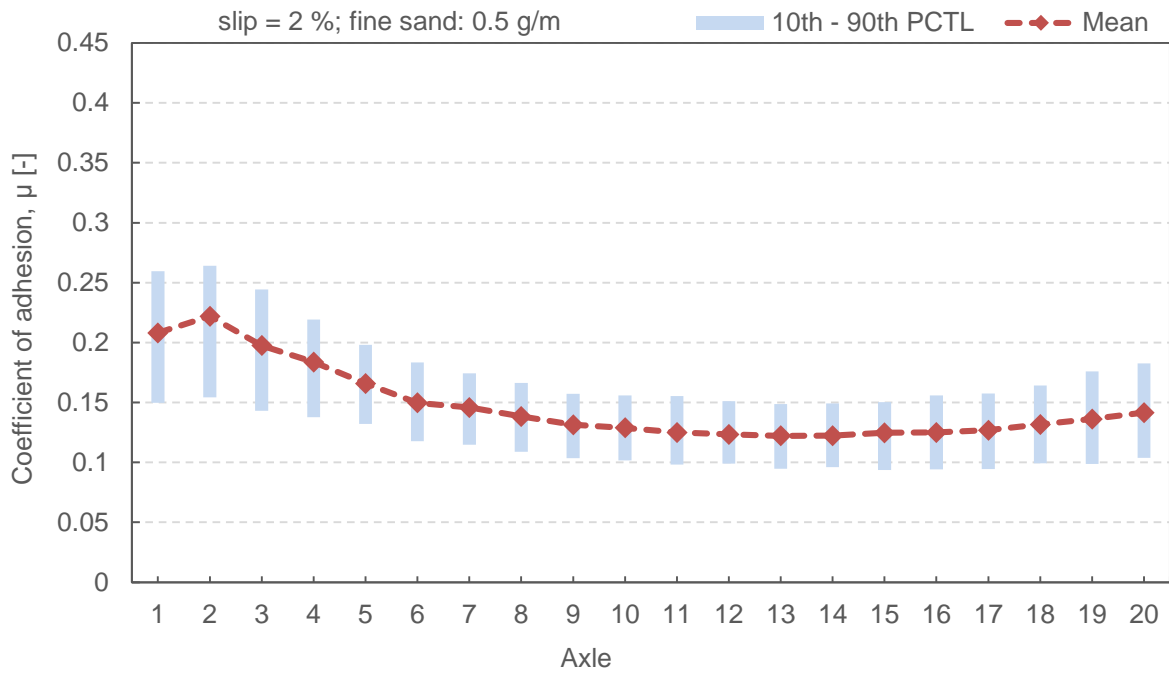
Table 1: Motion cases for diverse velocity relations.....	10
Table 2: Friction coefficients measured with a salient system tribometer.....	15
Table 3: Examples of wheel-rail adhesion coefficients	15
Table 4: Sand properties.....	21
Table 5: Yearly PM10 emission of the ÖBB	23
Table 6: Slip intervals for the evaluation	34
Table 7: Summary of the input parameters	35
Table 8: Settings for the comparative measurements.....	60

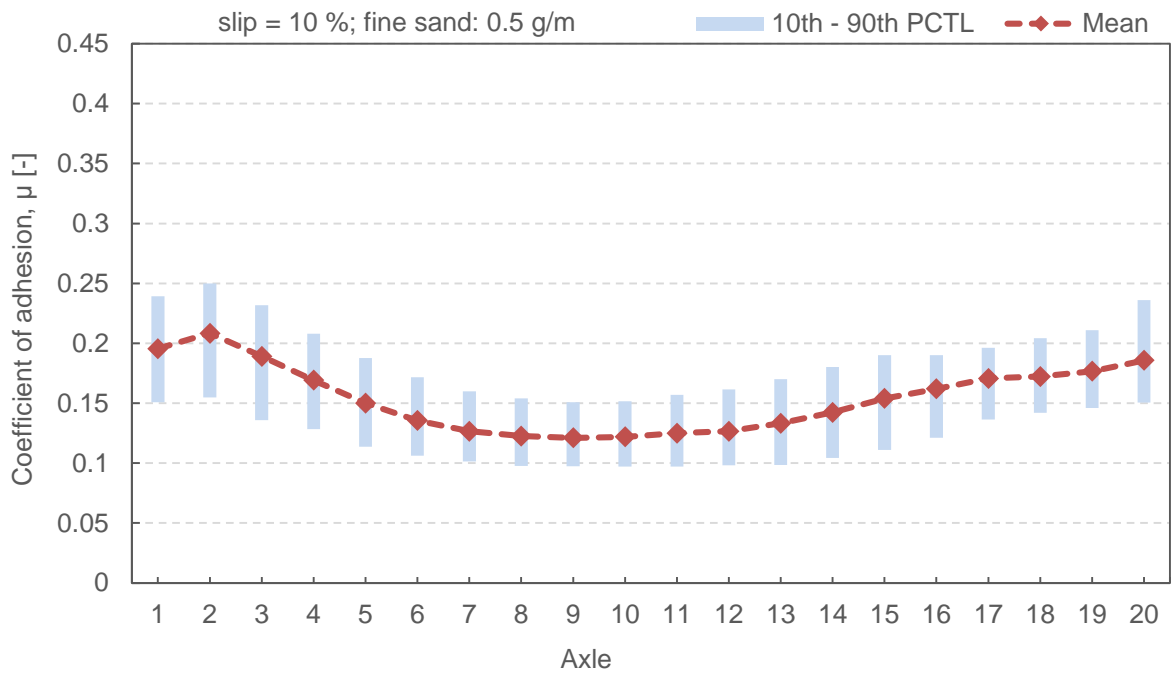
APPENDIX

In the appendix additional figures can be found about the experiment results.

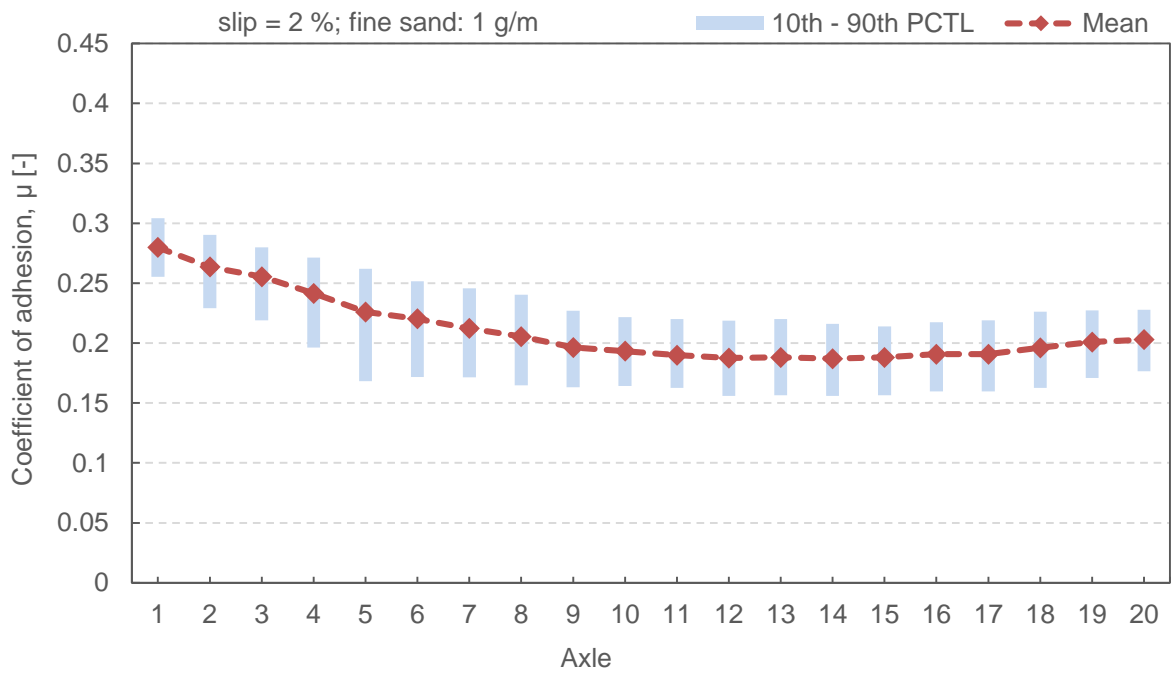
Single results with percentiles

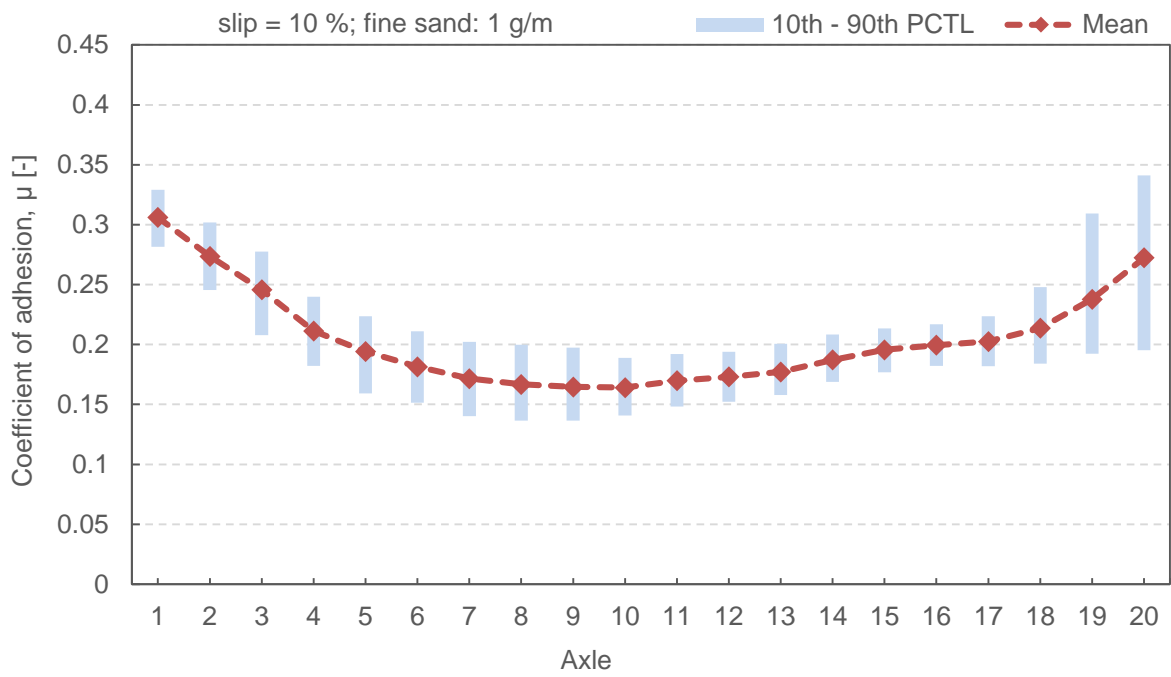
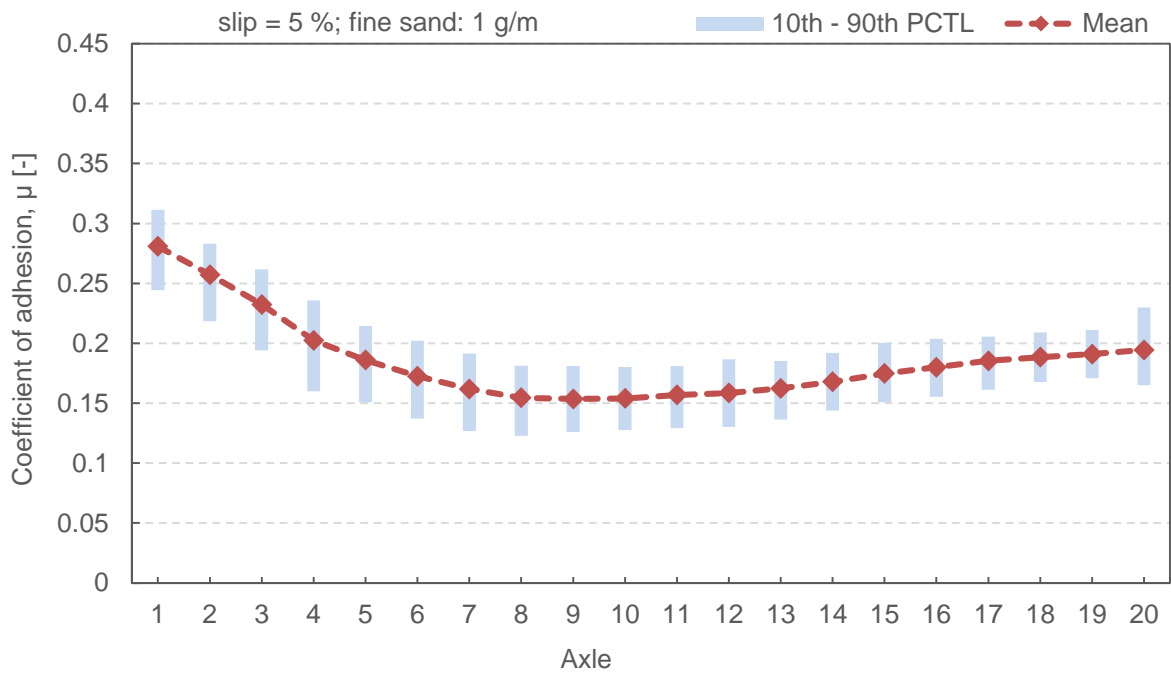
Fine sand: 0.5 g/m



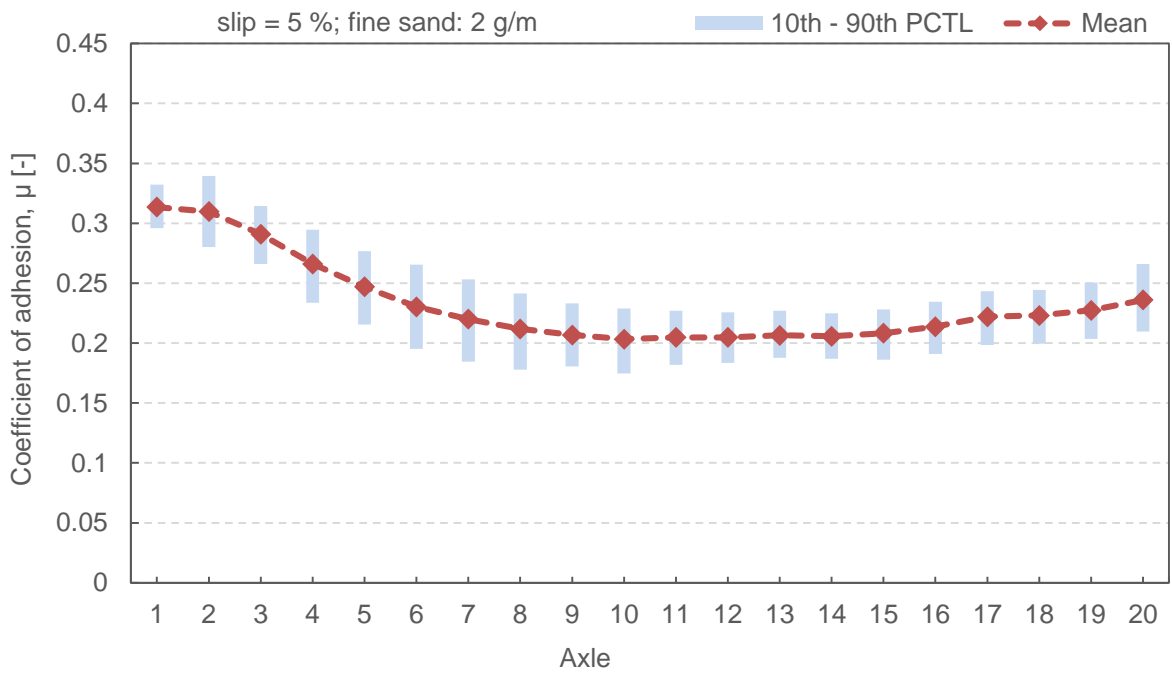
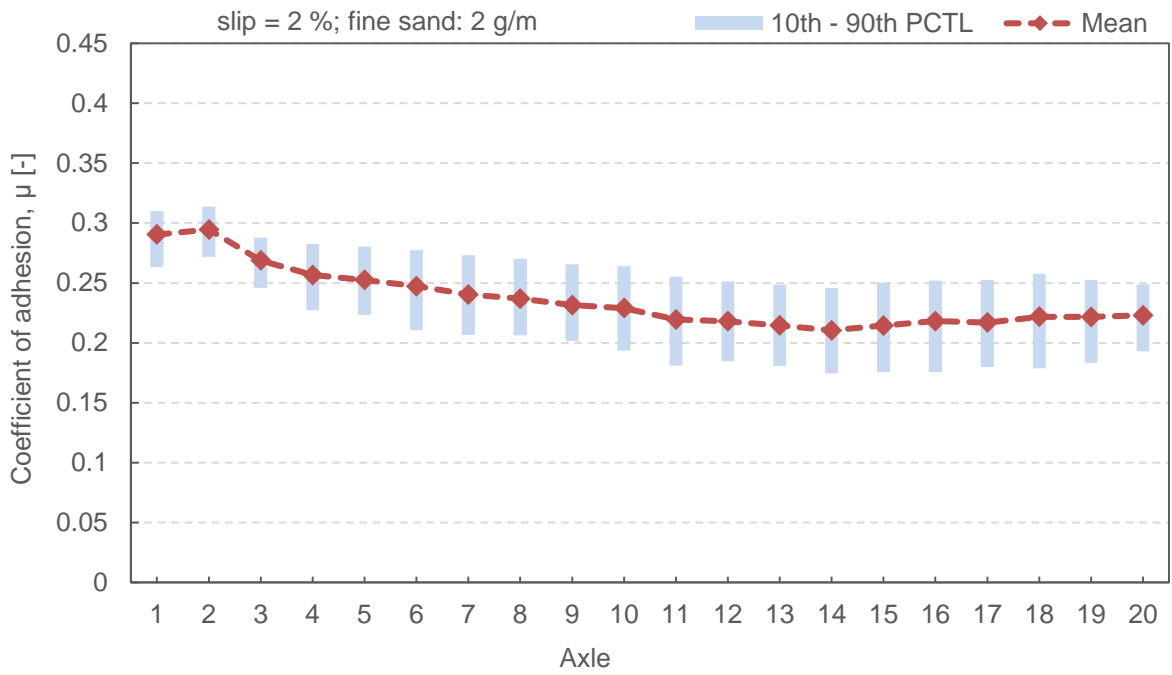


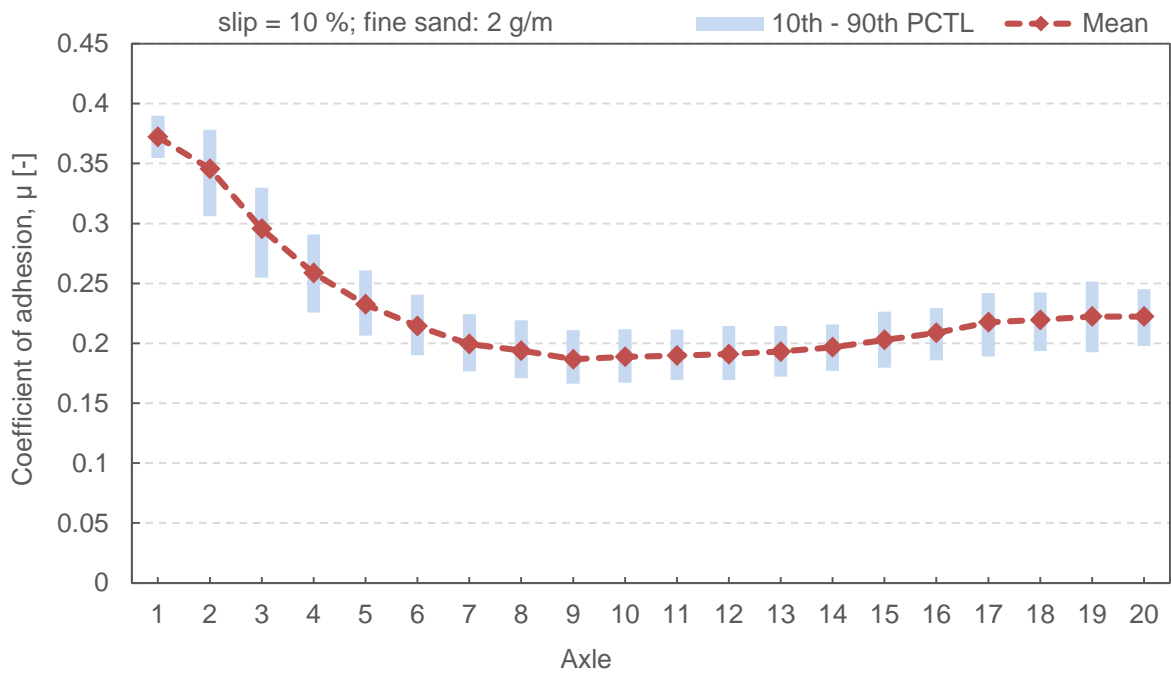
Fine sand: 1 g/m



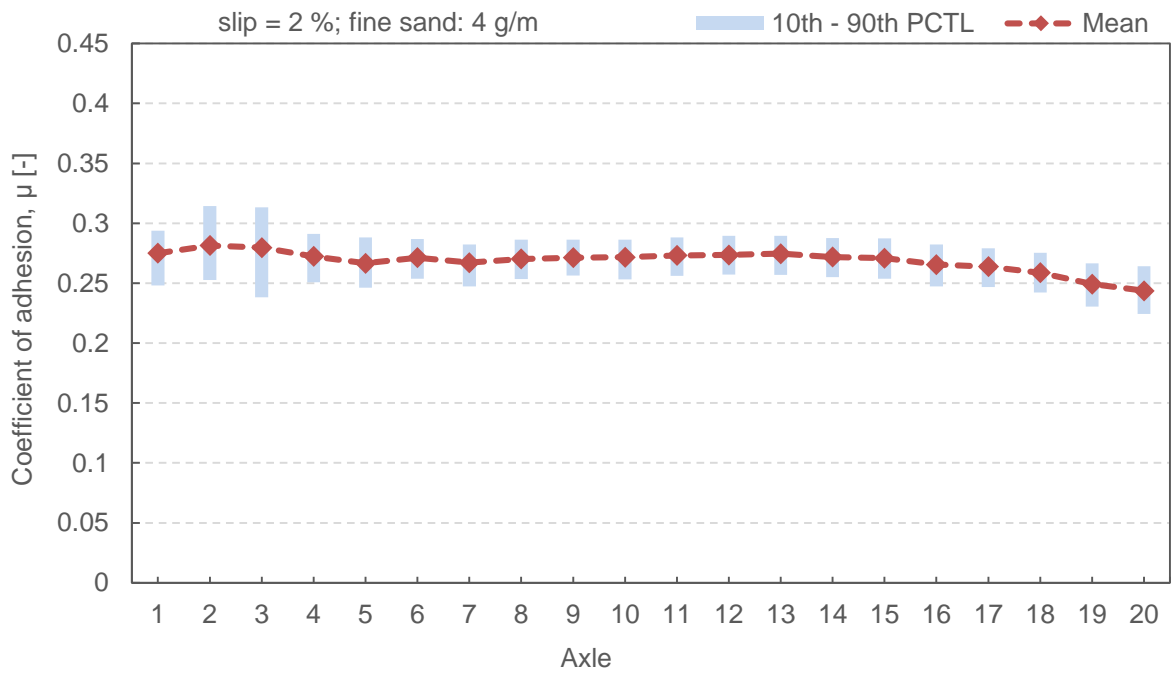


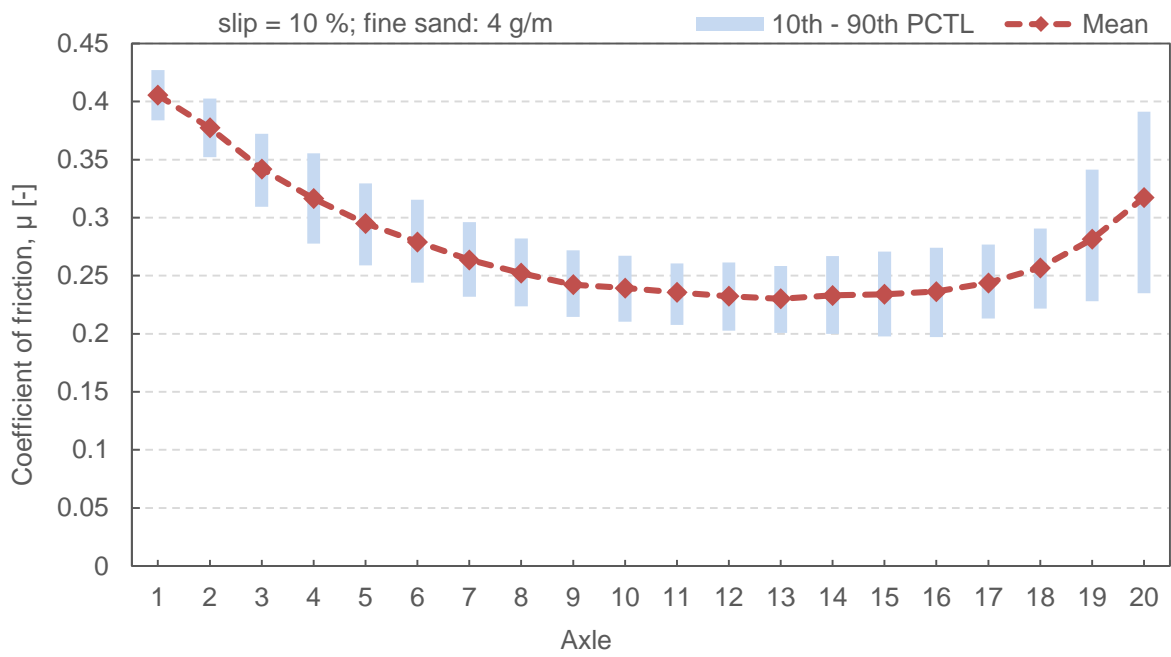
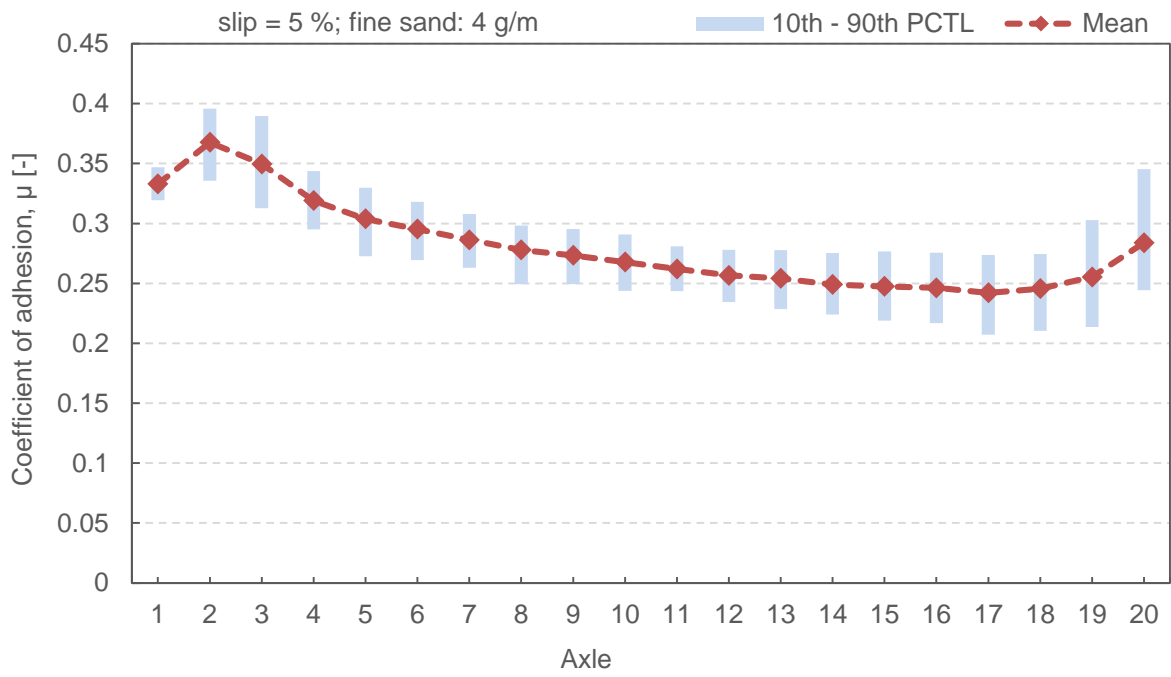
Fine sand: 2 g/m





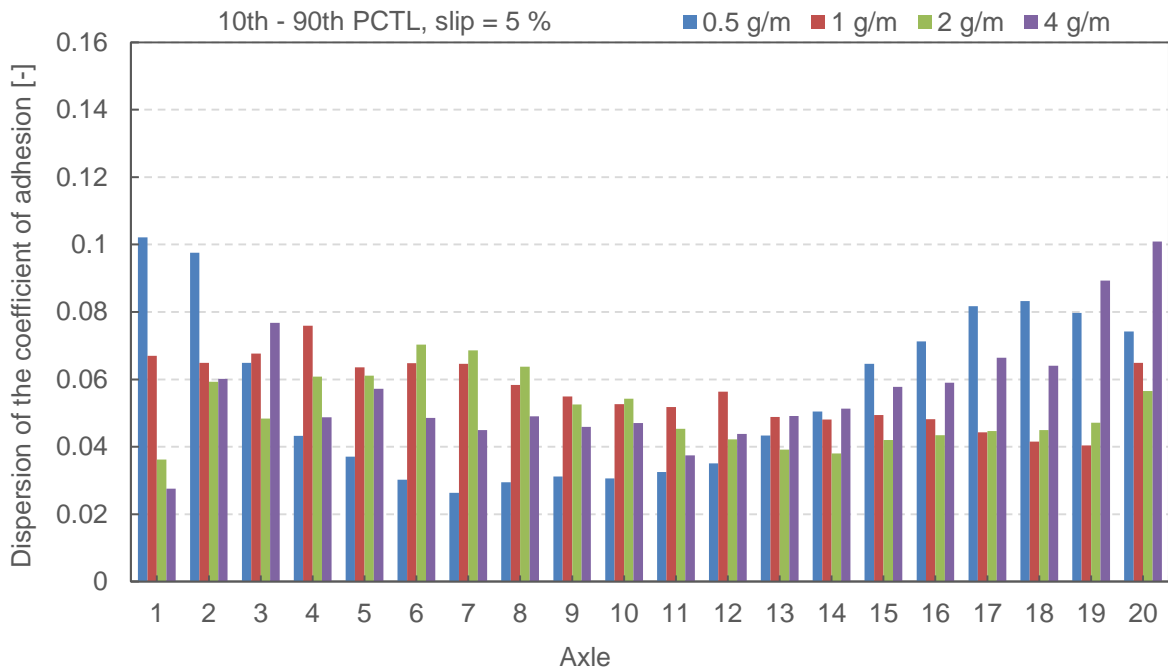
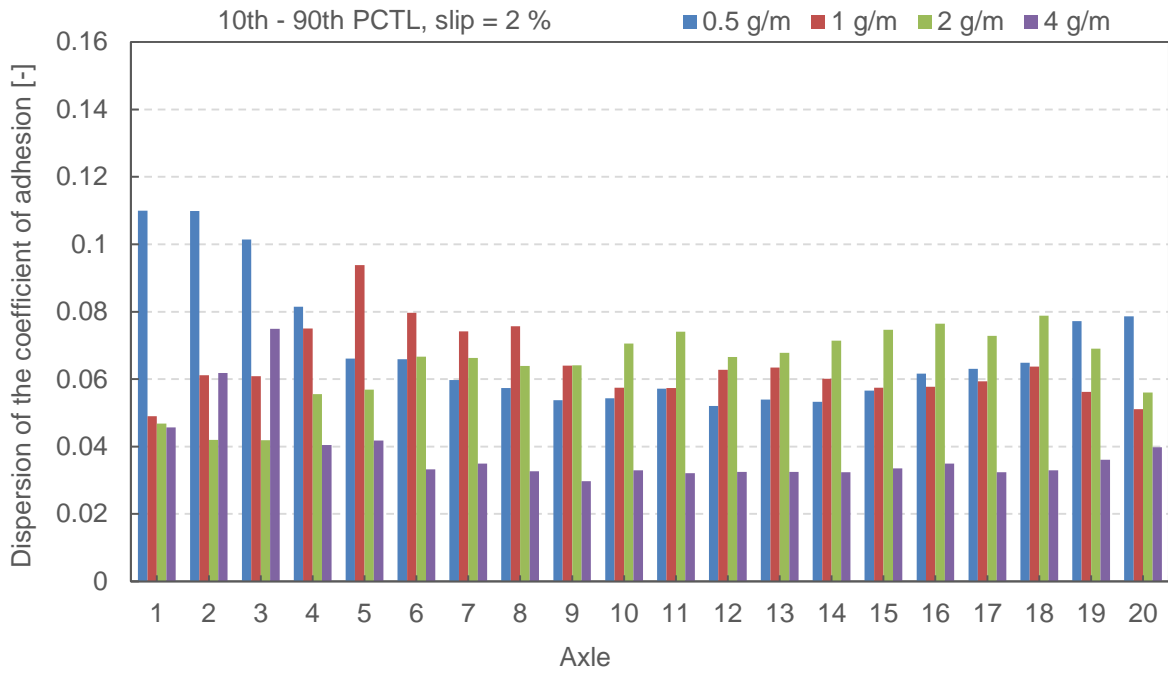
Fine sand: 4 g/m

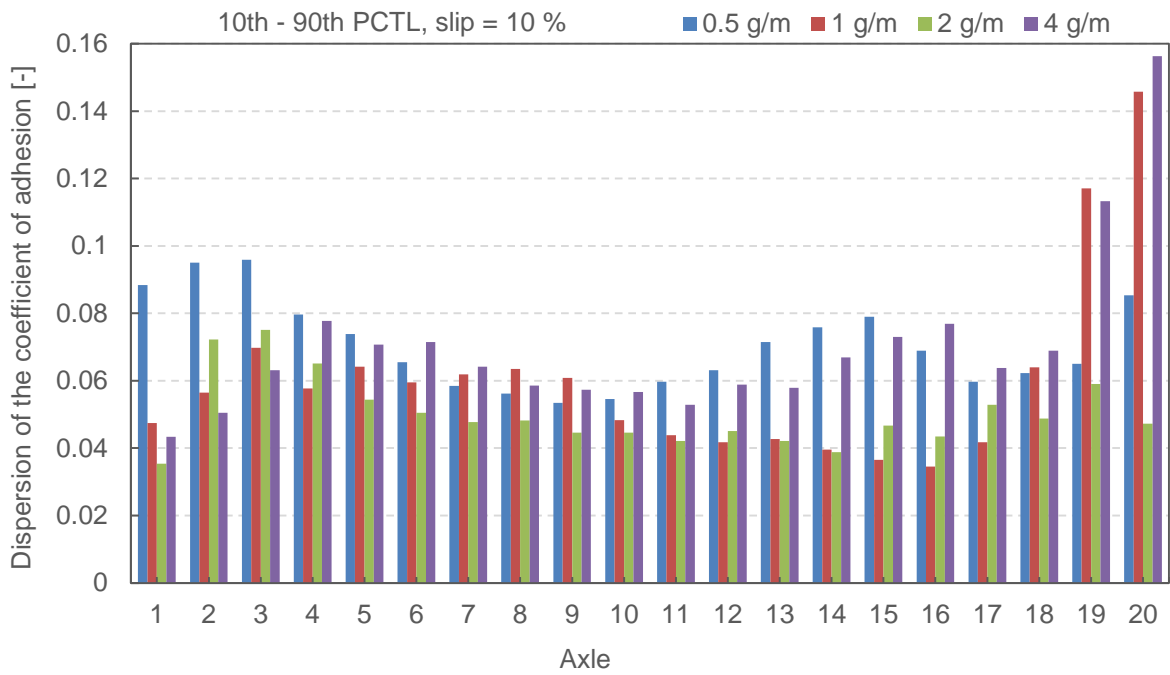




Dispersion of the adhesion coefficient

Comparison of the sand amount





Comparison of the slip values

